1972

Electrical And Thermal Conductivities Of Ion-selected Membranes

John Daniel Thorsley

ELECTRICAL AND THERMAL CONDUCTIVITIES OF ION-SELECTIVE MEMBRANES

by

John Daniel Thorsley

Department of Chemistry

Submitted in partial fulfillment

of the requirements for the degree of

Doctor of Philosophy

Faculty of Graduate Studies

The University of Western Ontario

London, Canada

June 1972

ABSTRACT

This thesis is concerned with the development and testing of methods for the measurement of electrical and thermal conductivities of ion-selective membranes, and an interpretation of the results obtained. Three types of membranes were studied: porous glass, cellulose and polyvinylbenzenesulfonate.

The electrical conductivity was measured in directions parallel and perpendicular to the membrane surface. The perpendicular method involved the optimum placement of the electrodes in relation to the membrane surface. A theory for the correction of overlap between the membrane and the cell faces was investigated. A method using mercury electrodes in contact with the membranes was also studied. It was found that, for polyvinylbenzenesulfonate membranes, the whole of the membrane's volume was available for conduction, rather than only the part occupied by water as is predicted by pore models of membranes. An anisotropy of the electrical conductivity was observed in porous glass and polyvinylsulfonate membranes which was ascribed to their method of manufacture.

An apparatus to measure the thermal conductivity was designed. A complete theory of its operation was developed and tested, including a method for correcting for thermal resistances at the membrane surfaces. It was found for polyvinylbenzenesulfonate membranes that the membranes behaved as a random mixture of a resin phase and a water phase with an anomalously high conductivity, possibly due to orientation of the water by the electrical double layer within the membrane. The concentration dependence of the conductivity of these membranes was found to be more complicated than a swelling effect. The temperature dependence of their thermal conductivity suggested that relatively short chain segments made up the membrane matrix.

ACKNOWLEDGEMENT

The publication of a thesis is not the result of the work of one person as is indicated on the title page. It is, rather, the culmination of the works of a great many people, who through previous publications or through personal contact have formed the ideas which are co-ordinated in the following pages. For the efforts of all of these people, I am deeply grateful.

I would especially like to thank my advisor, Dr. J.W. Lorimer, without whose understanding of the subject and his outstanding abilities in communication, this thesis would not be possible.

Special mention is also due to Dr. T.G. Brydges for his membranes and his knowledge, to Dr. D.G. Dawson for his helpful suggestions, to Miss Katie Ng for some conductivity measurements, to Mrs. Joyce Kilbourne for her typing skills, and to all the members of the L.G.F.C.B. Bridge Club.

This work was made possible by the financial assistance of the Defence Research Board for a research grant, and the Province of Ontario Graduate Fellowship program.

Finally, I would like to acknowledge the help of my wife, Sheila, whose understanding surpasses any words with which I can attempt to express it.

TABLE OF CONTENTS

LIST OF TABLES

LIST OF FIGURES

CHAPTER I

INTRODUCTION

Research into the transport properties of ion-selective membranes has shown promising results in several fields of technology [1,2]. The use of membranes in fuel cells, in some types of electrochemical batteries and in electrodialysis makes the investigation of their properties a worthwhile project. A systematic study of ion-selective membranes can lead to the ability to prepare membranes with properties suitable to many desired applications [3,4]. Also, the characterization of simple artificial membranes can lead to an understanding of the behaviour of the complex cell membranes that are necessary for life [5]. Therefore, a systematic study of the properties of several types of membranes, and a complete description of their properties and the interrelations among these properties will be a major step in the understanding and exploitation of ion-selective membranes.

The purpose of this work was the study of some methods of measuring two of the properties of ion-selective membranes and the testing of these methods on three types of artificial membranes. Particular attention was paid to

the methods employed so that reliable and accurate results could be obtained for all types of membranes. The first property studied, the electrical conductivity, is an important fundamental and practical characteristic [6]. It is involved in the interpretation of many transport phenomena across membranes. The thermal conductivity, the second property studied, is of fundamental importance in theories of energy transfer [7].

Before describing the types of membranes that were used, it is necessary to define what is meant by a membrane. According to Lakshminarayanaiah [8], an ion-selective membrane is a phase "acting as a barrier to the flow of ionic species present in the liquids and/or vapors contacting the two surfaces". In the case of ion-exchange membranes, the barrier behaves in the following way. The membrane is composed of polymer chains, crosslinked to form a matrix [9]. To the chains are attached charged groups, either negative as is the case with the membranes that were used here, or positive. The matrix is therefore characterized by the degree of crosslinking of the chains, by the capacity of the membrane which is related to the number of charged groups present, and by the water content which is related to the space available within the matrix structure through

which the ions and molecules pass during migration [10]. When an electrolyte is added, the ions with the same charge as the fixed groups in the membrane, called co-ions, will be excluded to an extent governed by the concentration of the external solution and the nature of the membrane. This is the basis of the model first proposed by Donnan [11]. For very low concentrations of external electrolyte, the co-ions will be completely excluded from the membrane. As the concentration increases, the number of co-ions will be equal to the number of counter-ions (those ions with a charge opposite to that on the membrane) minus the number of charges on the membrane matrix itself. In membranes with no ion-selective properties, there can be no distinction made between the positive and negative ions, since there are no fixed charges. When an electrical potential difference is applied across the membrane, flows of ions and solvent molecules are created. The ion flows are related to the electrical mobilities of the ions in the membrane, and to the ion-selective nature of the membrane itself. The electrical conductivity, related to this current flow, [6] is therefore of fundamental importance in understanding the properties of ions in the membrane matrix.

The thermal conductivity is related to the struc-

ture of the membrane matrix. In it is involved the excitation of sections of the polymer network by thermal energy [12]. The thermal conductivity is then dependent on the amount of crosslinking of the polymer chains, how the membrane was originally polymerized, and the number of fixed charges causing electrical repulsions within the membrane. Since the membranes are equilibrated in an electrolyte, the thermal conductivity should also depend on the amount of electrolyte that is present within the membrane, by analogy with calculations on membranes swollen by non-electrolytes [13].

It is therefore essential that accurate and reliable methods be developed to measure the electrical and thermal conductivities of ion-selective membranes so that these properties may be used for characterization and as basic quantities in theories of membrane transport.

Ion-exchange properties have been recognized since the middle of the nineteenth century [14]. Soils and clays with these properties were found and the responsible substances isolated [15]. Ion-exchange materials were first fabricated at the beginning of this century [16]. By 1914, detailed studies of the passage of current through membranes were being made. With the development of synthetic ion-

exchange resins in 1950 [17,18], a wide variation of the properties of the membrane, both physical and chemical, could be achieved and it became more feasible to use these to make a systematic study of the properties of membranes and to use this knowledge for studying the more complex problems of natural membranes. In the last 20 years a great deal of effort has been devoted to this field. The published work in the field up to 1969 has been surveyed by Lakshminarayanaiah [8,19].

Three types of ion-selective membranes were used in this work. They were chosen so that a wide spectrum of physical and chemical properties could be covered. The first type was a crosslinked copolymer of styrene and p-vinylbenzenesulfonic acid [4,20]. Membranes of this type have a high capacity (fixed charge density) and are intermediate in their tensile strength. The second, cellulose gel membranes, [21] have an intermediate capacity and a relatively low tensile strength. The third kind of membrane, porous glass, [22] has a low capacity and high tensile strength.

This thesis is divided into eight chapters. The second deals with the theories of transport in membrane systems. The third deals with the experimental methods

which are used frequently throughout the balance of this work. The next three chapters deal with the electrical conductivity of membranes. Chapter IV discusses types of cells which were designed to measure the electrical conductivity, $K_{\perp}$, perpendicular to the surface of the membrane. All of these cells were based on a design first used by Manecke and Bonhoeffer [23] and later modified by Lorimer et al [21]. Membranes were used which had a larger diameter than the electrodes in the cell and theoretical calculations [24] were used to account for any current flow through the part of the membrane that was not between the electrodes. The four cells used were similar, but the electrode size varied, as did the distance between the electrodes and the membrane surface. The fourth cell used mercury rather than platinum electrodes. This technique was used by Subrahmanyan [25] for the measurement of electrical conductivity. Chapter V deals with the electrical conductivity, $K_{\parallel}$, of a membrane parallel to its surface. Measurements of this type have been attempted by Hills [26] and Lorimer [21] using membrane rods or strips. All dimensions of the membrane must be known accurately for the success of their method. Therefore, a new type of cell was designed, based on a theory of van der Pauw [27]. This theory relies only on a precise

measurement of the thickness of the sample. The sample can be any shape as long as the thickness is uniform and there are no isolated holes. Chapter VI compares the results obtained normal to the membrane surface to those measured parallel to the surface. If the membrane is homogeneous, the two results should be the same, and the ratio of the two electrical conductivities will be unity. If, however, the two results are different, an anisotropy can be defined as

$$\alpha = \left| (K_{\perp} - K_{/\!/})/(K_{/\!/} + K_{\perp}) \right| . \qquad [I\text{-}1]$$

Such an effect may be caused by a surface layer on the membrane with properties different from the body of the membrane, or by some other structural peculiarity of the membrane.

Chapter VII is concerned with the thermal conductivity of ion-selective membranes. No measurements of this type have been reported before. Since it was impossible to insure the absence of contact films between the membrane and the heat source used, a complete theory of the apparatus was derived to take into consideration the existence of a reproducible contact film. The method was tested using polytetrafluoroethylene discs with a silicone oil film on the surface. It was then used for measurements on membranes.

These results were correlated to the swelling of membranes, since the thermal conductivity and the degree of swelling both reflect similar aspects of the polymeric structure of the membrane.

Chapter VIII is a summary of the results obtained and the possible explanations for these results.

CHAPTER II

THEORIES OF TRANSPORT IN MEMBRANES

1. Introduction

A complete theoretical description of the transport of ions and molecules in membranes can be considered to comprise, ideally, the following two steps:

1. Macroscopic transport equations are formulated in such a way that significant transport coefficients are defined and related to experimentally-accessible quantities.

The most comprehensive theory available for this purpose is the thermodynamics of irreversible processes, which was first applied to membrane phenomena in a systematic way by Staverman [28]. Two versions of the irreversible thermodynamic theory are in use: one dealing with discontinuous systems and one with continuous systems. The discontinuous version, as applied to membrane phenomena, has been reviewed in a number of places [8,19,29-34] and is valuable because of its simple and straightforward description of experimentally-observed phenomena. The continuous version is necessary for the proper consideration of the processes taking place within the membrane, and has also

been reviewed [29-31,34]. Some authors have considered in detail the relation between these two versions [29,30,31,34]. Older continuous theories of transport in membranes may be classified as approximations to the more rigorous irreversible thermodynamic theory. Reviews on these aspects are also available [19,35].

2. Molecular models that are in accord with current theoretical ideas in electrolyte and polymer theory are constructed, and calculations of the macroscopic transport coefficients are carried out and compared with experiment.

In general, progress in this direction has been slow and uncertain, because of the inherent complexity of the simplest models and the complicated nature of the necessary molecular theories of equilibrium and transport. Approximate theories [36,40] of this type are useful as guides for the prediction and correlation of membrane properties.

In this chapter, the irreversible thermodynamic theory will be discussed in detail, and molecular theories will be surveyed briefly.

2. Irreversible Thermodynamics of Transport in Membranes

(a) Discontinuous Systems

(i) General Relations

The thermodynamics of irreversible processes relates the driving forces (or affinities) applied to a membrane to the fluxes of solute or solvent that result. These processes are irreversible in a thermodynamic sense. If a process in a system is reversible, the change in the entropy of the system is exactly equal to the heat flow from the surroundings, Q, divided by the absolute temperature, T. That is,

$$\Delta S = Q/T \; . \qquad [II-1]$$

However, the processes that are being considered here are irreversible. In this case the entropy change is greater than that predicted for a reversible change [29]. In other words, the entropy change consists of two parts. One part is an external part that is equal to the value for the reversible process. The second part is an internal production of entropy caused by the presence of irreversible processes:

$$\Delta S' = Q/T + \Delta_i S \qquad [II-2]$$

It is this second term that characterizes irreversibility.

During the nineteenth century, several phenomeno-

logical laws were developed for specific irreversible processes. These laws gave the flux produced as being directly proportional to the applied force. Thus, Ohm's law gives the flow of current as proportional to the applied voltage, Fourier's law gives the heat flow as proportional to the temperature gradient, and Fick's law gives the diffusion flow of matter as proportional to the concentration gradient. If more than one of these forces are applied simultaneously, the resulting flows will be dependent on all of these forces. In membrane systems, the affinities actually used in experiments are differences in various intensive quantities. Research has been devoted to four of these affinities: an electrical potential difference (ΔE), a pressure difference (ΔP), a concentration difference (ΔC) which is related to a difference in chemical potential ($\Delta \mu$), and finally, a temperature difference (ΔT). (See [19] for examples.) For each of these affinities, there is an associated flux. For example, if only an electrical potential difference is acting on the membrane, there will be a current flow across the membrane. In this situation, the electrical conductivity and the transport numbers of ions and the solvent can be measured. Similarly, a pressure difference will cause a streaming potential and a temperature

difference will cause thermoosmosis, among other effects.

In the most general case, any force can give rise to any flow. For instance, a voltage applied across an ion-selective membrane results in a flow of matter, both solute and solvent. Therefore, a theory is needed that relates the fluxes to all of the forces. A general theory was developed by Onsager [41] in 1931. He showed that if there are n independent fluxes, J_i, and a corresponding affinity X_i for each flux, then the fluxes and forces are related by the following equation:

$$J_i = \sum_{j=1}^{n} L_{ik} X_k \qquad (k = 1,2,3....n). \qquad [II-3]$$

The fluxes and forces are chosen so that they satisfy the relation

$$dS/dt = \sum_i J_i X_i \qquad [II-4]$$

where dS/dt is the rate of entropy production due to the irreversible processes that are occurring in the system. Further restrictions can be placed on equation [II-3] with the use of Onsager's reciprocal relations:

$$L_{ik} = L_{ki} . \qquad [II-5]$$

These relations have been tested and confirmed experimentally in a number of cases [42].

In order to obtain expressions suitable to the conditions of the experimental measurements, a suitable model must be constructed. It consists of two reservoirs I and II separated by a membrane as shown in Figure [II-1].

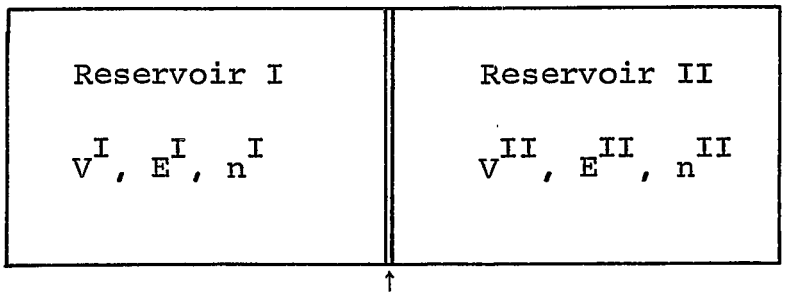

FIGURE [II-1]

This system is discontinuous as defined by de Groot [29,30] since the physical properties are not continuous functions of the spatial co-ordinates but are discontinuous at the membrane boundary. The differences between continuous and discontinuous treatments of membrane systems will be discussed later. The two reservoirs have volumes V^I and V^{II}, electrical potentials E^I and E^{II}, and masses n^I and n^{II}. No chemical reactions are to take place in the system.

Since the system is closed, the total mass of each component must be constant, and the law of conservation of mass is given by

$$dn_k^I + dn_k^{II} = 0 \qquad (k = 1,2.....r) \qquad [II-6]$$

and $$dn^{I} + dn^{II} = 0 , \qquad [II-7]$$

and r is the number of components in the system.

The change in the energy of each reservoir consists of two parts: that part which is exchanged with the surroundings, $d_e U$, and that part which is exchanged with the other reservoir, $d_i U$. The total energy change for the first reservoir can therefore be expressed as

$$dU^{I} = d_e U^{I} + d_i U^{I} \qquad [II-8]$$

and by a similar equation for the second reservoir. Since the energy of the system only changes if energy is exchanged with the surroundings and not simply moved from one reservoir to the other, the law of conservation of energy can be written as

$$d_i U^{I} + d_i U^{II} = 0 . \qquad [II-9]$$

Now, if the two reservoirs are considered separately, they are open systems. Suppose that a heat flow $d\bar{q}$ per mole into an open system at pressure P causes a molar increase in energy of $d\bar{U}$ and an amount of work $-Pd\bar{v}$ to be done on the system. $\bar{v}$ is the molar volume. Then the first law of thermodynamics can be written

$$d\bar{q} = d\bar{U} + Pd\bar{v} . \qquad [II-10]$$

The enthalpy of the system can now be defined as

$$H = nh = U + PV \qquad [II-11]$$

where n is the total number of moles in the system. Each reservoir is at uniform electrical potential so that there is no electrical work term in the equation for each reservoir separately. We obtain from equations [II-10] and [II-11] and the relation $d\bar{Q} = nd\bar{q}$,

$$d\bar{Q}^{I} = dU^{I} + P^{I}dV^{I} - h^{I}dn^{I} \qquad [II-12]$$

and a similar expression for reservoir II.

If the total system is considered however, then electrical work is done moving dn_k moles of each component k between the reservoirs. This work is equal to

$$\sum_{k=1}^{r} z_k F(E^{II}dn_k^{II} + E^{I}dn_k^{I}). \qquad [II-13]$$

With the aid of equation [II-8], this becomes

$$\sum_{k=1}^{r} z_k F(E^{II} - E^{I})dn_k^{II}. \qquad [II-14]$$

The factor F is the Faraday constant (96,487 J mol^{-1}) and z_k is the signed charge ("valence") of component k.

The total heat transferred between reservoirs can now be calculated from equations [II-12] and [II-14].

$$d\bar{Q} = dU + P^{I}dV^{I} + P^{II}dV^{II} + \sum_{k=1}^{r} z_k F(E^{II} - E^{I})dn_k^{II} \qquad [II-15]$$

where the total energy change, dU, is the sum of the energies of each reservoir, and the enthalpy terms cancel one another.

The heat absorbed by the two reservoirs can be split into the part absorbed from the surroundings and the part absorbed from the other reservoir, in the same manner as the energy change in equation [II-8]:

$$d\bar{Q}^{I} = d_e\bar{Q}^{I} + d_i\bar{Q}^{I}, \qquad \text{[II-16]}$$

and similarly for reservoir II. The heat and the energy received by the total system can now be expressed as

$$d\bar{Q} = d_e\bar{Q}^{I} + d_e\bar{Q}^{II} \qquad \text{[II-17]}$$

$$dU = d_eU^{I} + d_eU^{II}. \qquad \text{[II-18]}$$

If these two expressions are substituted into equation [II-15], then we obtain

$$d_e\bar{Q}^{I} + d_e\bar{Q}^{II} = d_eU^{I} + d_eU^{II} + P^{I}dV^{I} + P^{II}dV^{II} + \sum_{k=1}^{r} z_k FE^{I}dn_k^{I} + \sum_{k=1}^{r} z_k FE^{II}dn_k^{II}. \qquad \text{[II-19]}$$

The sizes of the two reservoirs are independent and thus this equation can be separated into an equation concerning each reservoir only:

$$d_e\bar{Q}^{I} = d_eU^{I} + P^{I}dV^{I} + \sum_{k=1}^{r} z_k FE^{I}dn_k^{I} \qquad \text{[II-20]}$$

and a similar expression for the second reservoir. The last equation is concerned only with changes taking place between the reservoir and the surroundings. If the relations between external and internal quantities are used, then equations

may be obtained for the changes between the two reservoirs. Therefore, if equations [II-12], [II-16], [II- 8] and [II-20] are employed, the following result is obtained for reservoir I:

$$d_i\bar{Q}^I = d_iU^I - h^I dn^I - \sum_{k=1}^{r} z_k FE^I dn_k^I \qquad [II-21]$$

With the help of equation [II-9], and the equation for reservoir II,

$$d_i\bar{Q}^I + \sum_{k=1}^{r}(h^I + z_k FE^I)dn_k^I + d_i\bar{Q}^{II} + \sum_{k=1}^{r}(h^{II} + z_k FE^{II})dn_k^{II} = 0 \qquad [II-22]$$

In order to establish the relationship between the fluxes and the forces in the system, an expression for the entropy production (equation [II-4]) must be obtained. This can be done by applying the second law of thermodynamics, using Gibbs' equation and considering each reservoir separately. For reservoir I, the result obtained is

$$T^I dS^I = dU^I + P^I dV^I - \sum_{k=1}^{r} \mu_k^I dn_k^I \qquad [II-23]$$

where S is the entropy as before, and μ_k is the molar chemical potential of component k. The total change in entropy for the system is the sum of the two separate entropies:

$$dS = (dU^I + P^I dV^I)/T^I + (dU^{II} + P^{II} dV^{II})/T^{II} - \sum_{k=1}^{r}(\mu_k^I dn_k^I/T^I + \mu_k^{II} dn_k^{II}/T^{II}). \qquad [II-24]$$

If equations [II-7], [II-8] and [II-9] are now employed, then

$$dS = (d_e U^I + P^I dV^I)/T^I + (d_e U^{II} + P^{II} dV^{II})/T^{II} + (1/T^I - 1/T^{II}) d_i U^I + \sum_{k=1}^{r} (\mu_k^{II}/T^{II} - \mu_k^I/T^I) dn_k^I , \quad [II-25]$$

and the application of equations [II-20], [II-21] and [II-25] leads to

$$dS = d_e \bar{Q}^I/T^I + d_e \bar{Q}^{II}/T^{II} + d_i \bar{Q}^I/T^I + d_i \bar{Q}^{II}/T^{II} + (h^I dn^I/T^I + h^{II} dn^{II}/T^{II} + \sum_{k=1}^{r} (\mu_k^{II}/T^{II} - \mu_k^I/T^I)\ dn_k^I . \quad [II-26]$$

Equation [II-22] can now be used to substitute for $d_i \bar{Q}^{II}$, giving

$$dS = d_e \bar{Q}^I/T^I + d_e \bar{Q}^{II}/T^{II} + (d_i \bar{Q}^I + h^I dn^I)(1/T^I - 1/T^{II}) + \sum_{k=1}^{r} (\mu_k^{II}/T^{II} - \mu_k^I/T^I) dn_k^I + \sum_{k=1}^{r} z_k F (E^{II} - E^I) dn_k^I/T^{II} . \quad [II-27]$$

The entropy change in the system consists of two parts, as indicated in equation [II-2]. The external part is the entropy exchanged with the surroundings:

$$d_e S = d_e \bar{Q}^I/T^I + d_e \bar{Q}^{II}/T^{II} \quad [II-28]$$

The internal part is due to the irreversible processes which are taking place inside the system. Equation [II-27] gives

this as

$$d_i S = (d_i \bar{Q}^I + h^I dn^I)(1/T^I - 1/T^{II}) + \sum_{k=1}^{r} [(\mu_k^{II}/T^{II} - \mu_k^I/T^I + z_k F(E^{II} - E^I))/T^{II}] dn_k^I. \quad [II-29]$$

The internal entropy changes for each reservoir can be separated in equation [II-29]:

$$d_i S^I = d_i \bar{Q}/T^I + h^I dn^I/T^I - \sum_{k=1}^{r} \tilde{\mu}_k^I dn_k^I/T^I \quad [II-30]$$

with a similar result for reservoir II (using equation [II-6]) and where

$$\tilde{\mu}_k = \mu_k + z_k FE \quad [II-31]$$

is the electrochemical potential.

The forces that are acting on this system are a temperature difference and a difference in electrochemical potential. Since the general Onsager theory of irreversible processes assumes that the forces are caused by small changes of the state variables from their equilibrium values, the forces are best expressed in their infinitesimal form [21]. Therefore, the forces can be written

$$X_u = -(1/T^I - 1/T^{II}) = -(T^{II} - T^I)/T^I T^{II} = -dT/T^2 \quad [II-32]$$

$$\tilde{X}_k = -(\tilde{\mu}_k^{II}/T^{II} - \tilde{\mu}_k^I/T^I) = -d(\tilde{\mu}_k/T) = -d\tilde{\mu}_k/T + \tilde{\mu}_k dT/T^2 \quad [II-33]$$

The force is always taken as acting from reservoir II to reservoir I. Equation [II-29] now becomes

$$d_i S = -(d_i \bar{Q}^I + h^I dn^I) dT/T^2 + \sum_{k=1}^{r} d(\tilde{\mu}_k/T) dn_k^I \qquad [II-34]$$

The entropy production is the time derivative of the internal part of the entropy change:

$$d_i S/dt = -(d_i \bar{Q}^I/dt + h^I dn^I/dt) dT/T^2 - \sum_{k=1}^{r} d(\tilde{\mu}_k/T) dn_k/dt \qquad [II-35]$$

The time rate of change in the heat absorbed is the heat flow, J_q, and the time rate of change in the number of moles, n, is the flow of matter, J_k. The use of this information, along with equations [II-32] and [II-33] leads to the following result:

$$d_i S/dt = J_q X_u + \sum_{k=1}^{r} (hX_u + \tilde{X}_k) J_k \qquad [II-36]$$

The chemical potential is a function of temperature, pressure and composition:

$$d\mu_k = d\mu_k(T) - S_k dT \qquad [II-37]$$

where $d\mu_k$ is a function of temperature, pressure and composition, and $d\mu_k(T)$ is a function of pressure and composition only. If these equations are incorporated into equation [II-36], the following result is obtained:

$$d_i S/dt = J_q X_u + \sum_{k=1}^{r} J_k (d\tilde{\mu}_k(T) - (h_k - h) dT/T)/T \qquad [II-38]$$

where $\tilde{\mu}_k(T)$ contains the electrical term as was the case with $\tilde{\mu}_k$. Now equation [II-3] can be employed to obtain the phenomenological equations. The Onsager coefficients are chosen so that a factor of T is incorporated into the entropy production:

$$J_i = - \sum_{k=1}^{r} L_{ik}(d\tilde{\mu}_k(T) - (h_k - h)dT/T) - L_{iq}dT/T \qquad [II-39]$$

$$J_q = - \sum_{k=1}^{r} L_{qk}(d\tilde{\mu}_k(T) - (h_k - h)dT/T) - L_{qq}dT/T \qquad [II-40]$$

The phenomenological coefficients obey Onsager's relations as stated in equation [II-5].

The total transported heat of component k, Q_k, can be defined now by the equation

$$L_{iq} = L_{qi} = \sum_{k=1}^{r} Q_k L_{ik} \qquad [II-41]$$

and, using the nomenclature recommended by Tyrrell [43], equations [II-39] and [II-40] become

$$J_i = - \sum_{k=1}^{r} L_{ik}(d\tilde{\mu}_k(T) + (Q_k - h_k + h)dT/T) \qquad [II-42]$$

$$J_q = - \sum_{k,j=1}^{r} Q_k L_{jk}(d\tilde{\mu}_k(T) - (h_k - h)dT/T) - L_{qq}dT/T \qquad [II-43]$$

When the temperature difference is zero, the quantity Q_k is just the heat flow accompanying a unit flow of matter.

The heat of transfer, Q_k^*, is defined by the equation

$$Q_j^* = Q_j - h_j , \qquad [II-44]$$

and can be easily substituted into equations [II-42] and [II-43] above.

These equations describe a system made up of a membrane between two electrolyte reservoirs under conditions of a concentration difference, an electrical potential difference, a temperature difference, and (implicit in $d\tilde{\mu}_k(T)$) a pressure difference.

(ii) Measurement of Electrical Conductivity

In this thesis, measurements of electrical conductivity were made under the conditions $dP = 0$, $dT = 0$, $d\mu_k = 0$, $k = 1,2,.....r$, and $dE \neq 0$. The electrical current density is

$$I = F \sum_{k=1}^{r} z_k J_k \qquad [II-45]$$

so that, from equation [II-42], under the above restrictions,

$$I = - \sum_{j,k=1}^{r} z_j z_k L_{jk} F^2 dE$$

$$\equiv - L_E F^2 dE \qquad [II-46]$$

The electrical conductivity, κ, of a membrane of thickness ℓ may then be defined as

$$\kappa = I\ell/(-\Delta E) = L_E \ell F^2 \qquad [II-47]$$

where ΔE is the difference in electrical potential across the membrane. The equivalence of L_E in equations [II-46]

and [II-47] follows by considering thin slices of homogeneous membrane of thickness $d\ell$. For each slice, L_E will be the same, so that integration of $\kappa = Id\ell/(-dE)$ by adding up contribution to dE from each slice gives equation [II-47]. Heterogeneous membranes will be considered later. Other electrical conductivities, for example, the conductivity at zero volume flow, can be defined [44]. With careful experiments, using small direct current voltages in a cell with the same solution at the same temperature and pressure on each side of the membrane, equation [II-46] will hold, but volume flow can occur. If alternating voltages are used, even if there are differences in concentration, pressure and temperature across the membrane, there is no volume flow. However, if the measured conductivity is independent of frequency, it should be identical with the direct current conductivity given by equation [II-46], since on each half of the alternating current cycle, equal and opposite volume flows can occur without hindrance. Experiments to test this point have been reported by Meares and Ussing [45], who found the values measured at 1000 kHz to be essentially the same as those from a direct current method for various concentrations of sodium ions.

(iii) Measurement of Thermal Conductivity

For thermal conductivity measurements, the membrane is enclosed by an impermeable heat source and an impermeable heat sink. The membrane is therefore a closed system and no net flow can occur. The total volume flow is

$$J_v = \sum_{i=1}^{r} \bar{V}_i J_i \qquad [II-48]$$

where V_i is the partial molar volume of species i. At $d\mu_i(T,P) = 0$, equations [II-42], [II-43] and [II-45] give

$$\begin{aligned} J_v &= - L_p dP - L_{PE} dE - L_{PT} dT/T \\ I/F &= - L_{PE} dP - L_E dE - L_{ET} dT/T \\ J_q &= - L_{PT} dP - L_{ET} dE - L_T dT/T \end{aligned} \qquad [II-49]$$

where

$$L_p = \sum_{i,k=1}^{r} \bar{V}_i \bar{V}_k L_{ik} \qquad L_{PE} = \sum_{i,k=1}^{r} \bar{V}_i z_k F L_{ik}$$

$$L_{PT} = \sum_{i,k=1}^{r} \bar{V}_i Q_k L_{ik} \qquad L_{ET} = \sum_{i,k=1}^{r} Q_k z_k F L_{ik}$$

$$L_T = L_{qq} - \sum_{i,k=1}^{r} Q_k L_{ik} (h_k - h) \qquad [II-50]$$

Since there is no net electric current, dE may be eliminated using equation [II-45]. And for no volume flow, a pressure difference given by the first of equations [II-49] arises as a consequence of the temperature difference and J_q becomes

$$J_q = \left[(L_{PT} - L_{PE} L_{ET}/L_E)^2 / (L_P - L_{PE}^2/L_E) - (L_T - L_{ET}^2/L_E) \right] dT/T \qquad [II-51]$$

The thermal conductivity under these conditions is

$$k_T = -(L_{PT}-L_{PE}L_{ET}/L_E)^2/(L_P-L_{PE}^2/L_E) + (L_T-L_{ET}^2/L_E) \qquad [II-52]$$

If the terms concerning the pressure are negligible (see page 184) and k_T is independent over a finite range T to $T + \Delta T$, then reasoning analogous to that leading to equation [II-47] gives

$$k_T = (L_{qq} - \sum_{i,j=1}^{r} Q_i Q_j L_{ij})\ell/T \qquad [II-53]$$

The thermal conductivity defined here is called the "external" thermal conductivity by Haase [13], a definition which will be examined in more detail below.

(iv) Heterogeneous Membranes

Kedem and Katchalsky [46] have considered electrical conductivities in membranes composed of series and parallel elements, under very general conditions where net volume flow may or may not occur. For the case of no volume flow, their equations take on the simple forms expected for electrical resistors in series or parallel.

Suppose a membrane is made up of p homogeneous elements that are parallel to the direction of the flow. Of a total cross-sectional area A, the r^{th} element has an area A_r. The total current is the sum of the individual currents i_r, so that the total current per unit area is

$$I = \sum_{r=1}^{p} i_r/A = \sum_{r=1}^{p} A_r I_r/A = \sum_{r=1}^{p} \sigma_r I_r, \qquad [II-54]$$

where σ_r is the fraction of the surface occupied by element r. Since the elements are in parallel, the voltage across each one is identical and equation [II-47] becomes, for each element

$$\kappa_r = F^2 \ell \sum_{j,k=1}^{n} z_j z_k L_{jk} dE, \qquad [II-55]$$

and from equations [II-54] and [II-55],

$$\kappa_p = \sum_{r=1}^{p} \sigma_r \kappa_r, \qquad [II-56]$$

where κ_p is the total conductivity across this membrane.

If the conductivity is measured at right angles to the previous direction, it will become a series of layers. If there are s layers in series in any membrane, each with a thickness ℓ_r, then the total potential difference will be the sum of the potential differences across each element r. The current densities will be the same since the cross-sectional area of each element is identical and it is assumed that there are no contact effects at the ends of the elements. Then, using equation [II-47], the result for each element is

$$I/F = - \sum_{j,k=1}^{n} z_j z_k L^r_{jk} dE_r, \qquad [II-57]$$

and

$$\kappa_{sr} = F^2 \ell \sum_{j,k=1}^{n} L^r_{jk} dE_r \qquad [II-58]$$

where κ_{sr} is the conductivity of the r^{th} element. Using equation [II-57], the total series electrical conductivity is given as

$$1/\kappa_s = \sum_{r=1}^{s} \lambda_s/\kappa_{sr} = \sum_{r=1}^{s} \ell r/\ell \kappa_{sr} \qquad [II-59]$$

where κ_s is the fraction of the total length of the membrane that is occupied by element r.

These results suggest that an anisotropy of the electrical conductivity of a membrane can be caused by the existence of layers of different conductivity. This anisotropy can be characterized by measuring the electrical conductivity in perpendicular directions.

(v) Other Transport Coefficients for Membranes

For flows of charged (ionic) constituents, the mass transport number t_k of constituent k can be defined as the flux of k divided by the total flux of charge:

$$t_k = J_k / \sum_{i=1}^{r} z_i J_i , \qquad dP = dT = d\mu_i = 0, \; i = 1,2....r \qquad [II-60]$$

With the use of this equation, along with equation [II-44], equation [II-42] becomes

$$I/F = - \sum_{k=1}^{r} t_k (d\tilde{\mu}_k(T) + (Q^*_k + h)\, dT/T - L_E F dE . \qquad [II-61]$$

This equation can be used to eliminate dE from the flux equation to give

$$J_i = t_i I/F - \sum_{k=1}^{r} M_{ik} (d\tilde{\mu}_k(T) + (Q_k^* + h)\, dT/T) \qquad [II-62]$$

and

$$J_q = \sum_{k=1}^{r} t_k Q_k I/F - \sum_{j,k=1}^{r} Q_k M_{kj} (d\tilde{\mu}_k(T) + (h-h_k)\, dT/T)$$

$$- (L_{qq} - \sum_{j,k=1}^{r} Q_j Q_k t_j t_k L_E)\, dT/T \qquad [II-63]$$

where

$$M_{ij} = L_{ij} - t_i t_j L_E = M_{ji} \qquad [II-64]$$

These equations will be used below in the discussion of ionic mobilities.

(b) Continuous Systems

(i) General Relations

When considering transport through membranes from the point of view of discontinuous systems, the membrane was treated as a "black box" in which the details of the transport processes occurring inside it were not considered. If we wish to look at processes inside the membrane, two extra features are needed. First, a suitable model must be constructed which contains sufficient detail to account for observed phenomena. Secondly, a general theory which describes the behaviour with time of a "macroscopic" element

of the volume in the system must be set up. This volume element contains a large enough number of molecules that its motion in time can be considered to be continuous, and will be called a "hydrodynamic" volume element.

From the equations of conservation of mass, of balance of forces and of energy flow in such a system, plus the use of the Gibbs equation, the rate of production of entropy and the equations for the flux of matter and heat can be derived in forms analogous to the equations found above for discontinuous systems. Three important differences appear, however. First, gradients replace differences, so that the forces causing flows are the local values of the gradients of chemical potential, pressure, temperature and electrical potential at given locations in the system. Secondly, the fluxes of matter are defined relative to the motion of the centre of mass of the system:

$$\underline{J}_i = c_i(\underline{v}_i - \underline{v}), \qquad i = 1,2.....r, \qquad \text{[II-65]}$$

where c_i and $\underline{v}_i$ are the concentration and velocity of substance i, and $\underline{v}$ is the velocity of the centre of mass of the system:

$$\underline{v} = \sum_{i=1}^{r} c_i\underline{v}_i / (\sum_{i=1}^{r} c_i). \qquad \text{[II-66]}$$

It should be noted that $\underline{J}_i$, $\underline{v}_i$, and $\underline{v}$ are vectors. Thirdly, the coefficients L_{ij}, in the analog to equation [II-39],

$$J_i = -\sum_{k=1}^{r} L_{ik}(\nabla\tilde{\mu}_k(T) - h_k\nabla T/T) - L_{iq}\nabla T/T , \qquad [II-67]$$

are local values which hold for flows measured relative to the centre of mass only. The term in h is dropped from equation [II-67] because of the definition of the heat flow in a continuous system [43].

If mechanical equilibrium is established rapidly in comparison with other processes, then a general theorem (Prigogine's theorem) shows that the rate of production of entropy due to irreversible processes is independent of the choice of reference velocity [29]. Thus, fluxes

$$\underline{J}_i^r = c_i(\underline{v}_i - \underline{v}_r) , \qquad [II-68]$$

may be used in conjunction with a convenient choice of $\underline{v}_r$. For ease in relating the theory to experimental results, $\underline{v}_r$ is chosen to be zero relative to the coordinates of the laboratory; that is, in membrane systems, $\underline{v}_r$ is taken to be the velocity of the membrane, which in most cases is zero relative to the laboratory. Prigogine's theorem requires some modification if the temperature difference across the membrane is not zero, but holds rigorously if a modified heat flux

$$\underline{J}'_q = \underline{J}_q - \sum_{i=1}^{r} h_i\underline{J}_i , \qquad [II-69]$$

is used in place of $\underline{J}_q$. The expression for the rate of

entropy production is unchanged by using this transformed heat flux. If there are no fluxes of matter present, then $\underline{J}'_q = \underline{J}_q$. The flow equations can now be put into a particularly useful form:

$$\underline{J}_i^r = c_i(\underline{v}_i - \underline{v}_r)$$

$$= -\sum_{j=1}^{r-1} L_{ij}^r(\nabla\tilde{\mu}_j(T) + Q_j^*\nabla T/T) \qquad i = 1,2,\ldots r-1 \quad \text{[II-70]}$$

$$\underline{J}'_q = \sum_{j,k=1}^{r-1} L_{jk}^r(Q_k^* + h_k)\nabla\tilde{\mu}_k(T) - (L_{qq} + \sum_{j,k=1}^{r-1} h_j Q_k^* L_{jk})\nabla T/T \quad \text{[II-71]}$$

Note that the coefficients L_{ij}^r and Q_j^* have values that depend on the choice of the frame of reference.

(ii) Measurement of Electrical and Thermal Conductivities

By definition, and using equations [II-70] and [II-71] for continuous systems, the local electrical conductivity is

$$\kappa = -\underline{I}/\nabla E = F^2 \sum_{j,k=1}^{r-1} z_j z_k L_{jk}^r = F^2 L_E^r$$

$$\nabla\mu_i = \nabla P = \nabla T = 0, i=1,2,\ldots n, \quad \text{[II-72]}$$

and the thermal conductivity is

$$k_T = -\underline{J}'_q/T = L_{qq} - \sum_{j,k=1}^{r} Q_j Q_k^* L_{jk}$$

$$J_i = 0, \qquad i = 1,2,\ldots r. \quad \text{[II-73]}$$

Since the electric current is defined as

$$\underline{I} = F \sum_{i=1}^{r} z_i \underline{J}_i = F \sum_{i=1}^{r} z_i c_i (\underline{v}_i - \underline{v}_r) , \qquad [II-74]$$

then for electrolyte systems in general, with $z_r = 0$ (that is, the charge of the frame of reference, usually the solvent), conservation of charge gives the relation

$$\sum_{i=1}^{r} z_i c_i = 0 , \qquad [II-75]$$

so that the current density, and hence the electrical conductivity is independent of the choice of the frame of reference. In a membrane, however, the membrane matrix carries the charge $z_r c_r$, so that

$$z_r c_r + \sum_{i=1}^{r-1} z_i c_i = 0 . \qquad [II-76]$$

Thus, from equation [II-71], using the velocity of the membrane $\underline{v}_r$ as the reference velocity,

$$\underline{I} = F \sum_{i=1}^{r-1} z_i c_i (\underline{v}_i - \underline{v}_r)$$

$$= F \sum_{i=1}^{r-1} z_i c_i \underline{v}_i \qquad [II-77]$$

if $\underline{v}_r = 0$. The transport coefficients will always refer to a frame of reference fixed on the membrane. L_{qq} however, does not involve the frame of reference.

The conductivities defined above are local values, or "internal" conductivities according to Haase [13]. Their

relation to the external quantities, which are the quantities accessible to experiment, will be discussed in section (c), (ii) below.

(iii) Flows Relative to the Solvent: Convective Contributions

Sometimes two reference velocities are used in describing transport in membranes. This choice has been discussed extensively (see the summary by Helfferich [47]) but in a less general way than given here.

In aqueous electrolyte systems, ionic mobilities (related to the phenomenological coefficients in section (d)) are almost always referred to the solvent water as a frame of reference, and tabulated values are almost invariably referred to this frame. Let us suppose that, in a membrane, the mobilities retain their values relative to the solvent. Since the solvent can move relative to the membrane, the mobilities measured relative to the membrane will be equal to the mobilities in free solution plus a correction factor for the "convection" of the solvent. Of course, equality of the mobilities in the membrane (even if they were referred to the solvent) and in the external solution would not be expected to hold unless the paths and interactions of ions in the membrane were essentially those

in bulk solvent. However, no assumptions of this kind are necessary in a general description of these so-called "convection" contributions to transport coefficients.

Let component r be the membrane, and component o be the single solvent. Then equation [II-65] becomes

$$\underline{J}_i^r = c_i(\underline{v}_i - \underline{v}_r) \qquad \text{[II-78]}$$

and

$$\underline{J}_i^o = c_i(\underline{v}_i - \underline{v}_o) \qquad \text{[II-79]}$$

so that

$$\underline{J}_i^r = \underline{J}_i^o + \underline{J}_o^r\, c_i/c_o \qquad \text{[II-80]}$$

and

$$\underline{J}_r^r = \underline{J}_r^o + \underline{J}_o^r\, c_r/c_o = \underline{0} \qquad \text{[II-81]}$$

where the superscript r refers to the membrane as the reference frame, the superscript (or subscript) o refers to the solvent, and

$$\underline{J}_o^r = c_o(\underline{v}_o - \underline{v}_r) \qquad \text{[II-82]}$$

Since, from equations [II-3], [II-32] and [II-33]

$$\underline{J}_i^r = -\sum_{j=1}^{r-1} L_{ij}^r\, \nabla\tilde{\mu}_j(T) + L_{iq}^r\, \nabla T/T \qquad \text{[II-83]}$$

where the summation does not include the membrane phase r and similarly

$$\underline{J}_i^o = -\sum_{j=1}^{r-1} L_{ij}^o\, \nabla\tilde{\mu}_j(T) + L_{iq}^o\, \nabla T/T \qquad \text{[II-84]}$$

where the solvent does not enter the summation, therefore, from equations [II-83], [II-84] and [II-81],

$$- \sum_{j=1}^{r} L_{ij}^{r} \nabla\tilde{\mu}_j(T) - L_{iq}^{r} \nabla T/T = - \sum_{j=1}^{r} L_{ij}^{o} \nabla\tilde{\mu}_j(T) - L_{iq}^{o} \nabla T/T$$

$$- \sum_{j=1}^{r} L_{oj}^{r} \nabla\tilde{\mu}_j(T) - L_{oq}^{r} \nabla T/T \qquad [II-85]$$

Therefore, take

$$L_{iq}^{r} = L_{iq}^{o} + L_{oq}^{r} \qquad [II-86]$$

$$L_{ij}^{r} = L_{ij}^{o} + L_{ij}^{r} \qquad [II-87]$$

For the case of electrical conductivity, the conductivities relative to the membrane and the solvent are

$$\kappa^{r} = F^2 \sum_{i,j=1}^{r-1} z_i z_j L_{ij}^{r} = F^2 L_E^{r} \qquad [II-88]$$

$$\kappa^{o} = F^2 \sum_{i,j=1}^{r-1} z_i z_j L_{ij}^{o} \qquad [II-89]$$

so that

$$\kappa^{r} = \kappa^{o} + F^2 \sum_{i,j\neq r}^{r-1} z_i z_j c_i L_{oj}^{r}/c_o \qquad [II-90]$$

But, equation [II-60] gives

$$\sum_{j=1}^{r-1} z_j L_{oj}^{r} = t_o L_E^{r}, \qquad [II-91]$$

and from equation [II-76], using $z_r c_r$ as the charge on the membrane in this case, equation [II-89] becomes

$$\kappa^{r} = \kappa^{o} - F^2 z_r c_r t_o L_E^{r}/c_o = \kappa^{o} - z_r c_r \kappa^{r} t_o^{r}/c_o \qquad [II-92]$$

For a cation exchange membrane, z_r is negative, and t_o^r is almost always positive. Thus, the conductivity relative to the membrane will be larger than that relative to the solvent by the term $-z_r c_r \kappa^r t_o^r / c_o$, called the "convection conductivity" [47].

The situation with L_{qq} is much more complicated because of the way the heat flow is defined.

(c) Mobilities in Membranes

In general, the mobility of a species i is defined as the velocity of i per unit potential gradient. We shall consider electrical mobilities u_i^E first. Thus, for $\nabla P = \nabla T = \nabla \mu_i = 0$,

$$u_i^r = -(\underline{v}_i - \underline{v}^r)/\nabla E \qquad \text{[II-93]}$$

Dividing the top and bottom of this equation by c_i, and using the definitions of $\underline{J}_i$ and the transport number t_i, the result obtained is

$$u_i^r = t_i^r L_E F/c_i = t_i^r \kappa^r / F c_i . \qquad \text{[II-94]}$$

As above, the mobility relative to the membrane can be considered to be made up of a mobility relative to the solvent plus a convective contribution:

$$\begin{aligned} u_i^r &= u_i^o + \sum_j z_j L_{oj}^r F/c_o \\ &= u_i^o + t_o^r \kappa^r / F c_o \\ &= u_i^o + u_o^r \end{aligned} \qquad \text{[II-95]}$$

From this follows the very important relation

$$u_r^o + u_o^r = u_r^r = 0 \qquad \text{[II-96]}$$

that is, the mobility of the solvent relative to the membrane is equal and opposite to the mobility of the membrane relative to the solvent. If, for example, theoretical expressions or experiment give the mobility of a polyelectrolyte molecule in solution as independent of molecular weight, then the mobility of water in a membrane composed of the polyelectrolyte should be equal and opposite, if other effects such as cross-linking of the molecules to form the membrane are negligible.

Completely analogous results hold for the thermal mobility, u_{iq}.

(d) Relations between Discontinuous and Continuous Systems

If linear relations between local fluxes and forces at a point inside a membrane can be written, and similar relations can be written for a membrane phase of arbitrary size using fluxes and forces measured in the phases external to the membrane, the two descriptions should be related. Theoretical investigations of the relations between the continuous and discontinuous descriptions have been described by Kirkwood [5], de Groot and Mazur [30] and

Caplan and Mikulecky [32]. We take a simplified point of view here.

Consider a system composed of a circular capillary connecting two reservoirs. The reservoirs are at different temperatures, pressures and compositions, and the capillary walls carry fixed charges. If the diameter of the capillary is large compared to molecular dimensions, the concept of a hydrodynamic volume element at a point inside the capillary is valid, and local fluxes and forces can be defined. Axial gradients of temperature, pressure and composition will exist in the capillary. Radial gradients will also exist, because of the electrical double layer. If there is local thermodynamic equilibrium at any cross-section of the capillary, the flux observed externally will be the total flux over any cross-section of the capillary, under steady-state conditions, and the axial concentration gradient will be

$$\partial \bar{c}_i / \partial x = dc_i / \ell \qquad \text{[II-97]}$$

where $\bar{c}_i$ is the average concentration across the capillary, x is measured along the length ℓ of the capillary, and dc_i is the <u>infinitesimal</u> difference in external concentration across the capillary. Similar equations hold for the average local pressure, temperature and electrical potential.

The "external" L_{ij} is then related to an average $L_{ij}^{(i)}$, averaged over a radial plane in the capillary, by

$$\ell L_{ij} = L_{ij}^{(i)} \qquad \text{[II-98]}$$

Similar considerations will hold for membranes of structure more complex than a single capillary.

If the external difference in concentration is finite, then equation [II-98] no longer holds, and we can no longer expect the fluxes observed externally to be linear functions of the forces measured externally.

If a steady state does not exist, but thermodynamic equilibrium is established rapidly at any given cross-section of the capillary relative to the relaxation time for the transport processes which are taking place, the average coefficients $L_{ij}^{(i)}$ are of use, and equation [II-98] should again hold for infinitesimal external differences.

For heterogeneous membranes, equation [II-98] can be written for each homogeneous part. If the diameter or length of the capillary is so small that the concept of a hydrodynamic volume element is no longer valid, the discontinuous description of transport processes is the only useful one.

Equation [II-98] may be used to relate "external" and "internal" mobilities, provided these quantities are

independent of the magnitude of the "external" forces; i.e. if measurements are made so that the electrical mobility, for example, is obtained for the limit $dE \rightarrow 0$.

(e) The Onsager Relations

Two points of view may be taken concerning the Onsager reciprocal relations. They may be considered as postulates to be checked experimentally. Evidence for the correctness for electrokinetic and other electrochemical processes has been reviewed by Miller [42]. The reciprocal relations can also be deduced from theory. Onsager's proof [41] assumed: (1) microscopic fluctuations as the ultimate source of irreversible phenomena; (2) the time symmetry of physical laws (principle of microscopic reversibility); (3) the relaxation of microscopic fluctuations is described by macroscopic phenomenological laws. The third assumption of Onsager has been criticized, and alternate derivations based on the master equation of irreversible statistical mechanics [48] and on the fluctuation-dissipation theorem [49] have been described.

3. Microscopic Theories of Transport in Membranes

(a) Double Layer Theories

The simplest microscopic picture of a membrane is a random collection of polymer chains carrying fixed charges, with counter-ions and co-ions near the chains. Even this model is difficult to describe mathematically, and several more specific models have been proposed.

Kobatake and Fujita [37] assumed that the membrane could be represented by a capillary with fixed charges on its walls, while Deryagin and his co-workers [39] used a slit instead of a capillary. Both solved the linearized Poisson-Boltzmann equation, and used a mixture of thermodynamic and hydrodynamic theory to calculate the transport coefficients. The condition that the concentration of mobile ions in the capillary or slit is much greater than the concentration of fixed charges was also used. This condition, along with the linearized Poisson-Boltzmann equation, makes their calculation of interest only for membranes of very low charge density.

Dresner [36] used the rigorous solutions of the non-linear Poisson-Boltzmann equation for a capillary and for a charged rod to make similar calculations, but assumed a salt-free membrane; i.e., one with only fixed charges and

counter-ions present. These computations still require rigorous comparison with experiment.

Double layer theories are closely connected with the theory of the equilibrium properties of membranes. The simplest equilibrium theory, that of Donnan (see Introduction) has been modified by including double layer contributions and contributions from the elastic free energy of the polymer network. One such theory is that of Rice and Harris [50]. This aspect of ion exchange has been reviewed by [51].

(b) Activated Transport Theories

Danielli [52] and Eyring and his co-worker [53] have discussed the application of the theory of absolute reaction rates to transport in membranes. For a brief review, see [19]. The phenomenological coefficients L_{ij} become combinations of rate constants in this theory, and little is gained except for a rather more pictorial concept of transport.

(c) Thermal Conductivity

Haase [13] has discussed models for the interpretation of the thermal conductivity in systems consisting of a membrane and a non-electrolyte, and a few tentative measurements have been correlated with theory. No theory or measurements for electrolyte membrane systems have been

developed, but data and qualitative theories for solid high polymers [12] may be useful additional guides.

CHAPTER III

GENERAL EXPERIMENTAL METHODS

1. Types of Membranes

(a) Polyvinylbenzenesulfonate membranes

The membranes of this type used were described by Brydges, Dawson and Lorimer [4]. Data for the membranes used are given in Table [III-1]. The density and heat capacity were determined for membranes equilibrated in conductivity water.

Before a membrane was used for a measurement, it was soaked for several days in the potassium chloride solution which was to be used in the measurement. This was done in order to equilibrate the membrane with that particular solution. When a membrane was to be used for measurement at a different concentration of electrolyte, it was first removed from the old solution, any excess solution on its surface was wiped off using tissue ('Kimwipe') and it was then soaked for several days in several changes of the new solution.

(b) Cellulose membranes

Textile cellulose, 8 percent by weight cellulose (degree of polymerization 250) was supplied by Courtaulds (Canada) Limited, Cornwall, Ontario. The method used for the preparation of the cellulose membranes was similar to the one described by Lorimer, Boterenbrood, and Hermans [21]. The mold consisted of a Plexiglass ring placed between two porous porcelain plates. The ring was placed on one of the porcelain plates (presoaked in conductance water in order to remove any air bubbles) and viscose was poured into the resulting container. Any air bubbles in the viscose were then removed and the second porcelain plate, again presoaked in conductance water, was carefully placed on top of the Plexiglass ring, making sure that no air bubbles were introduced in the process. This assembly was immersed in an ammonium sulfate solution, 15 percent by weight, for 24 hours, when coagulation of the cellulose had taken place. The cellulose membrane was then removed from the mold and boiled in another portion of the same solution for 15 minutes. The resulting product was then washed with conductivity water to remove the previous solution. Cellulose membranes of various thicknesses and diameters were prepared by changing the dimensions of the Plexiglass ring used in the mold. The

membranes of this type used in this work are shown in Table III-2].

The preparation of these membranes for use in measurements was the same as that used for the polyvinylbenzenesulfonate membranes in the preceding section. All cellulose membranes used were prepared from the same sample of Textile viscose.

(c) Porous Glass Membranes

Porous glass sheets (Corning type 7930 porous Vycor) were supplied by the Corning Glass Company, Corning, New York. All samples supplied were 0.48 cm thick. Two different methods were used to cut circular sections from the sheets. In one method a rotating table was used and an abrasive cutter was clamped above it. When the table was rotated, the blast of abrasive from the nozzle of the instrument provided a circular cut of the desired size. A motor was used to turn the table so that the cut would be uniform. Circular pieces were also cut using a glass drill.

Glass cutting equipment was also used in order to cut the sheets parallel to their faces so that pieces of different thicknesses could be obtained. The membranes were then cleaned by warming them in a solution containing nitric acid and a small amount of potassium chlorate [54].

TABLE [III-1]

PHYSICAL CHARACTERISTICS OF POLYVINYLBENZENESULFONATE MEMBRANES

NUMBER	THICKNESS	CAPACITY*	WATER CONTENT*	HEAT CAPACITY†	DENSITY‡
	cm	meq/g dry	g/g dry	$J\ g^{-1}$	$g\ cm^{-3}$
1	0.163	1.72	0.856	0.599	1.123
8	0.058	1.74	0.500	0.567	1.166
9	0.056	1.77	0.788	0.636	1.140
11	0.065	2.47	1.358	0.724	1.128
12	0.076	2.24	0.710	0.620	1.181
13	0.061	2.30	0.826	0.644	1.156
17	0.051	1.03	0.232	0.472	

* i.e. for 1 g of dry membrane in the H^+-form.

† for 1 g of water-swollen membrane in the K^+-form.

‡ for 1 cm^3 of water-swollen membrane in the K^+-form.

TABLE [III-2]

DIMENSIONS OF CELLULOSE MEMBRANES

(water-swollen)

NUMBER	THICKNESS	DIAMETER
	cm	cm
1	0.112	2.50
2	0.183	2.50
3	0.232	2.50
4	0.315	2.50

As with the other types of membranes described previously, the porous glass membranes were equilibrated in the appropriate potassium chloride solutions for 24 hours before any measurement was taken.

The apparent capacity of porous glass was estimated by discontinuous acid-base titration [55] and was found to be 0.023 meq/gm of water-saturated glass at pH 6, which is approximately the pH of solutions equilibrated with atmospheric CO_2.

2. Apparatus

(a) Water

Water was obtained during the first part of this research from the regular city supply and later from a predistilled supply on tap, which had an electrical conductivity of about $2 \times 10^{-5}\ \Omega^{-1}\ cm^{-1}$. In both cases, this water was redistilled using a Corning water still (model AG-2). The final product, which was used in the preparation of all solutions, had an electrical conductivity in the range of $1 - 2 \times 10^{-6}\ \Omega^{-1}\ cm^{-1}$:

(b) Solutions

Quantities of reagent grade potassium chloride were recrystallized once from conductivity water prepared

above and dried at 150°C for 24 hours. It was then placed in a platinum crucible which had been previously heated under an atmosphere of dry nitrogen to constant weight in a tube furnace. The potassium chloride was then fused in the same furnace under a stream of dry nitrogen. The crucible and its contents were then cooled in a desiccator and then were weighed on a Mettler (model H) balance, previously used for weighing the crucible alone.

One litre flasks were fitted with male glass joints. Glass caps would then fit over these to seal the container. These flasks were washed with conductivity water and dried at 110°C whenever they were recharged with new solution.

The amount of conductivity water required to give the desired concentration, calculated by the method below, was added to the flask. This amount was determined by weight using a Mettler top loading balance (model K7), weighing the water inside the solution flask. The crucible containing the potassium chloride was then added, forming a solution of the proper concentration.

The weight of the water required for one litre of solution is given to a sufficiently good approximation by

$$W = (1000 - \bar{V}_{KCl} C)\rho_w , \qquad [III-1]$$

where $\bar{V}_{KCl}$ is the partial molar volume of potassium chloride, C its molar concentration and ρ_w the density of water. The observed weight of water is given by

$$W_{obs} = W - (0.880)\rho_a \bar{V}_w \qquad [III-2]$$

taking the density of the balance weights, ρ_a, as 8.4 g cm^{-3} as is specified in the Mettler balance instructions. The partial molar volume of potassium chloride was taken from MacInnes [56]. The density of water at 25°C and that of moist air was taken from the Handbook of Chemistry and Physics (45th edition, pages 2129 and 2136 respectively).

The potassium chloride was fused in quantities of such a size that about 650 cm^3 of solution resulted. The concentrations were reproducible to ± 0.01 percent when measured by conductivity. This accuracy was confirmed by the reproducibility of the results using solutions made at different times.

(c) Thermostats

Glass tanks with a capacity of about 20 litres were used as containers for the constant temperature baths. Two types of circulators were used to control the temperature: a Bronwill Constant Temperature Circulator made by Bronwill Scientific Division, Will Corporation; and a Haake-Universal-

Thermostat Unitherm, Haake Corporation K. G., Berlin. These circulators were used interchangeably and their performance was found to be equivalent.

The temperature could be maintained constant to within 0.01°C. The cells were either equilibrated with the thermostatic bath or constant temperature water from the thermostatic bath was circulated through them, using the pumping facility on the circulator. In this case, the water was first passed through copper tubing within the bath in order to ensure that small local temperature variations caused by the heater of the circulator were removed. For the thermal conductivity cell, an auxilliary pump was used to ensure an adequate flow of water at constant temperature. This pump was placed in the line after the cell so that it would not affect the temperature of the water.

(d) Resistance Measurements

The resistance measurements were made using a Janz-McIntyre bridge [57] which incorporated a General Radio Company Impedance Comparator, type 1605-AS5 for the ratio arms, power supply and phase-sensitive detector. The variable arm of the bridge was composed of precision decade resistors varying in value from steps of 0.01 ohms to steps of 10,000 ohms. The bridge was calibrated by measuring the

resistances of several type 500 (General Radio Company, Concord, Mass.) standard resistors, which, in turn, had been compared with Leeds and Northrup Company standard resistor number 1594832 in a direct current potentiometer circuit. The results are shown in Table [II-3]. The accuracy of the resistors was found to be always better than 0.01 percent. A four leads method [58] was used when experimental measurements were being taken to insure that any resistance due to the leads to the cell would be cancelled out.

(e) Temperature Measurement

Copper-constantan thermocouples were used for temperature measurement in the thermal conductivity cell [59]. To prepare the thermocouple, the insulation was stripped from the end of each wire, the ends were wound together, and a small amount of soft solder applied to hold them. The voltage drop was measured with a Sargeant recorder, model SR, placed in the copper side of the thermocouple.

All thermometers and thermocouples were calibrated against a 0.01 degree mercury-in-glass thermometer certified by the National Bureau of Standards.

CHAPTER IV

ELECTRICAL CONDUCTIVITY PERPENDICULAR TO THE MEMBRANE SURFACE

1. Theory

Most attempts to measure the electrical conductivity of a membrane normal to its surface have inherent inaccuracies. This has been caused by the failure to take into account the "overlap" of the membrane surface with the measuring cell. That is, when a membrane is placed between two electrodes, its diameter is made larger than that of the electrode chambers so that it can be supported directly between them. The part of the membrane which is not directly between the electrodes will cause a distortion of the current lines [60]. This causes a lowering of the resistance across the cell. Therefore, the results will produce a value for the electrical conductivity that is higher than the actual value.

It is very difficult to cut a membrane in such a way that it is exactly the same size as the measuring electrode. If it is slightly smaller at any point, errors due to the leakage of current past the membrane may be very important. It may also not be desirable to do so if contact between the membrane and the electrodes is not wanted.

Therefore, if the overlap is to be accounted for, it should be done so mathematically. This problem has been solved for the type of apparatus used in this research by Barrer, Barrie and Rogers [24] using methods described by Tranter [61]. The boundary conditions for the problem are shown in Figure [IV-1] on a cross-section of a cylindrically symmetrical membrane. The electrodes are situated at $z = 0$ and $z = 1$ and extend from $r = 0$ to $r = a$. The shaded areas are the boundaries of the membrane.

The major difficulty in solving the equations for this system lies in the mixed boundary condition along the surface of the membrane. If a constant flux is assumed along the membrane surface, the concentration will vary with r. But if the concentration is taken to be constant, the flux will vary with r. The problem is to apply both conditions simultaneously. The problem is treated by first obtaining a solution of Laplace's equation using the boundary condition of constant flux per unit area to derive an expression for the mean concentration over the face $z = 1$. This result can then be related to this constant concentration C [24].

The solution of the problem gives the following result for the resistance across the cell:

$$R = [\ell/\pi a^2 \kappa][1 - 16Sn/\pi^2] \qquad [IV-1]$$

where ℓ is the thickness of the membrane sample, a is the radius of the electrodes and κ is the electrical conductivity of the membrane. The quantity Sn is defined by the following equation;

$$Sn = \sum_{q=1,3,5,\ldots}^{\infty} \frac{1}{q^2} \left(\frac{I_1(q\alpha)}{K_1(q\alpha)}\right) [I_1(q\beta)K_1(q\alpha) - I_1(q\alpha)K_1(q\beta)] \qquad [IV-2]$$

in which $I_1(x)$ and $K_1(x)$ are modified Bessel functions of the second kind with argument x and

$$\alpha = \pi a/\ell, \qquad \beta = \pi b/\ell. \qquad [IV-3]$$

The quantity q is an index which takes all odd values of the positive integers.

Equation [IV-1] makes it possible to calculate the resistance across the membrane from its electrical conductivity. If, however, there is an electrode chamber between the electrode and the membrane that has been filled with electrolyte, then there will be an extra resistance that must be added to the result. In this case, equation [IV-1] becomes

$$R = R_o + l_{eff}/[\pi a^2 \kappa] \qquad [IV-4]$$

where R_o is this extra resistance and l_{eff} is the effective

FIGURE [IV-1]

ELECTRICAL CONDUCTIVITY CELL

BOUNDARY CONDITIONS

FOR

THEORY

The cell is cylindrically symmetrical in r.

The hatch marks designate the outer edge of the cell, and the broken lines represent the electrodes.

FIGURE [IV-1]

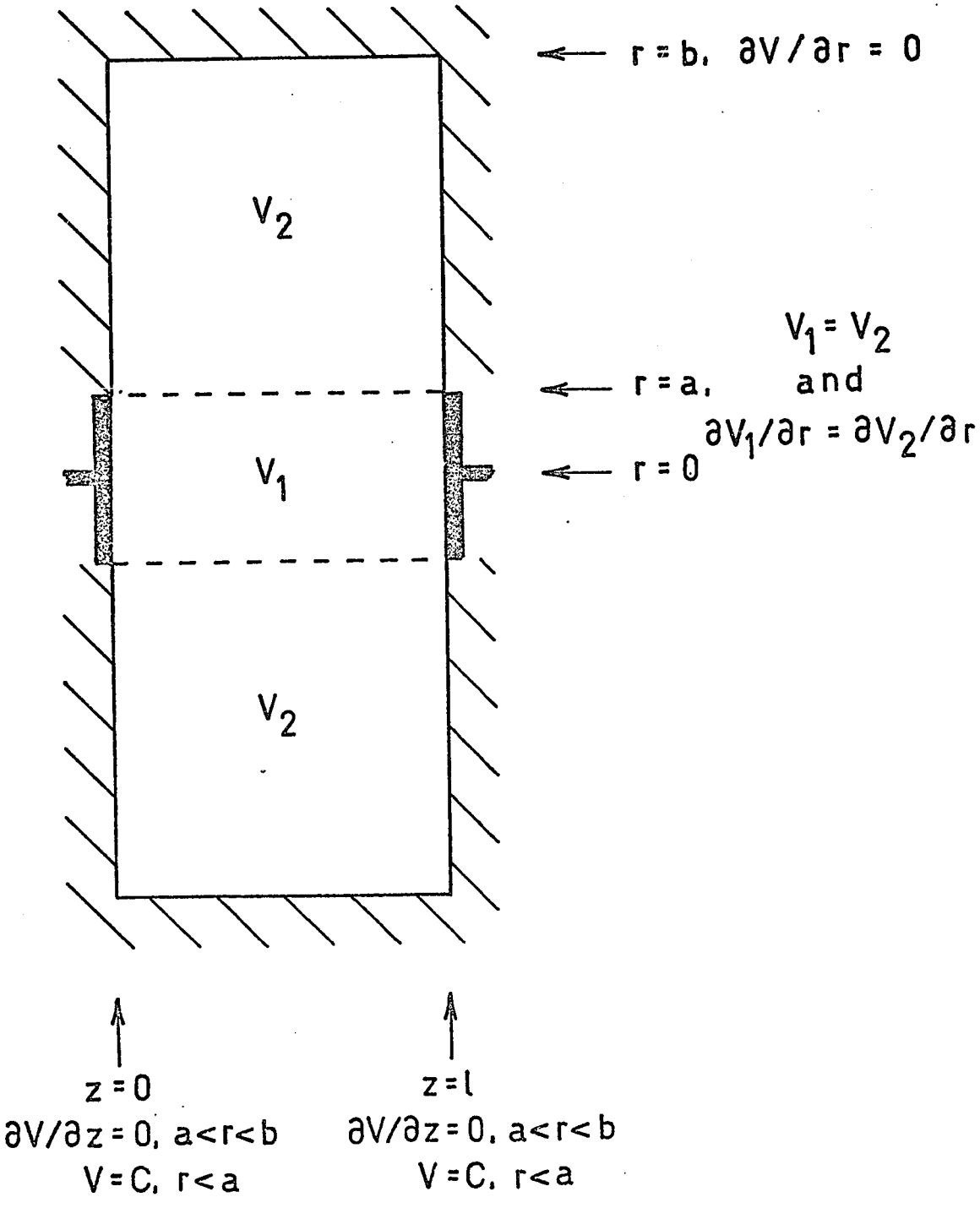
r = b, ∂V/∂r = 0
V2
V1 = V2
r = a, and
∂V1/∂r = ∂V2/∂r
V1
r = 0
V2
z = 0
∂V/∂z = 0, a<r<b
V = C, r<a
z = l
∂V/∂z = 0, a<r<b
V = C, r<a

thickness of the sample and is defined, from equation [IV-1] as

$$l_{eff} = l(1 - 16Sn/\pi^2) . \qquad [IV-5]$$

This addition to the theory involves an approximation because the theory has been derived with the electrodes in contact with the membrane surface. It can be expected that the error introduced in the result will be small if either the thickness of the electrode chamber is small in comparison to the thickness of the membrane, or the resistance of the electrode chamber is small compared to that of the membrane. In both of these cases, the extra resistance R_o will be small compared to the total resistance across the cell.

From equation [IV-4] it can be seen that a plot of the resistance across the membrane against the effective thickness of the membranes as calculated from the theory should give a straight line whose slope, m, is proportional to the inverse of the electrical conductivity:

$$m = 1/\pi a^2 \kappa , \qquad [IV-6]$$

and whose intercept, R_o, is the resistance across the electrode chambers of the cell.

2. General Experimental Methods

Each cell design used was similar and a common method was used for the confirmation of the validity of the theory, and the acquisition of data.

Plexiglass test rings, similar to those used by Lorimer et al, [21] were manufactured in order to test the operation of each cell. There were twelve rings, three of which had approximately the same thickness (ℓ), in four different diameters (b). These dimensions are shown in Table [IV-1].

When a measurement was to be made, the appropriate test ring was placed into the cell and the two halves of the cell fitted together on an O-ring seal. The basic design of all cells is shown in Figure [IV-2] and is similar to the design used by Lorimer et al [21]. The major variations from the basic design are in the region of the electrodes. The inside of the ring was filled with potassium chloride solution of known concentration, either using filler holes into the electrode chambers, or by adding the solution before the cell was fitted together. Great care was taken to ensure that no air bubbles were trapped inside the test ring. The resistance across the cell could then be measured and the results from several test rings plotted against

TABLE [IV-1]

DIMENSIONS OF TEST RINGS

NUMBER	THICKNESS (cm)	RADIUS (cm)
1A	0.187	1.907
1B	0.250	1.904
1C	0.293	1.906
1D	0.460	1.903
2A	0.181	1.271
2B	0.249	1.270
2C	0.290	1.271
2D	0.472	1.270
3A	0.182	0.633
3B	0.246	0.633
3C	0.292	0.633
3D	0.462	0.631

FIGURE [IV-2]

ELECTRICAL CONDUCTIVITY

BASIC CELL DESIGN

The body of the cell was constructed of Plexiglass. The grooves in the cell faces were accurately machined in order to accommodate O-rings used for sealing the cell and for preventing leakage from the electrode chambers between the membrane and the cell face.

FIGURE [IV-2]

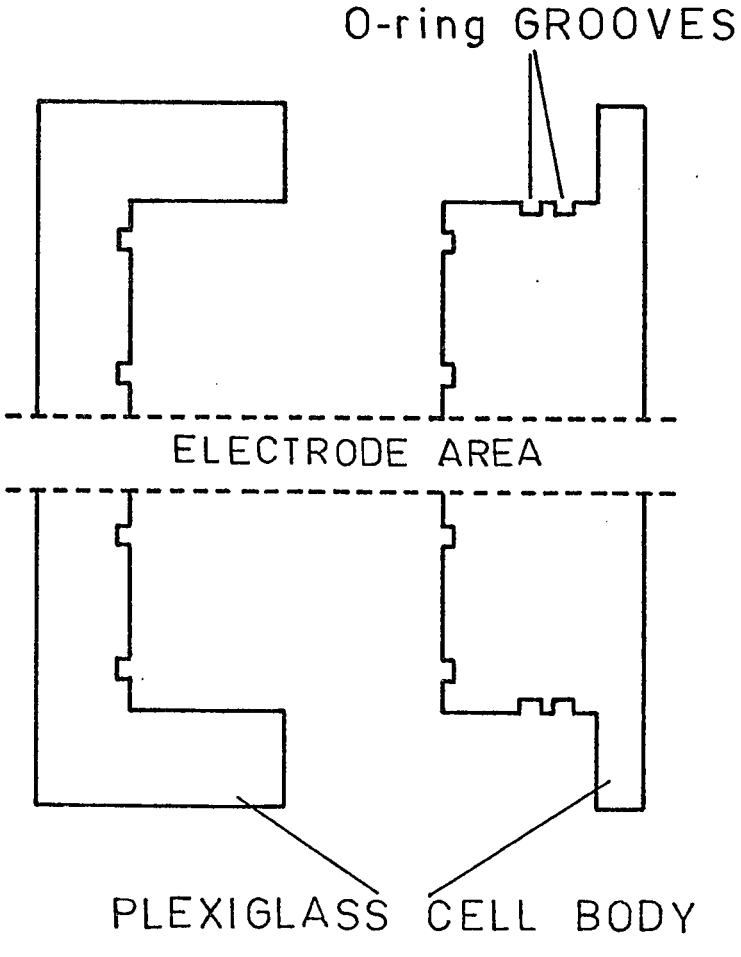

their effective thicknesses as calculated from equation [IV-5]. This method was used to test all cell designs except the last one (Cell Design IV) in which no direct method of testing could be used. The resistance between the cell and the constant temperature bath was measured to ensure that very little leakage to the bath took place. In all cases, this resistance was very large, of the order of 10^7 Ω.

This method thus employed a "liquid membrane" composed of potassium chloride solution of an accurately known concentration and therefore with an accurately-known electrical conductivity. The application of the theory to the results obtained from the test rings to calculate the electrical conductivity, therefore, will confirm or deny the applicability of the theory to the cell design.

When a membrane was to be measured, it was placed in the cell so that it was as nearly centred on the electrodes as possible. The two halves of the cell were pushed together until the membrane made contact with both halves. This could be observed by the wetting of the sides of the cell by the electrolyte in the membrane. The electrode chambers, if there were any, were then filled with potassium chloride solution of the same concentration as that used to soak the

membrane.

The cell was first equilibrated in a constant temperature bath. All cells were designed so that they could be immersed completely, except for the filler holes which were extended by means of Plexiglass tubing about 3 cm above the cell. All measurements were then taken at a Celsius temperature of 25.00 ± 0.01 K. Thermal equilibration usually took from 15 to 30 minutes each time a new membrane was placed in a cell.

The values for l_{eff} for both the test rings and the membranes and for each cell were obtained by use of a Fortran IV computer program. This program first calculated the modified Bessel functions to a sufficient accuracy, either by using the actual series expansion for the Bessel function for a value of the argument below 10, or by a suitably good approximation for values of the argument above 10 [62]. These were then used to calculate the series for Sn, including a number of terms predetermined to give the required accuracy. The value of the effective thickness, l_{eff}, could then be obtained using equation [IV-5]. The computer program used for these calculations is shown in Appendix I.

3. Cell Design Number I

(a) Design

The first cell with which measurements were taken is shown in Figure [IV-3]. This diagram is a cross-section of the cell and is drawn to scale. The electrodes were recessed from the surface of the membrane creating electrode chambers approximately 6 mm deep. These chambers were filled by means of filler holes from the outside. The electrodes were made of 0.025 cm platinum foil soldered onto brass plugs which screwed into place in the Plexiglass body of the cell. After they had been placed in position, the electrodes were platinized electrolytically using a standard platinizing solution at a current of about 50 milliamperes for six minutes for each electrode [63]. A handle made of brass was attached to the exterior of the cell to facilitate the suspension of the cell in the constant temperature bath.

(b) Experimental

The resistance was measured for all test rings using the method described previously. Each resistance measurement was taken at four different frequencies: 1, 2, 5 and 20 kHz. Potassium chloride solution of a concentration of 0.1158 N was used for all measurements.

FIGURE [IV-3]

CELL DESIGN NUMBER I

Cell is drawn to scale.

The cell body is constructed of Plexiglass.

The cross-hatched areas are made of brass.

The dashed lines indicate the positions of the filler holes and of the bolts used for holding the cell halves together.

FIGURE [IV-3]

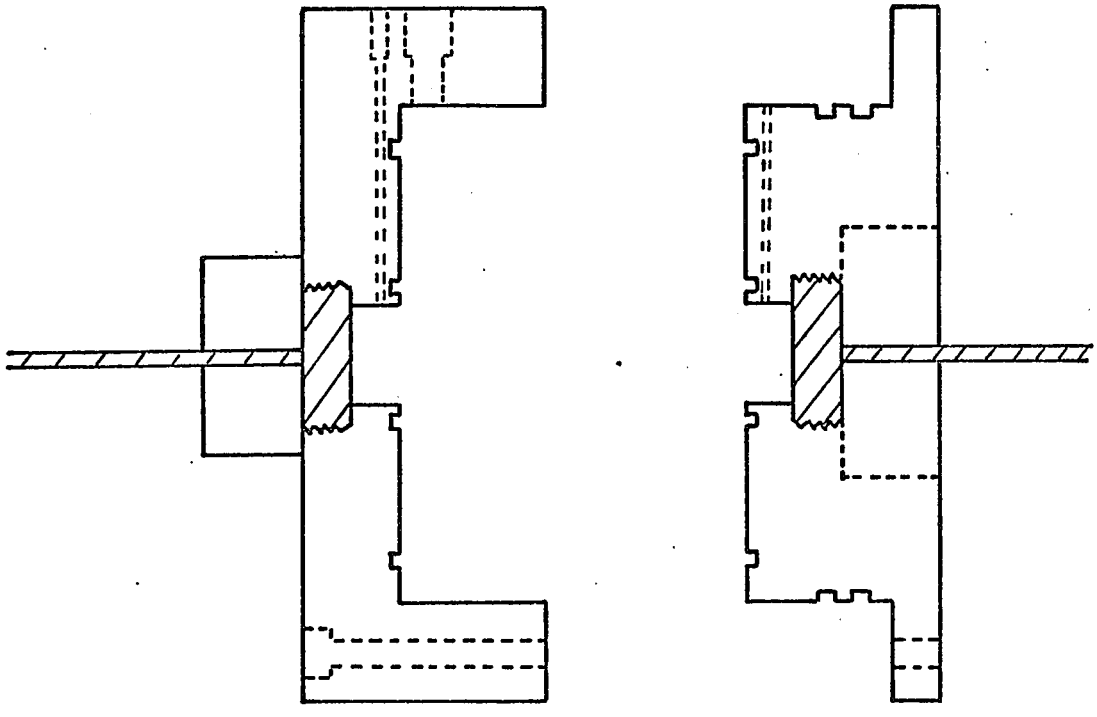

To demonstrate the current distribution in the cell, a two dimensional analog was constructed by cutting a piece of Teledeltos paper into the pattern shown in Figure [IV-4]. The electrodes shown were made of copper foil and were held onto the paper with Melton Silver solution grade EM55 obtained from Melton Metallurgical Laboratories, Poole, England. The percentage of potential difference between the electrodes was plotted with a Field Plotter, Servomex Controls Limited type FD 92.

(c) Results

The resistance measurements obtained from the test rings are given in Table [IV-2] and plotted in Figure [IV-5]. The radius of the electrodes in the cell were measured and found to be 0.478 cm. The theoretical electrical conductivity of the potassium chloride solution was 0.01516 ohm^{-1} cm^{-1} at 25°C [64].

The percentage potential difference across the Teledeltos paper is plotted in Figure [IV-4] showing the positions on the paper where the readings were taken.

(d) Discussion

The results obtained for the test rings give a family of straight lines which have a common origin but slightly different slopes. As the overlap becomes larger,

FIGURE [IV-4]

POTENTIAL MAP FOR ANALOG OF

CELL DESIGN NUMBER I

Diagram is one-half the actual size.

The interior of the diagram is Teledeltos paper, and the cross-hatched sections represent the electrodes.

The lines represent lines of constant potential, and the numbers show the percentage of the total potential drop which takes place to the left of that line.

FIGURE [IV-4]

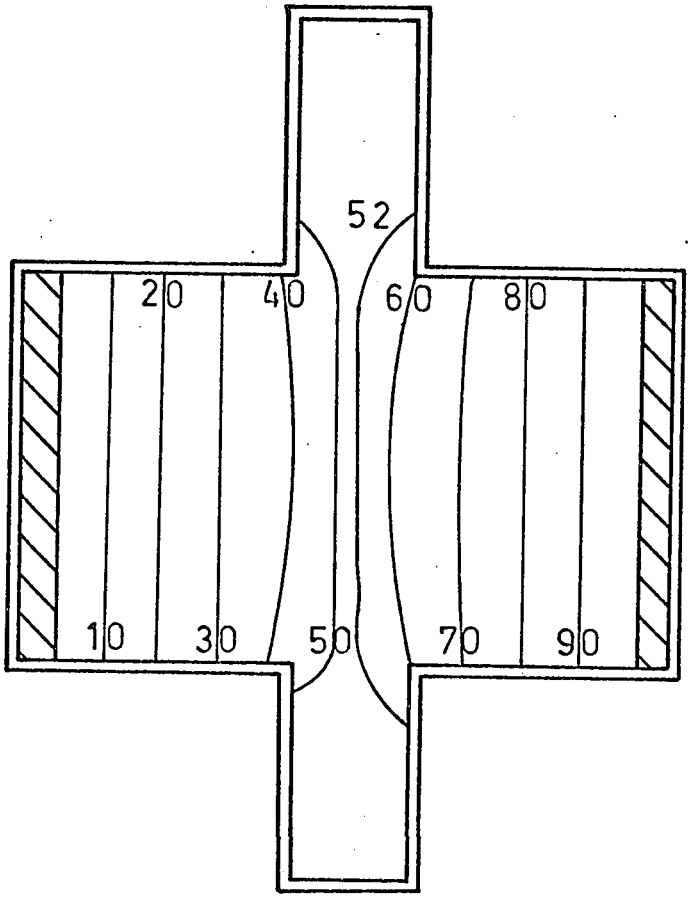

TABLE [IV-2]

MEASUREMENTS ON TEST RINGS --- CELL I

NUMBER	l_{eff}/cm	R/Ω
1A	0.164	134.0
1B	0.215	138.2
1C	0.245	140.9
1D	0.343	149.3
2A	0.162	134.3
2B	0.214	138.7
2C	0.243	141.3
2D	0.351	150.6
3A	0.163	134.6
3B	0.212	139.0
3C	0.246	141.9
3D	0.357	151.5

FIGURE [IV-5]

MEASUREMENTS ON TEST RINGS

CELL DESIGN NUMBER I

● Ring series # 1 R_o = 119.42

△ Ring series # 2 R_o = 119.90

○ Ring series # 3 R_o = 119.84

The slopes for these lines are shown in Table [IV-3]

FIGURE [IV-5]

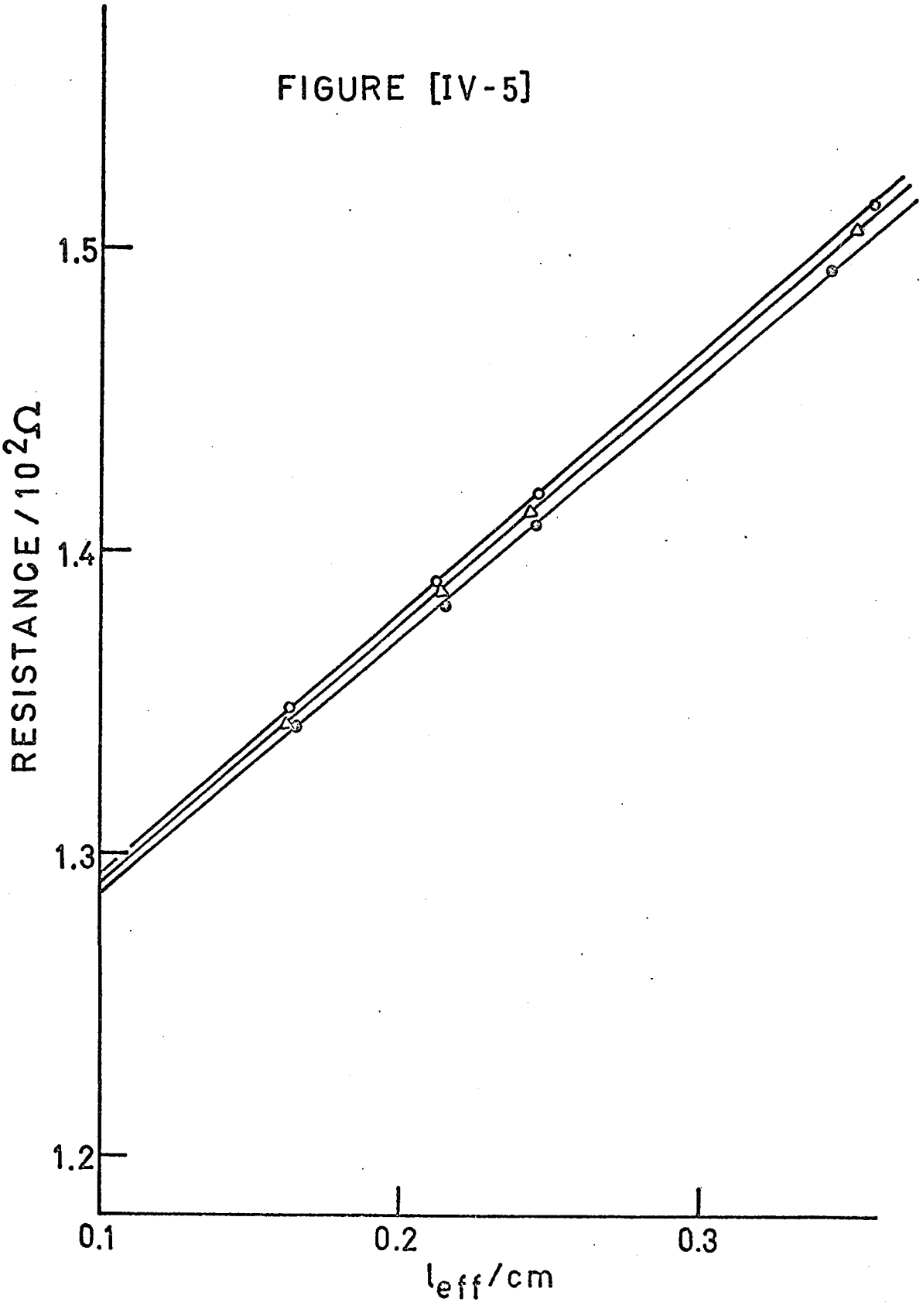

the slope of the line more closely approaches the correct value. This trend is shown in Table [IV-3]. In these data, it is assumed that the electrical conductivity is correct and the effective diameter of the electrodes (that is, the diameter that the electrodes would be if the slope agreed with the theoretical value) is calculated. The larger the diameter of the test ring, the larger is the overlap (defined as the difference between the test ring (or membrane) diameter divided by the electrode diameter, (b-a)/a) and the calculated diameter of the electrodes is closer to the actual diameter.

TABLE [IV-3]

EFFECTIVE ELECTRODE RADIUS FOR DIFFERENT RING SERIES

RING SERIES	OVERLAP (b-a)/a	SLOPE m ohm/cm	$1/\kappa m$ cm	$d=(4/\pi\kappa m)^{1/2}$ cm
1	2.868	95.99	0.6872	0.935
2	1.579	91.01	0.7248	0.961
3	0.284	88.13	0.748	0.976
DIRECT ELECTRODE MEASUREMENT	0	86.58		0.985

The cause for the discrepancy between the experimental results and the theory is almost certainly caused by the finite thickness of the electrode chambers. The theory used was derived with the electrodes in contact with the surface of the membrane. The approximation of using electrode chambers between the membrane and the electrodes will be good as long as the potential is constant on the interface between the membrane and the electrode chamber.

A two dimensional analog of the situation in the cell is shown in Figure [IV-4]. The copper electrodes represent the electrodes in the cell and the electrode section represents the electrode chambers. The wider section in the middle represents the membrane. As can be seen by the plot of the potential lines, there is a large bulge of these lines in the vicinity of the membrane-electrode chamber interface. The line for 50 percent potential difference is not exactly in the middle because the analogs of the two electrode chambers were not exactly the same size.

This distortion of the lines of potential makes it very evident that the boundary condition for constant potential has been violated for this cell design, and therefore either the theory or the cell design must be altered.

4. Cell Design Number II

(a) Design

This cell was designed in order to approximate the boundary conditions as closely as possible. This design is shown in Figure [IV-6] and is identical with the previous cell with the exception of the region in the vicinity of the electrodes. The electrodes were made of 0.20 cm platinum wire, cut and polished to make electrodes of that diameter. They were placed in the cell so that they were flush with the face of the cell. Therefore, there would be very little, if any, resistance due to the solution between the membrane and the electrodes. Filler holes were no longer required. Platinized electrodes could no longer be used since the platinum black would be removed by the physical contact with the membrane. Therefore, the electrodes were left with shiny platinum faces.

(b) Experimental

Plexiglass test rings were again used to test the cell. Since there were no filler holes, the cell was filled in the following way. Excess potassium chloride solution was placed in the female half of the cell, along with the test ring to be used. The two halves of the cell were then put together, keeping the test ring centred in the cell and

FIGURE [IV-6]

CELL DESIGN NUMBER II

The cell is drawn to scale.

The body of the cell is constructed of Plexiglass.

The black areas represent the platinum wires used for the electrodes.

FIGURE [IV-6]

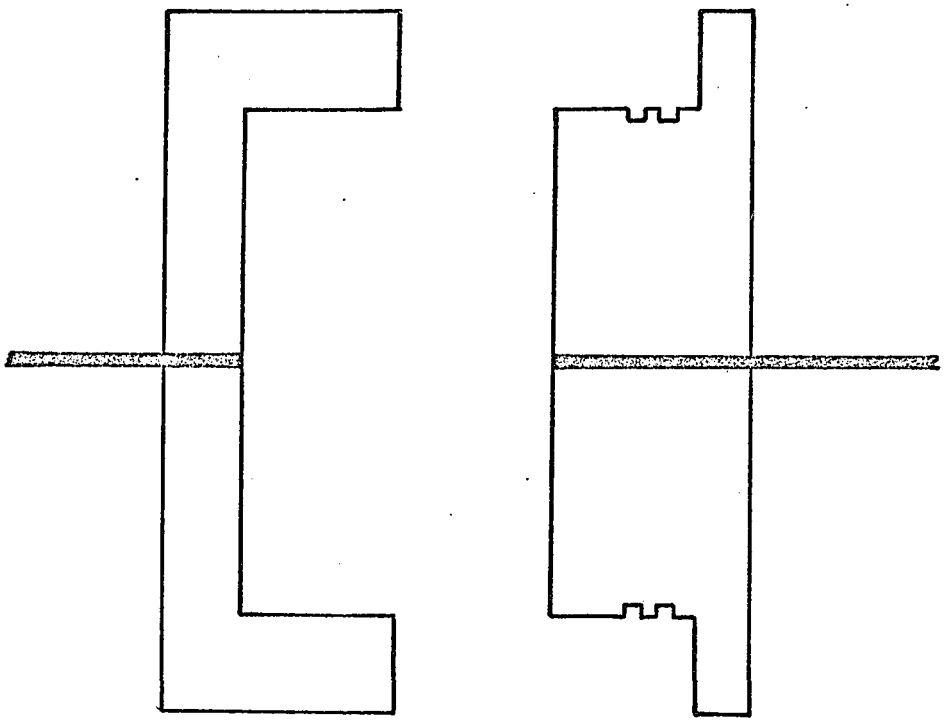

making sure that no air bubbles became trapped inside the test ring. The excess solution was then removed through a small hole drilled into the membrane chamber through the top of the cell.

The resistance was measured for the test rings using concentrations of potassium chloride solution of 0.1 N and 0.05 N. All resistance measurements were taken at four different frequencies of 20, 5, 2, and 1 kHz.

(c) Results

A strong dependence of the measured resistance on frequency was found. A typical set of measurements is shown in Figure [IV-7].

In order to obtain a result free from the polarization effect observed, the curve was extrapolated in the following way. According to [65], we can expect that a relationship of the following form holds for shiny platinum electrodes:

$$R = R_{\infty} + k/w^{n} \qquad [IV-7]$$

where R is the resistance across the cell measured at frequency w, R_{∞} is the resistance across the cell at very high frequency, and both k and n are constants.

Transposing R_{∞} to the left hand side and taking logarithms of the equation gives the result

FIGURE [IV-7]

FREQUENCY DEPENDENCE

OF

RESISTANCE

CELL DESIGN NUMBER II

TEST RING 2D

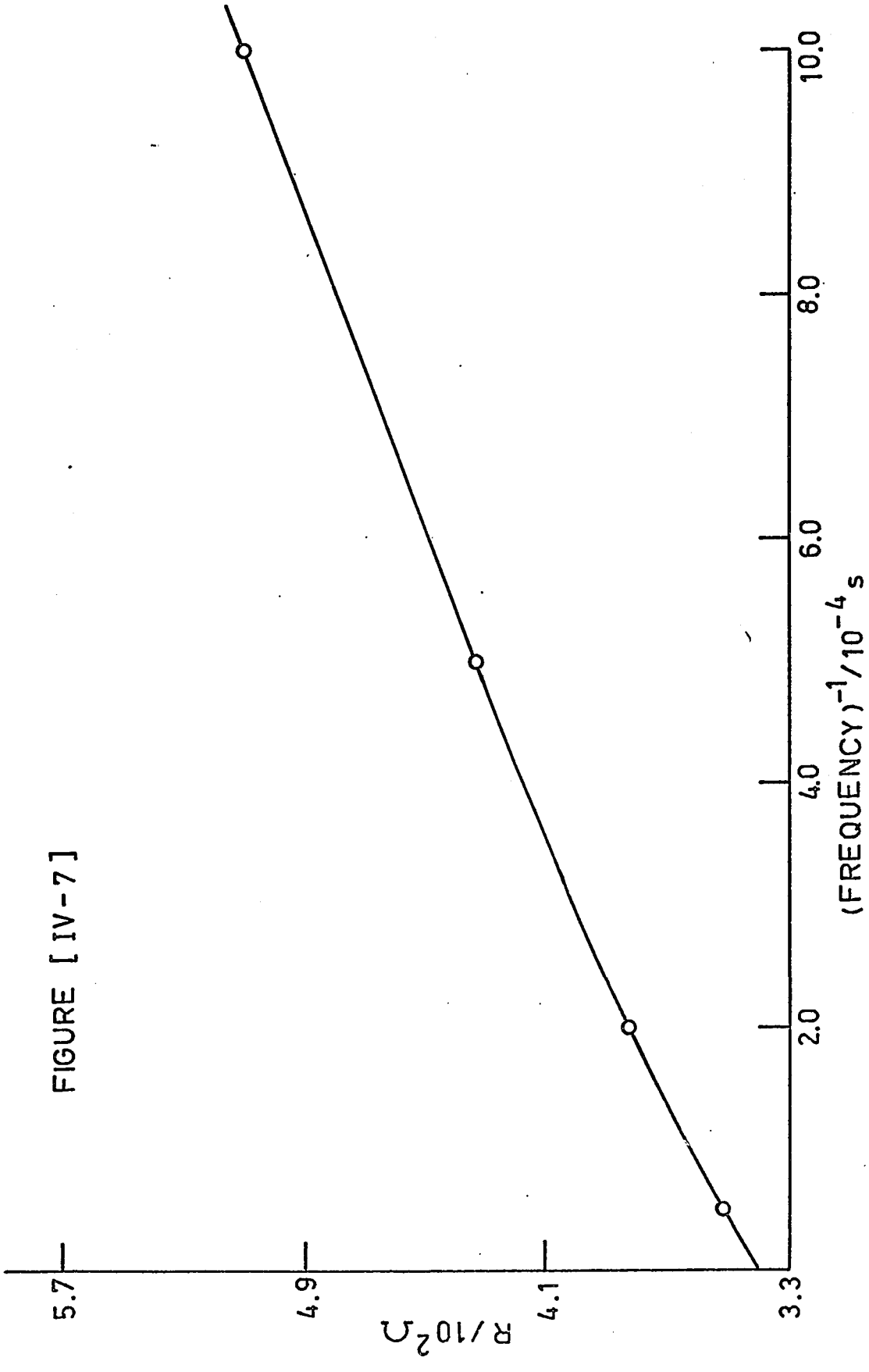

FIGURE [IV-7]

$$\log[R - R_\infty] = \log k - n\log w. \qquad [IV-8]$$

If the resistance has been measured at three different frequencies, a, b, and c, and the values obtained for the resistances were R_a, R_b, and R_c respectively, then these values can be substituted into equation [IV-8] to give three equations and three unknowns, R_∞, k, and n. By subtracting the first equation obtained in this way from the second and the third, k is eliminated and the problem is reduced to two equations and two unknowns:

$$\begin{aligned} \log[(R_a - R_\infty)/(R_b - R_\infty)] &= n\log b/a \\ \log[(R_a - R_\infty)/(R_c - R_\infty)] &= n\log c/a \end{aligned} \qquad [IV-9]$$

From these two equations, a value can be found for R_∞ by successive approximations. A value is assumed for R_∞. This is substituted into the left-hand side of equation [IV-9]. By substituting the values for the frequencies into the right-hand side of this equation gives the result $y = n$ where y is a known quantity.

This value can now be substituted into equation [IV-9] for n and antilogarithms taken to yield the following result:

$$(R_a - R'_\infty)(R_c - R'_\infty) = \frac{c}{a} e^y = p \qquad [IV-10]$$

Again, p is a known quantity. This equation is now solved

for a new value of resistance at very high frequency, R'_∞:

$$R'_\infty = pR_c - R_a \qquad \text{[IV-11]}$$

In this way, a new value of R_∞ has been generated and can be resubstituted into equation [IV-9] to obtain a better approximation. This iterative procedure can be carried on until the desired degree of precision has been obtained.

The value of the resistance at very high frequency was calculated by this method using a Fortran IV computer program. The initial value for R_∞ was calculated by assuming a linear relationship between the resistance and the inverse of the frequency for the data obtained at 20 and 5 kHz. The iterative procedure described above was repeated until the resistances obtained at 20, 5 and 2 kHz agreed to within 0.01 ohm when put into equation [IV-9]. The deviation of the resistance at 1 kHz was then calculated. It was in general lower than the value predicted by the linear relationship for the other frequencies by about 1.5 percent.

The results for test rings using 0.1 N potassium chloride solution are given in Table [IV-4] and plotted in Figure [IV-8]. The value of the power of the frequency in equation [IV-7] fell consistently between the values of 0.8 and 0.9. The results at very high frequency are given, along with results at 20 kHz with the electrodes platinized.

The resistances at very high frequency for one series of test rings using 0.05 N potassium chloride solution are also given in Table [IV-4]. These results are plotted in Figure [IV-9].

(d) Discussion

The values obtained for the electrical conductivity of potassium chloride solutions were in good agreement with literature values [64]. For unplatinized electrodes the value of the electrical conductivity is 0.01228 ohm^{-1} cm^{-1} for 0.01 N potassium chloride solution compared to an accepted value of 0.01218 ohm^{-1} cm^{-1} [64]. The intercept was found to be -25.3 ohm, indicating that the electrodes protruded slightly out of the face of the cell. For platinized electrodes, the electrical conductivity was found to be 0.01209 ohm^{-1} cm^{-1} and the intercept was -44.1 ohm. The increase in the size of the negative intercept is the addition of material to the electrodes by the act of platinization. The value of the electrical conductivity for the 0.05 N potassium chloride solution was found to be 0.00663 ohm^{-1} cm^{-1}. (Literature value, 0.00667 ohm^{-1} cm^{-1}.) The electrodes had been removed and replaced before these readings were taken and the value of the intercept, 2.5 ohm, shows that the electrodes were very

TABLE [IV-4]

MEASUREMENTS ON TEST RINGS --- CELL II

NUMBER	l_{eff}/cm	R_∞/Ω 0.05 N KCl	R_∞/Ω 0.1 N KCl	R^*_{20}/Ω 0.1 N KCl
1A	0.1070		245.7	223.6
1B	0.1207		281.3	256.5
1C	0.1274		296.9	275.3
1D	0.1429		334.6	311.7
2A	0.1053	488.0	240.9	218.6
2B	0.1215	559.5	280.7	257.1
2C	0.1270	588.7	294.9	271.8
2D	0.1433	662.9	337.0	310.6
3A	0.1057		242.0	220.9
3B	0.1200		278.1	256.7
3C	0.1272		297.9	272.8
3D	0.1430		335.0	308.6

* Resistance at 20 kHz

FIGURE [IV-8]

TEST RING RESULTS

CELL DESIGN NUMBER II

0.1 N KCl

o Test ring series # 1

◉ Test ring series # 2

Δ Test ring series # 3

For very high frequency using shiny platinum electrodes,

R_o = -25.3 Ω m = 2.49 x 10^3 Ω cm^{-1}

For 20 kHz using platinized platinum electrodes,

R_o = -44.1 Ω m = 2.53 x 10^3 Ω cm^{-1}

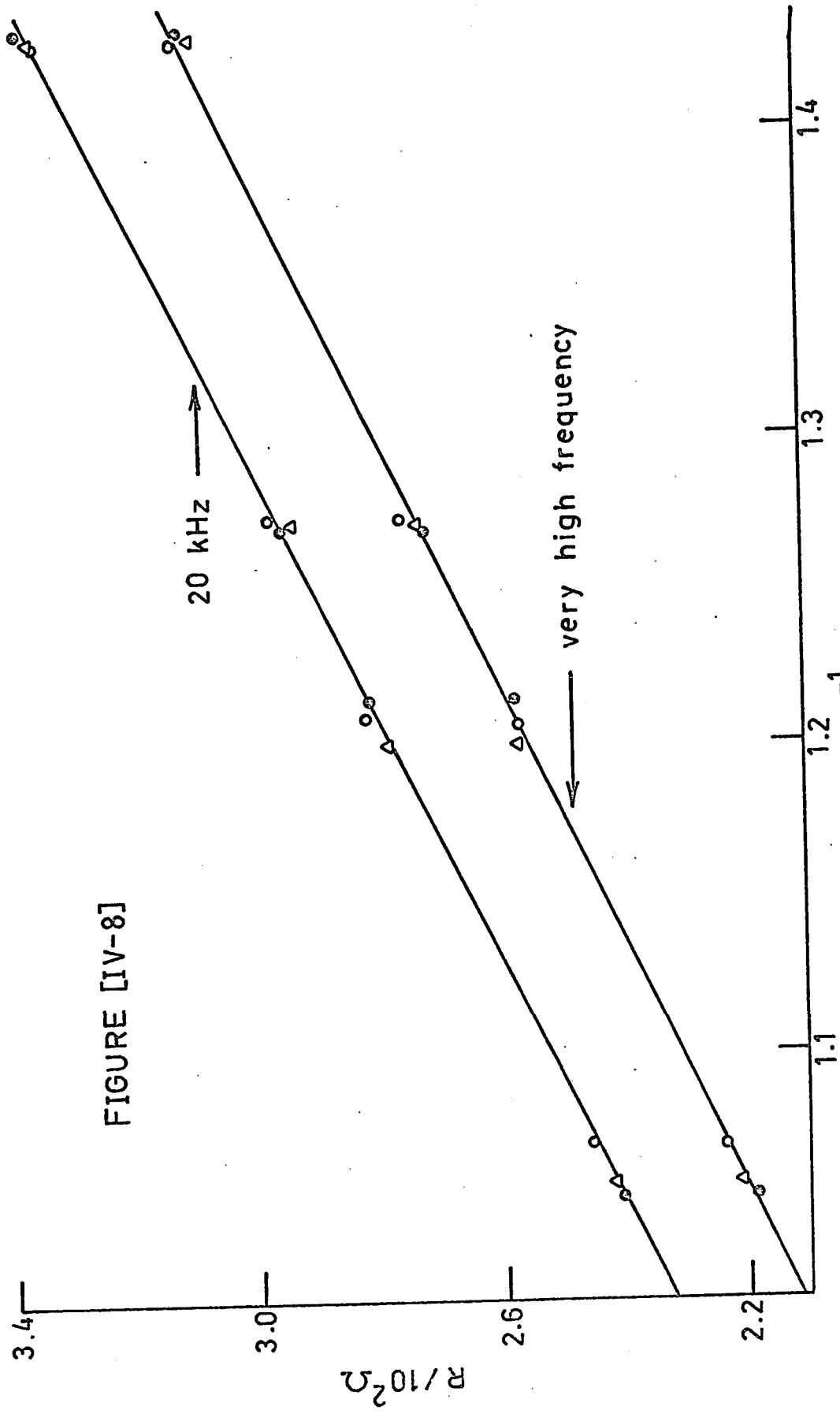
3.4
3.0
2.6
2.2
R / 10²Ω
1.1
1.2
1.3
1.4
l_{eff} /10⁻¹cm
20 kHz
very high frequency

FIGURE [IV-8]

FIGURE [IV-9]

TEST RING RESULTS

CELL DESIGN NUMBER II

0.05 N KCl

Results are for Test ring series # 2, at very high frequency using shiny platinum electrodes.

$R_o = 2.5\ \Omega$ $\qquad$ $m = 4.62 \times 10^3\ \Omega\ cm^{-1}$

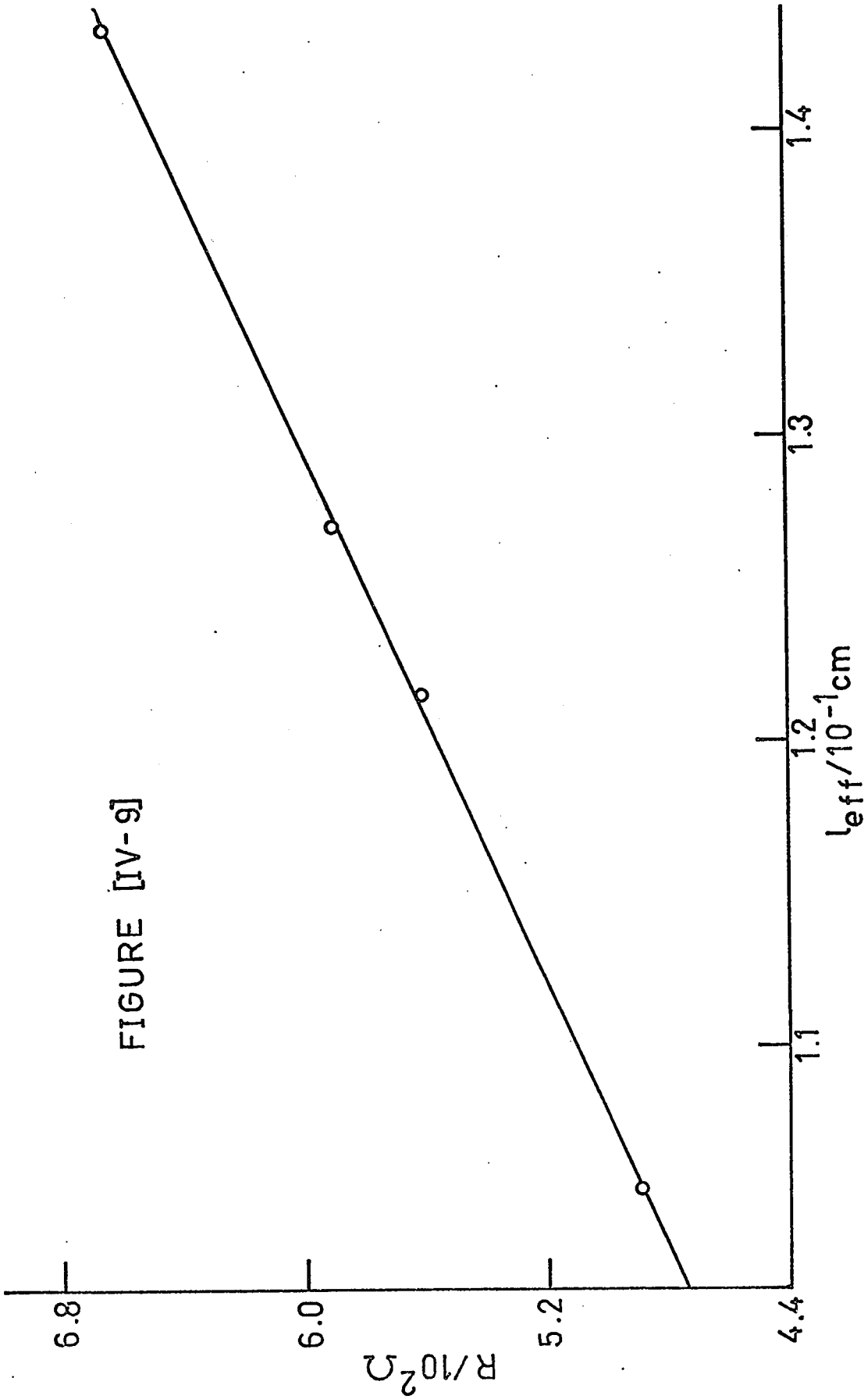

FIGURE [IV-9]

nearly flush with the faces of the cell.

This cell was designed in order to duplicate the boundary conditions in the theory for the overlap estimation as closely as possible. It does this, as shown by the results obtained. However, this design leads to some experimental and computational difficulties.

Firstly, the cell is difficult to fill when being tested with the test ring in place since there are no filler holes and no easy way to incorporate them into the design.

The major problem, however, with this cell design is the polarization of the electrodes. Not only is the resistance due to polarization large when compared to the actual resistance being measured, but also this value is continually changing at any given frequency. The values of k and n in equation [IV-8] change continually. Therefore, although the cell may be in thermal equilibrium, the resistances at the measured frequencies will continue to change with time. Therefore, not only is there no easy way to tell if the cell is in actual thermal equilibrium, but, since the measurements cannot be taken simultaneously, an additional error is involved, caused by the time needed in order to take these readings.

The final problem is the method used to estimate the polarization. The resistance at very high frequency was calculated so that the resistances at 20, 5 and 2 kHz would simultaneously satisfy equation [IV-8]. The resistance measurement at 1 kHz, however, was consistently lower than the value predicted by the calculated value of R_∞. This probably results in only a small error in the result for the resistance at very high frequency since the resistance is proportional to a negative power of the frequency and consequently this point is a large distance from the intercept. A large error in this point will therefore cause only a small error at the intercept. It is nevertheless a problem in the interpretation of the data and indicates a problem with the theory used. It is therefore desirable to platinize the electrodes so that these polarization effects can be minimized.

5. Cell Design Number III

(a) Design

The third cell design was an attempt to incorporate the best features of the two previous designs, platinized platinum electrodes and electrodes close to the membrane surfaces. Cell Design Number III is shown in Figure [IV-10]. It again employs the same basic cell design, identical with

cell number I except in the region of the electrodes. The electrodes were made by Engelhard Industries of Canada Ltd. to special order. They were 1.410 cm in diameter and were made out of 52 mesh platinum wire gauze. A circular piece of platinum foil was attached to the back of the outer edge of the electrodes to add to their rigidity. The electrodes were placed about 0.1 cm from the inner face of the cell so that they would not be in contact with a membrane and therefore could be platinized. However, they were still close enough to the membrane face so that no significant deviation from the theory of overlap should occur. Each electrode was fastened at its centre to a 0.15 cm platinum wire by means of a pressure weld. This wire was attached to a copper wire outside the electrode chamber area as shown in the diagram. Filler holes were drilled into the electrode chambers behind the mesh electrodes and these were used to fill the cell with solution.

(b) Experimental - Test rings

This cell was tested extensively using the test rings and concentrations of potassium chloride solutions of 0.1 N, 0.05 N, 0.01 N, and 0.005 N. For the second and fourth concentrations, the first two series of test rings was used. For the other concentrations, only the second

FIGURE [IV-10]

CELL DESIGN NUMBER III

The cell is drawn to scale.

The cell body is made from Plexiglass.

The cross-hatched areas designate brass (or copper) parts.

The black sections and electrodes are made from platinum.

The dashed lines indicate filler holes, screw locations and the bolts for joining the cell halves.

FIGURE [IV-10]

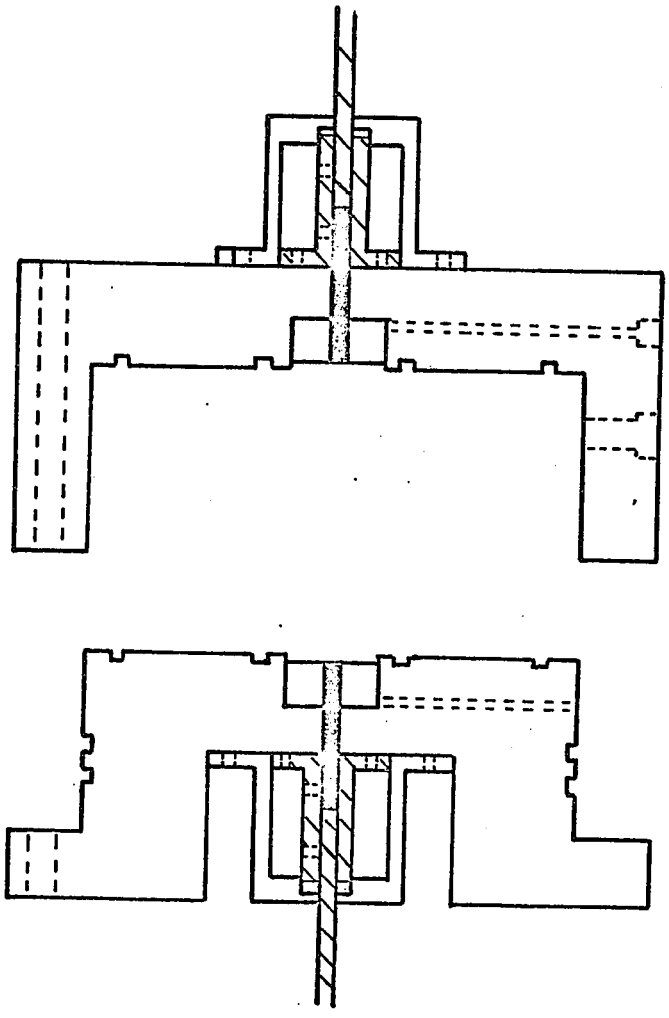

series of test rings was employed. In all the results obtained, the electrodes were platinized in the same way as was described for cell design number I.

(c) Results - Test rings

The results for the test rings for all concentrations of potassium chloride solution are shown in Table [IV-5]. Figure [IV-11] plots the results for 0.1 N and 0.05 N potassium chloride solution while Figure [IV-12] shows the results for 0.01 N, and 0.005 N potassium chloride solution.

(d) Discussion - Test rings

The results obtained for the electrical conductivities of the potassium chloride solutions agree very well with the literature values [64] over the complete range of concentrations studied. These values, experimental and from the literature, along with the values for the intercept, are given in Table [IV-6].

From the results obtained, it is evident that the cell design meets the requirements of the theory for the estimation of overlap for potassium chloride solution over the range of concentrations studied.

TABLE [IV-5]

MEASUREMENTS ON TEST RINGS --- CELL II

NUMBER	l_{eff}/cm	R/Ω			
		0.1 N	0.05 N	0.01 N	0.005 N
1A	0.1677		33.10		307.6
1B	0.2240		38.35		353.7
1C	0.2561		41.56		382.1
1D	0.3833		53.59		494.3
2A	0.1686	17.85	33.22	154.8	308.2
2B	0.2216	20.42	38.18	180.4	351.2
2C	0.2576	22.38	41.93	195.0	386.3
2D	0.3769	28.54	52.84	252.3	489.6

FIGURE [IV-11]

RESULTS ON TEST RINGS

CELL DESIGN NUMBER III

0.1 N KCl

The results are for Test ring series # 2.

0.05 N KCl

o Test ring series # 1

● Test ring series # 2

The slope and intercept values for these data are given in Table [IV-6].

FIGURE [IV-11]

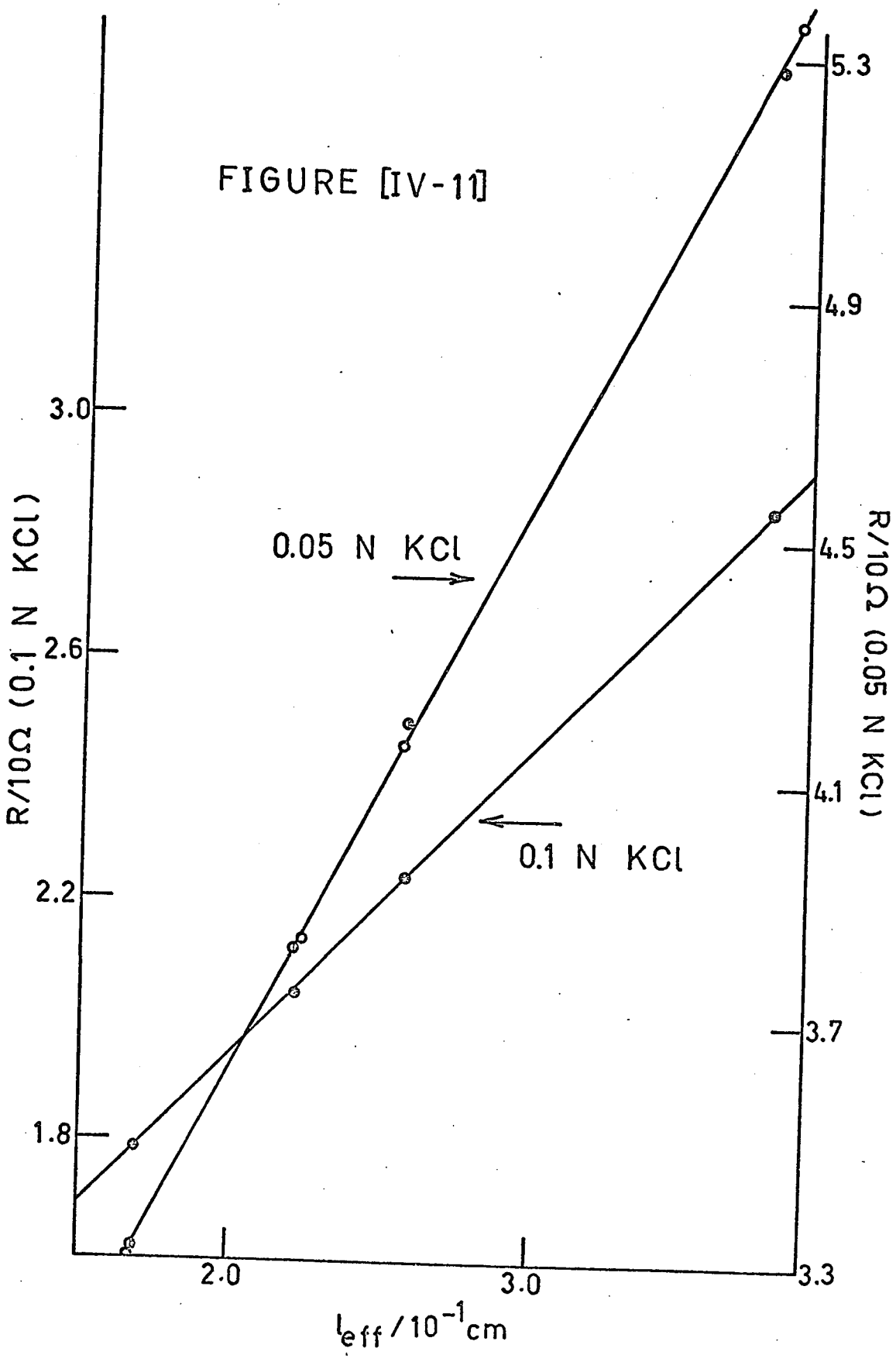
5.3
4.9
3.0
0.05 N KCl
4.5
2.6
4.1
0.1 N KCl
2.2
3.7
1.8
3.3
2.0
3.0
l_{eff} / 10^{-1}cm
R/10Ω (0.1 N KCl)
R/10Ω (0.05 N KCl)

FIGURE [IV-12]

RESULTS ON TEST RINGS

CELL DESIGN NUMBER III

0.01 N KCl

The results are for Test ring series # 2.

0.005 N KCl

- Test ring series # 1
- Test ring series # 2

The slope and intercept values for these data are given in Table [IV-6].

FIGURE [IV-12]

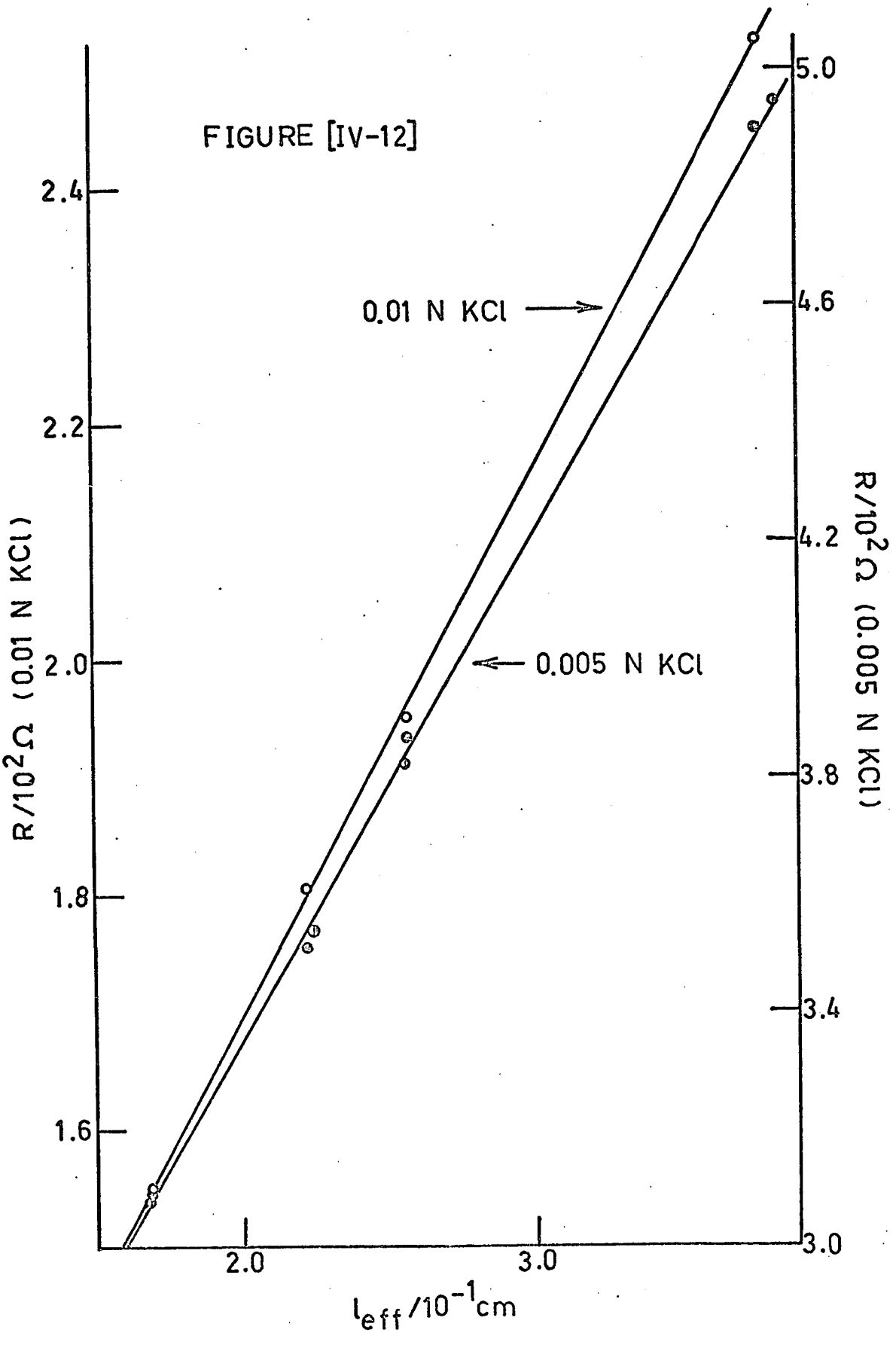
0.01 N KCl
0.005 N KCl
R/10²Ω (0.01 N KCl)
R/10²Ω (0.005 N KCl)
2.4
2.2
2.0
1.8
1.6
5.0
4.6
4.2
3.8
3.4
3.0
2.0
3.0
l_eff /10⁻¹cm

TABLE [IV-6]

ELECTRICAL CONDUCTIVITIES AND INTERCEPTS --- CELL III

NORMALITY KCl	SLOPE Ω cm^{-1}	INTERCEPT Ω	CONDUCTIVITY/Ω^{-1} cm^{-1} EXPERIMENT	LITERATURE [64]
0.1	51.85	9.00	0.0121	0.01218
0.05	94.22	17.41	0.00665	0.00669
0.01	445.4	81.11	0.00141	0.001413
0.005	867.9	161.34	0.000720*	0.0007168

* corrected for conductivity of solvent

(e) Experimental - Membranes

The three different types of membranes were used for measurement in this cell. The membrane to be measured was placed into the cell and the two halves of the cell were slid together until the presence of a slight pressure was observed on the sides of the membrane as the moisture in the membrane wetted the faces of the cell. The electrode chambers were filled with the same concentration of potassium chloride solution in which the membrane had been equilibrated.

The results on all types of membranes were taken in concentrations of potassium chloride solution of 0.1 N,

0.05 N, and 0.01 N.

The results for polyvinylbenzenesulfonate membranes were obtained by the use of membrane number 17 in Table [III-1].

(f) Results - Membranes

The results obtained for the membranes at the three concentrations are given in Table [IV-7]. Those for cellulose and polyvinylbenzenesulfonate are plotted in Figure [IV-13] and those for porous glass are plotted in Figure [IV-14]. The value of the resistance for the electrode chambers was taken from the values of R_o obtained from the test rings as shown in Table [IV-6].

TABLE [IV-7]

MEASUREMENTS ON MEMBRANES --- CELL III

MEMBRANE	KCl CONCENTRATION	CONDUCTIVITY (Ω^{-1} cm^{-1})
CELLULOSE	0.1 N	7.12×10^{-3}
	0.05 N	3.79×10^{-3}
	0.01 N	0.945×10^{-3}
P.V.B.S. #17	0.1 N	1.77×10^{-2}
	0.05 N	1.29×10^{-2}
	0.01 N	1.48×10^{-2}
POROUS GLASS	0.1 N	1.35×10^{-3}
	0.05 N	0.728×10^{-3}*
	0.01 N	0.280×10^{-3}*

* corrected for the conductivity of the solvent

(g) Discussion - Membranes

The uncertainty in the results obtained for polyvinylbenzenesulfonate membrane was very large. This effect is caused by the low resistance across this type of membrane, which was only about 10 percent of the total resistance reading. The rest of the resistance is due to the electrode chambers. Not only would this situation cause a large error in membrane resistances, but it would again cause a problem with the application of the overlap theory as was discussed earlier in this chapter. This situation causes the lines of constant potential to bend and the theory will be violated.

However, in the case of using membranes with a relatively high resistance when compared to the resistance of the electrode chambers, the cell design gave entirely satisfactory results. This was the case when the test rings were used as well as when cellulose and porous glass membranes were being measured.

FIGURE [IV-13]

ELECTRICAL CONDUCTIVITY OF MEMBRANES

CELL DESIGN NUMBER III

● data for potassium chloride solution [64].

◐ results for cellulose membranes.

○ results for polyvinylbenzenesulfonate membranes.

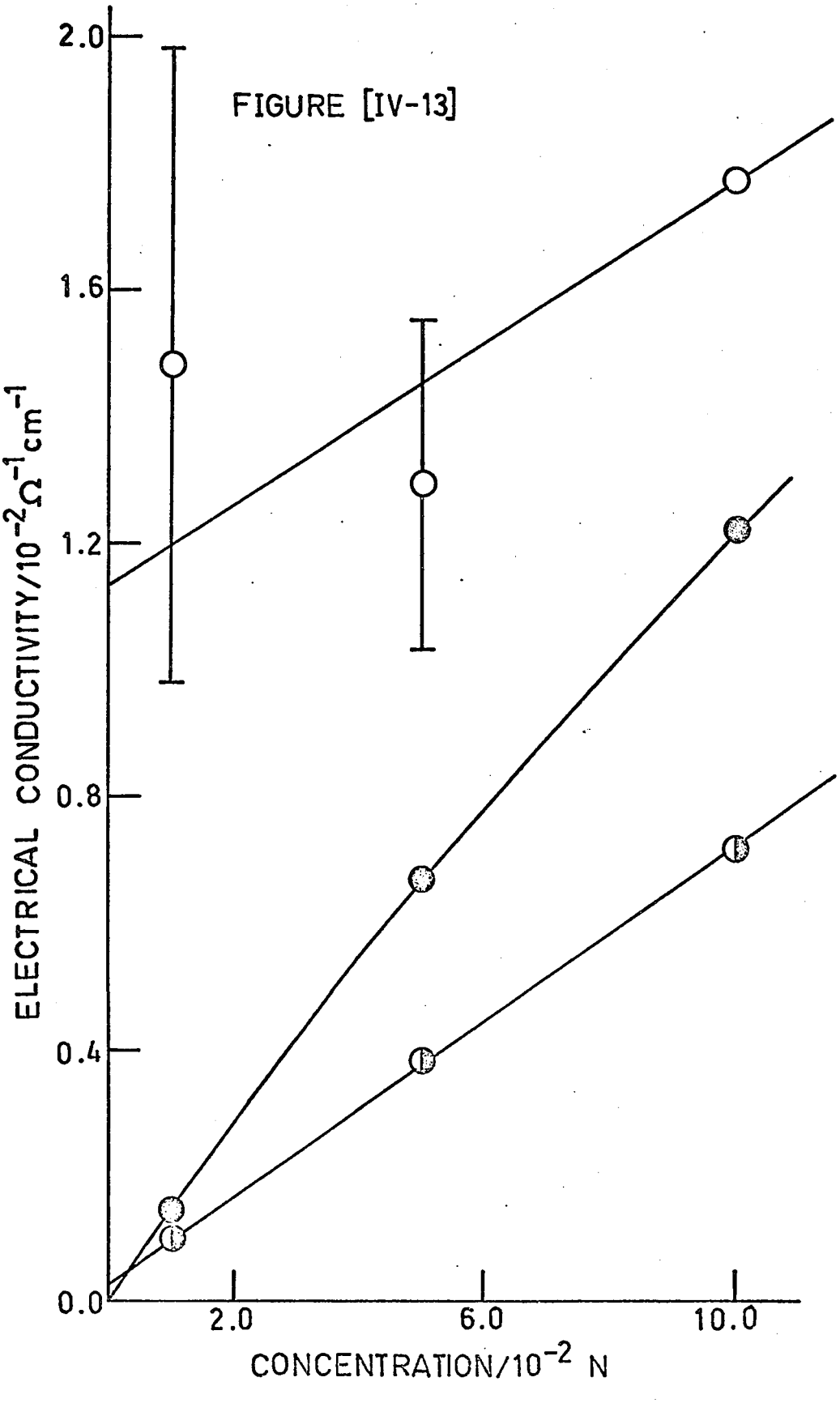
FIGURE [IV-13]
2.0
1.6
1.2
0.8
0.4
0.0
ELECTRICAL CONDUCTIVITY/$10^{-2}\Omega^{-1}cm^{-1}$
2.0
6.0
10.0
CONCENTRATION/10^{-2} N

FIGURE [IV-14]

ELECTRICAL CONDUCTIVITY OF MEMBRANES

CELL DESIGN NUMBER III

The results shown are those obtained for porous glass membranes.

FIGURE [IV-14]

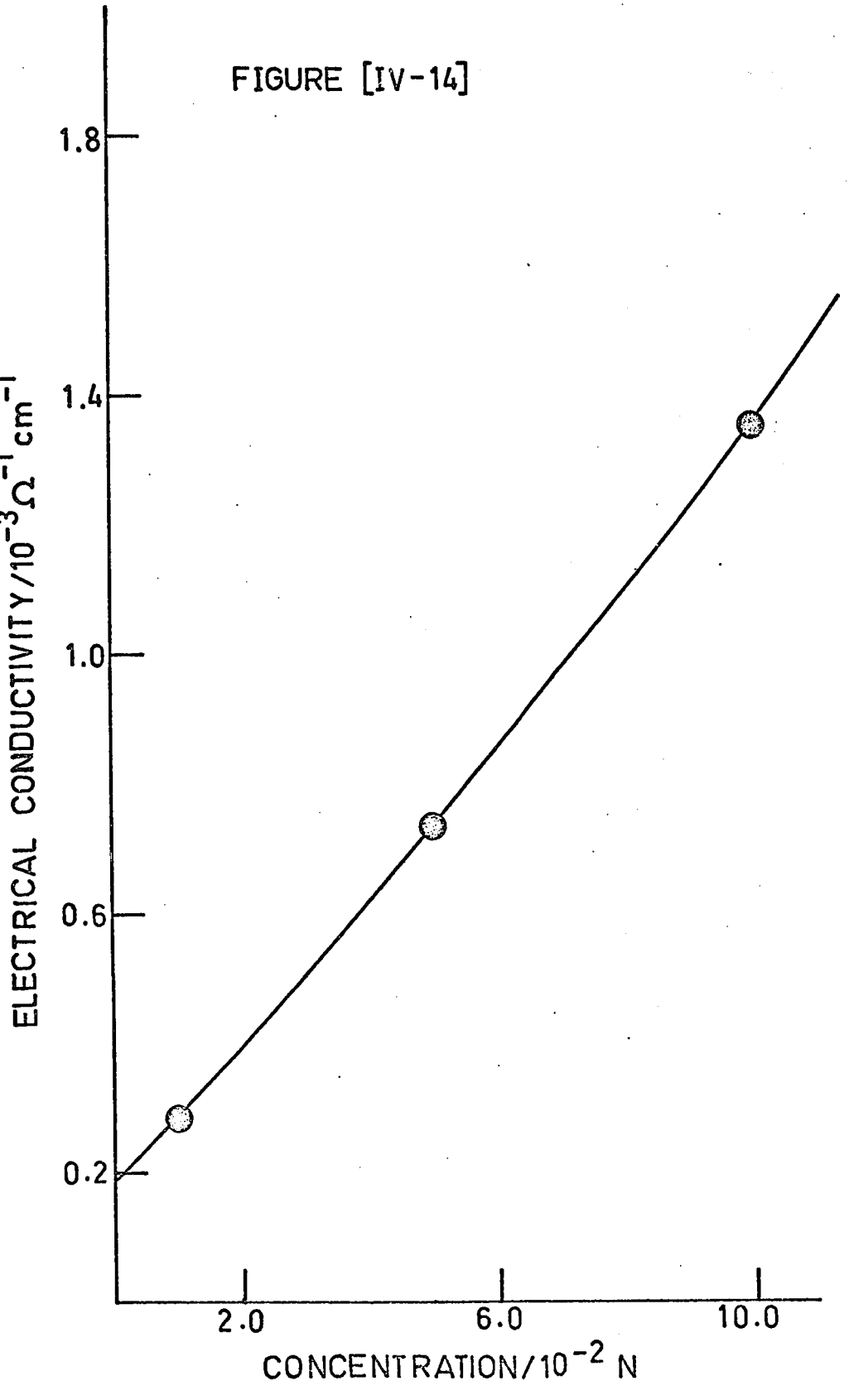
1.8
1.4
1.0
0.6
0.2
ELECTRICAL CONDUCTIVITY/$10^{-3}\Omega^{-1}cm^{-1}$
2.0
6.0
10.0
CONCENTRATION/10^{-2} N

6. Cell Design Number IV

(a) Design

This cell was a modification of cell design number I. It was the same in all features except that the electrode chambers were filled with mercury, similar to a method described by Subrahmanyan [25]. The platinum electrodes were left in place and used as the method by which contact between the mercury and the external circuit was achieved.

(b) Experimental

The membrane to be measured was prepared as usual and placed in the cell in the same manner as in cell number III. Mercury, equilibrated in the appropriate potassium chloride solution for 24 hours was then put into the "electrode chambers". The cell was then brought to thermal equilibrium and resistance measurements taken. All membranes were equilibrated in 0.1 N, 0.05 N, and 0.01 N potassium chloride solutions for measurement.

(c) Results

The results for the same membranes as were measured in cell number III are shown in Table [IV-8]. The total resistance across the cell when the polyvinylbenzenesulfonate membrane was being measured was only about 4 ohms and the

TABLE [IV-8]

ELECTRICAL CONDUCTIVITIES OF MEMBRANES

CELL DESIGN NUMBER IV

Membrane	KCl concentration	Electrical conductivity (Ω^{-1} cm^{-1})
cellulose	0.1 N	7.05×10^{-3}
	0.05 N	3.62×10^{-3}
	0.01 N	0.930×10^{-3}
porous glass	0.1 N	1.26×10^{-3}
	0.05 N	0.713×10^{-3} *
	0.01 N	0.271×10^{-3} *
P.V.B.S. #17	0.01 N	1.35×10^{-2}

* corrected for the conductivity of the solvent.

bridge would not balance because of capacitance effects. In order to obtain readings, a calibrated 100 ohm resistance was placed in series with the cell. This amount was then subtracted from the reading obtained from the bridge. A polarization effect was observed for the polyvinylbenzenesulfonate membranes. The data were, therefore, extrapolated to very high frequency in the same manner as the results for cell design number II. They could then be treated in the same way as the other results. A small variation in the values at different frequencies was found with time, but after temperature equilibration, the effect on the extrapolated value was negligible, and the readings at different frequencies could be taken with almost no change in these values during the time required to take the measurements. Polyvinylbenzenesulfonate membranes with a variety of properties were measured. The results are shown in Table [IV-9].

(d) Discussion

The results obtained by this method for the cellulose and porous glass membranes were approximately 2 percent lower than those obtained using cell number III. This discrepancy could be caused by various additive errors such as the measurement of the size of the electrodes in

TABLE [IV-9]

Electrical Conductivity of Polyvinylbenzenesulfonate Membranes

Membrane	Volume Fraction Water	Capacity (meq/g dry)	Electrical Conductivity ($10^2\Omega^{-1}cm^{-1}$)	Degree of Ionization	λ_1
1	0.516	1.72	1.57	0.226	15.3
9	0.496	1.77	1.71	0.238	13.6
11	0.629	2.47	1.65	0.369	14.4
12	0.470	2.24	1.78	0.334	14.1
13	0.508	2.30	1.75	0.342	13.9
17	0.225	1.03	1.77	0.210	14.1

the cells. Since this quantity is squared in the analysis of the data, a small error in its measurement would be magnified. However, Subrahmanyan [25] also found results for the same kind of method to be lower than those reported for the same kind of membrane by others [66]. The effect, then, may be peculiar to the method.

A problem with polarization is again evident. But in this case, it occurs only when the resistance across the membrane is very small. The results for polyvinylbenzenesulfonate are subject to little error from overlap since this cell design duplicates the boundary conditions of the theory as closely as possible. The interpretation of these results will be dealt with in the next section.

7. Interpretation of the Conductivity of Membranes

From equation [II-80], the flux $\underline{J}_i$ of an ion i, relative to the membrane is related to the flux $\underline{J}_i^o$ relative to the solvent by

$$\underline{J}_i = \underline{J}_i^o + c_i \underline{J}_o / c_o \qquad \text{[IV-12]}$$

If only electrical forces are present, equations [II-60] and [II-82] give

$$t_i = t_i^o + c_i t_o / c_o \qquad \text{[IV-13]}$$

The ion (equivalent) conductance is

$$\lambda_i^a = z_i t_i^a \kappa / |z_i| c_o \qquad [IV-14]$$

in an arbitrary frame of reference a, so that

$$\lambda_i = \lambda_i^a + z_i t_o \kappa / z_i c_o \qquad [IV-15]$$

The electrical conductivity of the membrane is, from equation [II-92]

$$\kappa = \sum_i |z_i| c_i \lambda_i = \sum_i |z_i| c_i \lambda_i^o + \sum_i z_i c_i t_o \kappa / c_o \qquad [IV-16]$$

The measurements in Table [IV-9] are for an external salt concentration of 0.1 N, while the fixed charge concentrations in the membranes are of the order of 2 N. Donnan exclusion therefore indicates that essentially only counterions 1 are present in the membrane, and thus, from [IV-16]

$$\kappa = |z_1| c_1 \lambda_1^o / (1 - z_1 c_1 t_o / c_o) \qquad [IV-17]$$

The concentration c_1 is the concentration of ions which contribute to the conductivity. If c_c is the stoichiometric concentration of counterions, an apparent counterion conductance may be defined as

$$\lambda_1 = \kappa / |z_1| c_c = c_1 \lambda_1^o / c_c (1 - z_1 c_1 t_o / c_o) \qquad [IV-18]$$

The concentration c_c may be calculated in two ways.

(a) If c_c' is the number of moles of counterions per

unit volume of water in the salt-free membrane,

$$c'_c = d_o X/\bar{w}$$

where X is the capacity (mol/g dry) and $\bar{w}$ is the water content (g/g dry) of the membrane and d_o is the density of water.

The data in Table [IV-9] can be used to calculate $\lambda'_1 = \kappa|z_1|c'_c$, which is found to be accurately proportional to the volume fraction of water v_o, in the membrane [4]:

$$v_o = \bar{w}d_r/(d_o + \bar{w}d_r) \qquad \text{[IV-19]}$$

where d_r is the density of the dry membrane: $d_r = 1.25$ g cm^{-3} [4].

(b) If c_c is the number of moles of counterions per unit volume of the whole membrane,

$$c_c = Xd_r(1 - v_o) = c'_c v_o \qquad \text{[IV-20]}$$

The values of λ_1 calculated using this value of c_c are constant for all of the membranes used (see Table [IV-9]). We conclude that the whole of the membrane is accessible for the transport of ions, and not just the solvent portion of the membrane. This conclusion is at variance with pore models of membrane which continue to be popular (e.g. [67, 68]). However, pore models ignore the kinetic motion of the polymer matrix [12]. The role of this factor will be

discussed below.

To proceed further with this interpretation, we need a microscopic model of a membrane. Katchalsky [69] has reviewed the use of a rigid charged rod as a useful model of a polyelectrolyte molecule in solution. We take as a model of a membrane a network of charged rods joined in series and parallel. Mazur and Overbeek [70] have shown in general that any model of this type will give transport equations of the form predicted by irreversible thermodynamics. Polyelectrolyte theory provides two features of this model which are of value. First, there is a fraction φ, of the counterions which is osmotically active [69]. The value of φ is determined by the charge density of the rod; i.e., some counterions are so strongly bound to the rod by the high electrostatic field that they do not contribute to the thermodynamic properties of a polyelectrolyte solution. We shall assume that this fraction also applies to conductance, so that $c_1 = \varphi c_c$. Secondly, liquid flow will occur parallel to the charged rods, since the flow is induced by the interaction of the applied electric field and the electric field of the double layer. Ion flow should also be parallel to the rods, on the average, since the distribution of counterions is determined by the field

of the double layer. We thus have randomly-oriented regions about the randomly-oriented network of charged rods, in which flow of ions and liquid occurs. A simple calculation [69] gives the effective ion conductance for this arrangement. The component of the field along a rod which makes an angle θ with the field is $E\cos\theta$. The component of the mobility along the rod is $u\cos\theta$. If we average over all angles which give contributions in the direction of the field, the average velocity is

$$\bar{v} = (uE/2) \int_0^{2\pi} \cos^2\theta \sin\theta \, d\theta = uE/3 \qquad [IV-21]$$

so that the effective conductance is $\lambda_1^o/3$.

When these factors are introduced into equation [IV-18], we find (with $z_1 = +1$)

$$\lambda_1 = \varphi\lambda_1^o/3(1 - \varphi c_c t_o/3c_o) \qquad [IV-22]$$

For polyvinylbenzenesulfonate membranes of the type used here, Stewart and Graydon [71] found experimentally that $t_o M_o X/\bar{w} = c_c t_o/c_o$ was almost constant for membranes with capacities of 1 to 4 meq g^{-1} in contact with sodium chloride solutions of concentrations from 0 to 4 M. M_o is the molecular weight of the solvent. The value of $c_c t_o/c_o$ rose from about 0.4 for low values of X to 0.6 for high values, with most values being about 0.5. Since $c_c t_o/c_o$

is the fraction of the total water in the membrane transported by electro-osmosis, it is reasonable to assume that this fraction depends only on the charge density along the chain, and not on the nature of the counterion.

The observed ratio $\lambda_1/\lambda_1^o = 0.190$ (taking λ_1^o = 73.52 for K^+, the value at infinite dilution in water [72]). With $c_c t_o/c_o = 0.5$, equation [IV-22] gives $\varphi = 0.44$. The polyvinylbenzenesulfonate membranes used here have degrees of ionization of 0.21 to 0.37 (defined as the number of sulfonate groups divided by the total number of vinyl groups). For this degree of ionization, data on polyelectrolyte solutions [69] give φ = 0.3 to 0.5. The value of φ is not very sensitive to the value of λ_1^o. Even if λ_1^o = 51.20, the value for K^+ in 2 N potassium chloride solution, is used [73], φ increases only to 0.58.

Equation [IV-18] contains an electro-osmotic contribution to conductance, which is analogous to the electrophoretic effect on a polyion in solution. A relaxation effect, caused by retardation of the motion of the counterions in the double layer by the high electric field, should also occur. Attempts to include an approximate relaxation effect [69] in equation [IV-18] lead to negative values of φ. We conclude that the mobility of the counter-

ions close to the polymer chains is very small; i.e., the relaxation effect is very large.

The above model also indicates that the counter-ions follow the thermal motion of the polymer chains, so that the whole volume of the membrane is available for conduction. The membrane therefore behaves as a poly-electrolyte solution, and not as a two-phase system. While the model is a simple one, it is more realistic for poly-vinylbenzenesulfonate membranes than are capillary models, and it gives results which are consistent with current ideas on the structure of polyelectrolyte solutions.

Similar calculations can be done for the cellulose and porous glass membranes using equation [IV-17]. The data used are shown in Table [IV-10]. The values for the water transport, the water content and for the internal concentrations are taken from Brydges [73]. The value for the electro-osmotic term is always small compared to unity so this term could be ignored and the value of φ calculated from the equation

$$\varphi = \kappa / (\sum_i |z_1| C_i \lambda_i) \qquad [IV-23]$$

The value of φ obtained for cellulose is greater than unity. This is possible [69] if there are solvent-counterion interactions.

TABLE [IV-10]

OSMOTIC COEFFICIENTS FOR CELLULOSE AND POROUS GLASS

MEMBRANE	C_{ext}	$K \times 10^3$	t_o *	$\bar{C}_1$ *	C_2 *	φ
CELLULOSE	0.1	7.05	-	0.1	0.1	1.6
	0.05	3.62	-	0.056	0.05	1.3
	0.01	0.930	97	0.0143	0.085	1.7
POROUS GLASS	0.01	0.271	40	0.104	0.012	0.1

* Values obtained or estimated from [73]

The value for porous glass is much smaller than expected. It is probable that only the volume of water in the membrane should be used to determine the internal concentrations. This method gives a more reasonable value of $\varphi = 0.4$. In this case it is more realistic to use a pore model of the membrane, since the membrane is very rigid and motion of the polymer chains will be severely limited.

8. Comparison With Other Work

Measurements of the electrical conductivity perpendicular to the membrane surface have been reported by other authors. Their methods have some similarities to those used in this work.

Breslau and Miller [68] have used a cell design similar to our cell number I. It suffers from the same problems as those pointed out for our cell. It has large electrode chambers which tend to make the measured resistance across the cell much larger than the actual resistance across the membrane. Also, no overlap correction has been made for the larger size of the membrane as compared to the electrodes.

Subrahmanyan [25] has used a method which was the basis of our cell number IV. Several suspected problems in

his design were removed. The large volume of mercury used as the electrodes could cause large capacitance effects in the apparatus hindering resistance measurements. Also, there was no mention of equilibration of this mercury in the same solution as the membrane. This omission could cause spurious solvent flows into the liquid electrodes.

CHAPTER V

ELECTRICAL CONDUCTIVITY PARALLEL TO MEMBRANE SURFACE

1. Theory

A theory has been developed by van der Pauw [27] for the measurement of the Hall effect and the specific resistivity of semiconductors of an arbitrary perimeter but of uniform thickness. If a method employing this theory is used, the only dimension that is required for the measurement of the specific resistivity, and therefore of the electrical conductivity, is the thickness. The shape of the sample is not restricted in its other two dimensions.

The following two conditions must be met if the theory is to hold rigourously. The electrodes must be at the circumference of the sample, and the contact between the electrodes and the sample must be sufficiently small. Secondly, there cannot be isolated holes in the sample.

The basic theory is first derived for a sample in the form of a semi-infinite plane of uniform thickness. Along the edge of the sample are placed four electrodes, designated P, Q, R, and S. The distances between each pair of electrodes are a, b, and c respectively. The problem is

diagrammed in Figure [V-1].

It is first necessary to show that the following relationship holds:

$$\exp(-\pi R_{PQ,RS} d/\rho) + \exp(-\pi R_{QR,SP} d/\rho) = 1. \qquad [V-1]$$

d is the thickness of the sample, ρ is the specific resistivity, and $R_{PQ,RS}$, $R_{QR,SP}$ are quantities with dimensions of resistance which are obtained by dividing the potential difference between the first two electrode positions indicated in the symbol, by the current passed between the second two positions.

The validity of this equation can be shown by solving the flow equation for the conditions required for the measurement of the "resistances". Since the problem is cylindrically symmetrical and is uniform in the z direction across the thickness, the solution of Laplace's equation that gives the distribution of potential [75] is

$$\nabla^2 V = 0, \quad \text{or} \quad \frac{1}{r}\frac{\partial}{\partial r}\left(r \frac{\partial V}{\partial r} \right) = 0 \qquad [V-2]$$

or

$$r \frac{dV}{dr} = \frac{dV}{d\ln r} = \frac{j\rho}{\pi d} \qquad [V-3]$$

where V is the potential, j is the current entering the sample at P (for the first resistance measurement) and leaving it at Q, as shown in Figure [V-1]. The potential

FIGURE [V-1]

SEMI-INFINITE PLANE

FOR

VAN DER PAUW THEORY

FIGURE [V-1]

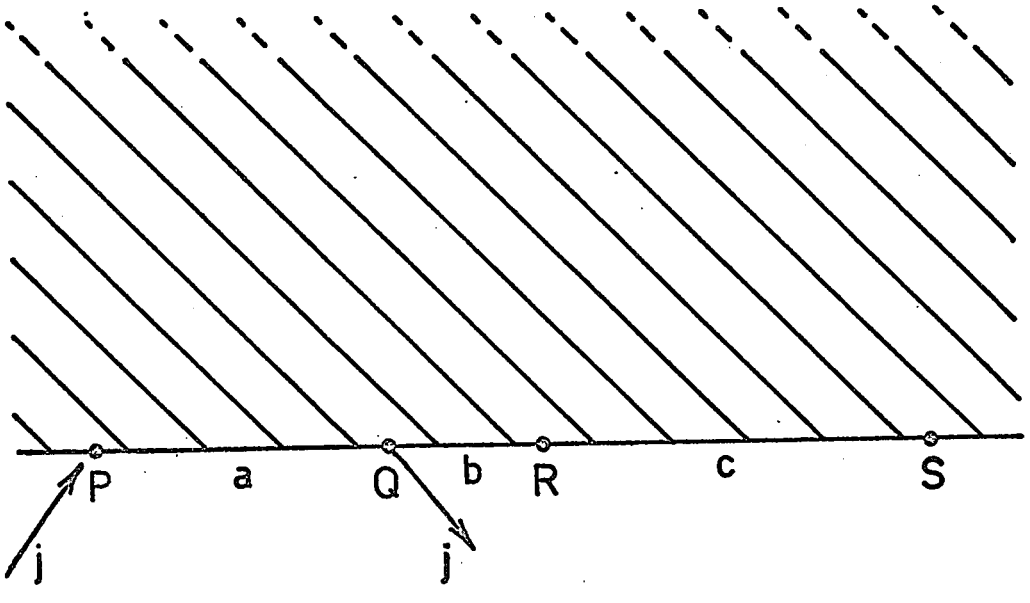

at position R under these conditions is

$$V_R = \frac{j\rho}{\pi d}[\ln r|_Q - \ln r|_P] \qquad [V-4]$$

$$V_R = \frac{j\rho}{\pi d} \ln b/(a + b) \qquad [V-5]$$

Similarly, the potential at position S can be found to be

$$V_S = \frac{j\rho}{\pi d} \ln(b + c)/(a + b + c) \qquad [V-6]$$

The potential difference can now be calculated by subtracting equation [V-6] from equation [V-4]. To obtain the resistance required in equation [V-1], this potential difference is divided by the current, j.

$$R_{PQ,RS} = \frac{\rho}{\pi d} \ln \frac{(a + b)(b + c)}{b(a + b + c)} \qquad [V-7]$$

The quantity $R_{PQ,RS}$ is referred to as a resistance, but it must be understood that it is not a conventional resistance. Usually, both the potential difference and the current are measured between the same two points. In this case, the positions across which the potential difference is measured are independent of the positions of the current electrodes.

In a similar manner, the other resistance required can be obtained. In this case, the current is passed between positions Q and R, while the potential difference is measured from position P to S.

$$R_{QR,SP} = \frac{\rho}{\pi d} \ln \frac{(a + b)(b + c)}{ac} \qquad [V-8]$$

This equation, and equation [V-7] can now be substituted into equation [V-1] and the following result is obtained:

$$(b(a + b + c) + ac)/(a + b)(b + c) = 1. \qquad [V-9]$$

By rearrangement of this equation, it is easy to see that the left hand side is indeed equal to unity, and therefore equation [V-1] does hold for a semi-infinite plane.

Now, from van der Pauw [27], the following equation is equivalent to equation [V-1] and is more convenient for obtaining the specific resistivity and therefore the electrical conductivity from experimental results:

$$\rho = \pi d \frac{(R_{AB,CD} + R_{BC,DA})}{2\ln 2} f\,(R_{AB,CD}/R_{BC,DA}) \qquad [V-10]$$

where f is a function of the ratio of the resistances only and is satisfied by the following relationship:

$$\frac{R_{AB,CD} - R_{BC,DA}}{R_{AB,CD} + R_{BC,DA}} = \frac{f}{\ln 2} \cosh^{-1} \frac{(\exp[\ln 2/f])}{2} \qquad [V-11]$$

In order to apply the theory to slabs of arbitrary shape, the technique of conformal mapping is introduced. Two facts are necessary to justify this step in the theory. Firstly, Riemann's Mapping Theorem [76] states that it is always possible to find an analytic function that will map a semi-infinite plane into a plane of arbitrary shape. Secondly, Laplace's equation is invariant under conformal

transformation [77]. This means that the potentials at corresponding points on the transformed problem will be identical to those on the semi-infinite plane. In the light of these facts, it can be seen that the theory is completely general for samples of arbitrary shape, subject to the restrictions enumerated earlier.

2. Cell Design

The design of the cell used for these measurements is shown in Figure [V-2]. The cell body was constructed of Plexiglass and the two halves of the cell were fitted together with a double O-ring seal in the same manner as all the cells used for the perpendicular measurement of electrical conductivity in the preceding chapter. The cell was cylindrically symmetrical, with the exception of four holes drilled into the side of the cell around the circumference to accommodate the electrodes. In the left half of the cell, the electrode chamber was U-shaped in cross section so that the cell could be used for different sizes of membranes by altering the thickness of the membrane chamber. The electrodes could slide to within 1.5 cm of the centre of the cell so that a sample of any size larger than 3 cm in diameter could be used.

The probe electrodes, supported on polytetrafluoroethylene plugs, are shown in Figure [V-3]. A double O-ring seal was used to hold the electrodes in the electrode chambers, so that they could slide back and forth in the electrode chamber. They could therefore make contact with samples of different diameters.

Two separate electrodes were constructed in each probe electrode, a larger one which was used as a current electrode, and a smaller one, bent so that it was very close to the larger electrode, to be used for the measurement of potentials. In this way, the problem of any polarization of the potential electrodes by the current was overcome [65]. Both electrodes were made from silver wires which were cemented in place with epoxy resin cement. These wires were led through the probe and attached to a larger copper wire so that electrical connections could be made more easily. One of the silver wires was insulated with a piece of polytetrafluoroethylene spaghetti so that the two electrodes were isolated from one another. Four identical probe electrodes were made for simultaneous use in the four electrode chambers in the cell.

FIGURE [V-2]

CELL DESIGN

MEASUREMENT PARALLEL TO THE MEMBRANE SURFACE

The diagram is drawn to scale.

The cell is made completely of plexiglass.

The O-ring seal is identical to those in Chapter IV.

The dashed lines show the position of one of the electrode chambers and of the tightening bolts.

FIGURE [V-3]

PROBE ELECTRODES

The diagram is drawn twice actual size.

The body of the electrode was made from polytetrafluoro-ethylene.

The black regions are made from silver wire.

Grooves in the side were made accurate dimensions in order to accommodate O-ring so that they would make a sliding seal when placed into the electrode chambers of the cell.

FIGURE [V - 2]

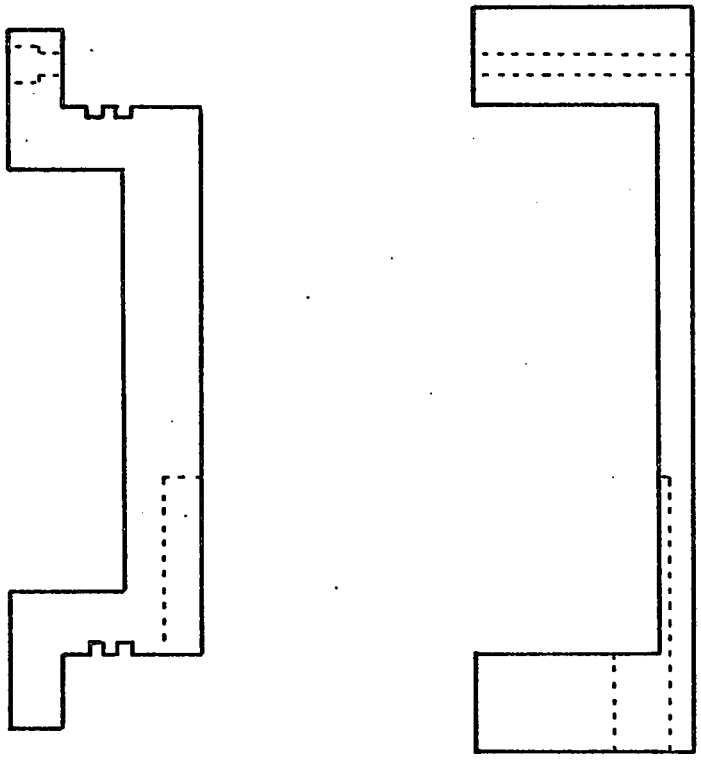

FIGURE [V - 3]

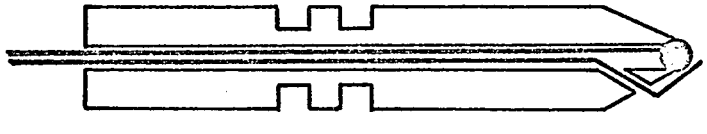

3. Experimental

(a) Method of Measurement

The electrodes were chloridized by passing a current of about 1 mA through 0.1 N hydrochloric acid solution for approximately 1 hour using the electrodes as the anode and a piece of platinum wire as the cathode [78]. All the electrodes were joined together so that they would be chloridized simultaneously. They were then allowed to equilibrate for three days in distilled water, and then for several hours in the same solution that was used for the equilibration of the membrane, before any measurements were made.

The circuit used for taking measurements is shown in Figure [V-4]. R_1 was a large resistance used for limiting the current flow to about 10 mA. R_S was a decade resistance box with decade steps from 0.1 to 1000 ohm across which the voltage drop was measured in order to determine the current accurately. S_1 was a double pole, double throw switch used for selecting either the decade resistance box, or the potential electrodes for determination of the potential difference. S_2 allowed the current flow through the cell to be reversed. S_3 was a switch for opening the circuit.

FIGURE [V-4]

EXPERIMENTAL SET-UP

S1 is the potential measuring switch. In the up position, the potential across points C and D on the sample is measured. In the down position, the potential across R_s (standard resistor) is measured to determine the current.

S2 is the current controlling switch. In the up position, current is allowed to flow between points A and B on the sample. In the down position, current flows through R_s for current measurement.

S3 is a switch used to arrest current flow.

R_1 is a large resistor used for changing the magnitude of the current.

FIGURE [V-4]

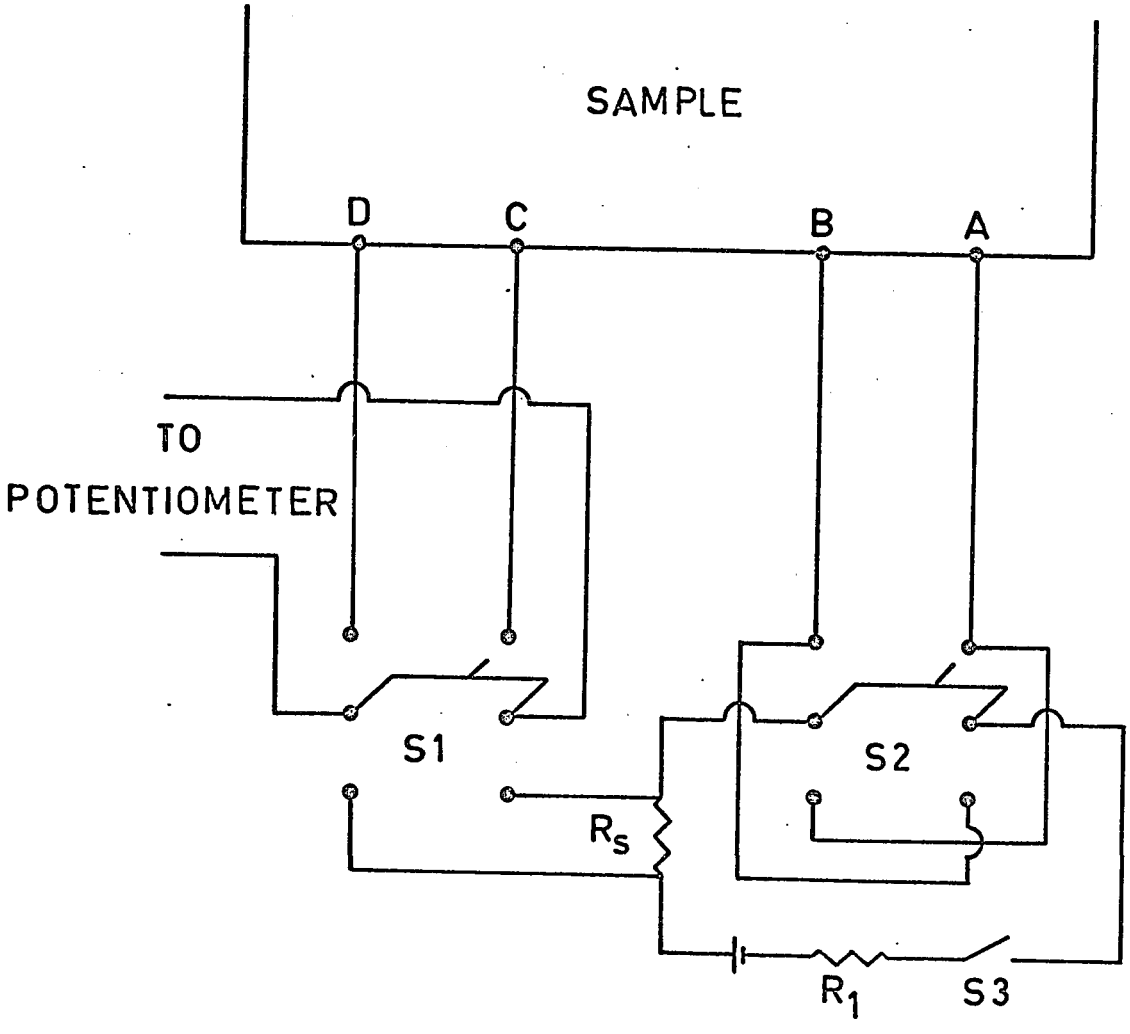

(b) Testing of Theory

The cell's operation and its agreement with predicted results were tested with potassium chloride solution. Spacers were placed between the two halves of the cell, along the outside edge so that a space was left inside the cell. This space was filled with potassium chloride solution of a known concentration. Readings were then taken in the following way. A current of about 10 mA was passed between the larger electrodes on two of the probe electrodes and the potential difference across the smaller electrodes on the other two probes was measured. The switch S_2 was then reversed, reversing the current, and another potential difference reading was taken. Half of the difference between these two readings was taken as the potential difference due to the current. This method was found to give reproducible results for a variety of current strengths. The size of the current was then obtained by changing the position of switch S_1 and measuring the potential difference across the known resistance R_s. One current electrode was then interchanged with one potential electrode and the measuring process was repeated. Potential difference measurements were taken using a type K-3 universal Potentiometer made by the Leeds and Northrup Co., Philadelphia.

Results were obtained for several different thicknesses of potassium chloride solution by varying the thickness of the spacers at the edge of the cell.

(c) Membranes

The membrane to be measured was placed into the cell and the two halves were fitted together so that the sample was held snugly. The probe electrodes were then adjusted so that all electrodes were in contact with the sample. Measurements were then made in the same manner as was used with the potassium chloride solution. Samples of cellulose membranes, porous glass membranes and polyvinylbenzenesulfonate membranes were measured in this way. In all cases both the membrane and the probe electrodes were equilibrated in the appropriate potassium chloride solution for several hours before any measurements were taken.

4. Results

(a) Testing of Theory

Measurements were made using potassium chloride solutions with concentrations of 0.05 N and 0.005 N. Six different thicknesses of the solution chamber were used.

Because of the design of the cell, excess solution was required to fill up the space left for the manipulation

of the electrodes. Therefore, the thickness of the solution layer in the cell was not uniform, as is required by the theory [27]. This excess solution would conduct current and reduce the potential difference across the cell, giving a conductivity which was higher than would be expected.

This effect was accounted for in the following way. It was assumed that the excess solution constituted an additive constant to the thickness of the potassium chloride solution sample. This is a valid assumption if the excess constitutes a reasonably small fraction of the total thickness of the sample. If the thickness then, is broken into two parts, equation [V-10] becomes

$$\rho = A(d + d') \qquad [V-12]$$

where d is the actual thickness of the sample as measured, d' is the part of the thickness contributed by the excess solution, and A is given by

$$A = \frac{\pi}{2\ln 2} \left(R_{AB,CD} + R_{BC,DA}\right) f\left(\frac{R_{AB,CD}}{R_{BC,DA}}\right) \qquad [V-13]$$

and is a function only of the resistances to be measured. Rearranging equation [V-12] gives

$$\frac{1}{A} = \frac{d}{\rho} + \frac{d'}{\rho} = kd + kd' \qquad [V-14]$$

Therefore, if the inverse of A is plotted against the thickness of the sample, the slope will be the electrical

conductivity of the sample; that is, of the potassium chloride solution.

The results are tabulated in Table [V-1] and plotted in Figure [V-5]. For 0.05 N potassium chloride solution at a Celsius temperature of 22 K, using a linear least squares fit for the data, a value for the electrical conductivity of 0.00645 ohm^{-1} cm^{-1} was obtained and for 0.005 N potassium chloride solution at 23 K, a value of 0.000694 ohm^{-1} cm^{-1} was found. The comparable literature values are 0.00642 and 0.000694 ohm^{-1} cm^{-1} respectively [64].

(b) Membranes

The results obtained for cellulose membranes, porous glass and polyvinylbenzenesulfonate membranes are shown in Table [VI-1] in the next chapter, along with the corresponding results normal to the membrane surface. No extra manipulation of the data was required since the non-uniformity of the sample thickness is peculiar to the use of liquid samples.

5. Discussion

The operation and theory of this type of cell appears to give good results. The difficulties in testing resulted from the necessity of using a liquid standard, but

TABLE [V-1]

TESTING OF CELL WITH KCl

THICKNESS (cm)	$R_{AB,CD}$ (ohm)	$R_{BC,DA}$ (ohm)	f	ρ_{app} (ohm-cm)	$d\kappa_{app} \times 10^4$ (ohm^{-1})
---- 0.005 N at 22.0°C ----					
0.655	367.0	556.8	0.9852	1352.3	4.844
0.585	408.3	620.9	0.9850	1344.0	4.353
0.505	453.8	705.5	0.9834	1304.7	3.871
0.425	532.4	824.3	0.9837	1285.4	3.306
0.345	643.5	1000.8	0.9834	1264.2	2.729
0.270	788.4	1241.2	0.9825	1220.1	2.213
---- 0.05 N at 23°C ----					
0.655	36.60	58.42	0.9815	138.4	47.33
0.575	41.60	65.72	0.9822	137.3	41.89
0.490	46.66	75.66	0.9803	133.2	36.79
0.410	53.90	88.30	0.9794	129.3	31.71
0.330	65.09	106.51	0.9794	125.7	26.25
0.250	82.35	135.33	0.9793	120.7	20.71
0.175	113.01	187.13	0.9788	116.3	15.05

FIGURE [V-5]

TESTING OF ELECTRICAL CONDUCTIVITY CELL

WITH

POTASSIUM CHLORIDE SOLUTION

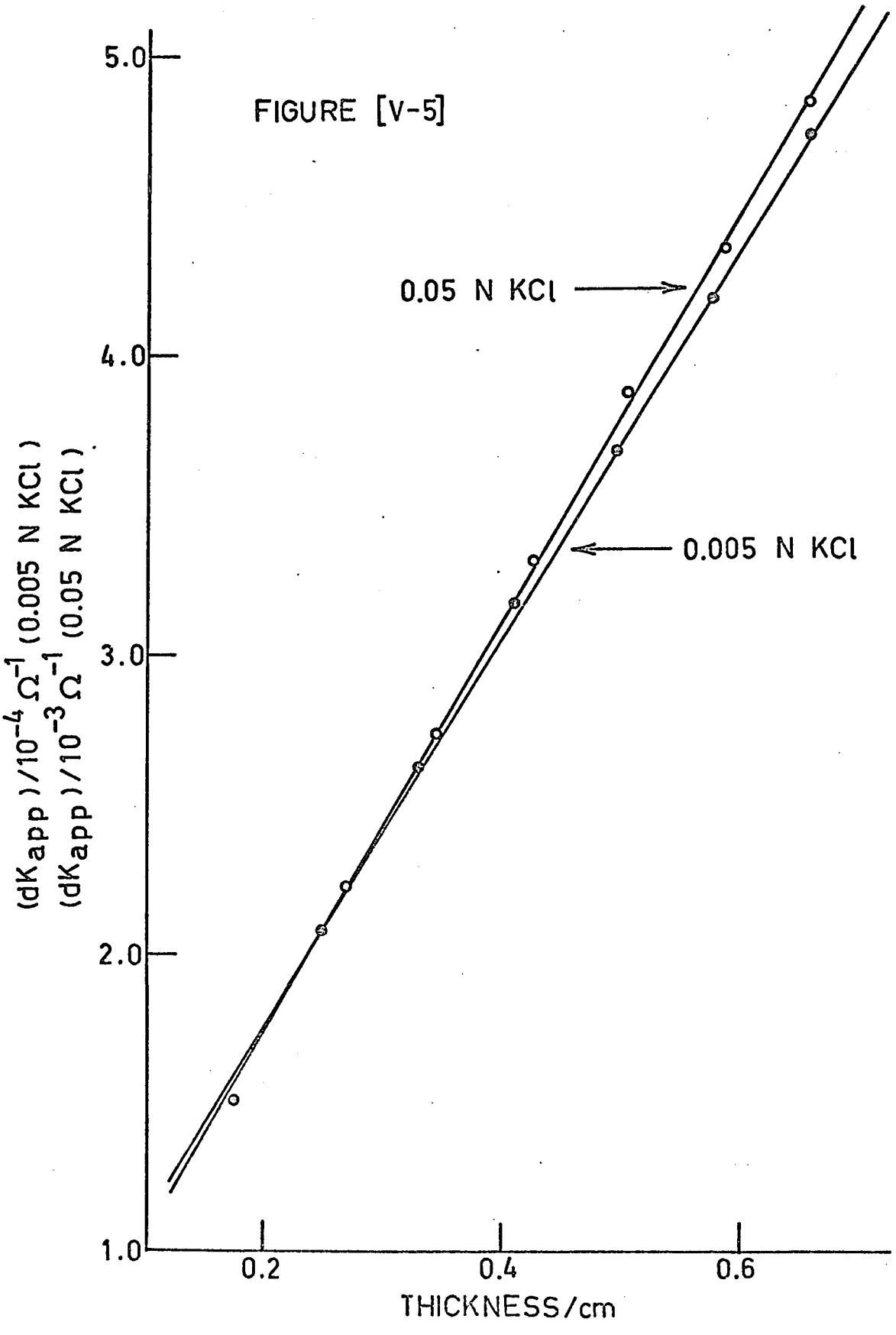
FIGURE [V-5]
0.05 N KCl
0.005 N KCl
5.0
4.0
3.0
2.0
1.0
0.2
0.4
0.6
THICKNESS/cm
$(dK_{app})/10^{-4}\Omega^{-1}$ (0.005 N KCl)
$(dK_{app})/10^{-3}\Omega^{-1}$ (0.05 N KCl)

even with the extra correction factor, the agreement appears to be quite acceptable.

A comparison of the results obtained for membranes from the two methods so far described can also give some indication of the acceptability of not only this method, but the method for the measurement of electrical conductivity perpendicular to the membrane surface. This can only be done with some discussion of the anisotropy of the membranes, however, and this will be done in the next chapter.

6. Comparison with Other Work

Few results for the electrical conductivity parallel to the membrane surface are available. Meares and Ussing [14] have performed both alternating and direct current measurements using methods described by Hills, Jakubovic and Kitchener [80], and by Lorimer [21]. The major difference between their method and ours is the membrane shape. Their membrane must be cut into a strip of uniform and accurately known dimensions. In the method used in this work, only the thickness need be uniform.

CHAPTER VI

ANISOTROPY OF MEMBRANES

1. Theory

The anisotropy, α, of the electrical conductivity of a membrane can be defined as follows:

$$\alpha = \frac{\rho_{//} - \rho_{\perp}}{\rho_{//} + \rho_{\perp}} = \frac{\kappa_{\perp} - \kappa_{//}}{\kappa_{\perp} + \kappa_{//}} \qquad [VI-1]$$

where $\rho_{//}$ is the specific resistivity of the membrane parallel to its surface, and $\rho_{\perp}$ is the specific resistivity measured perpendicular to the membrane surface, and $\kappa_{//}$ and $\kappa_{\perp}$ are similarly defined electrical conductivities. The value of this anisotropy can vary from zero, when the electrical conductivity is the same in both directions, to 1, when the electrical conductivity is very small in one direction compared to the other. A plot of the anisotropy as a function of the ratio of the specific resistivities is shown in Figure [VI-1]. The allowable values of the anisotropy fall on the curve.

2. Results

The results obtained for the electrical conductivity normal to the membrane surface in chapter IV are

FIGURE [VI-1]

GRAPH OF ANISOTROPY

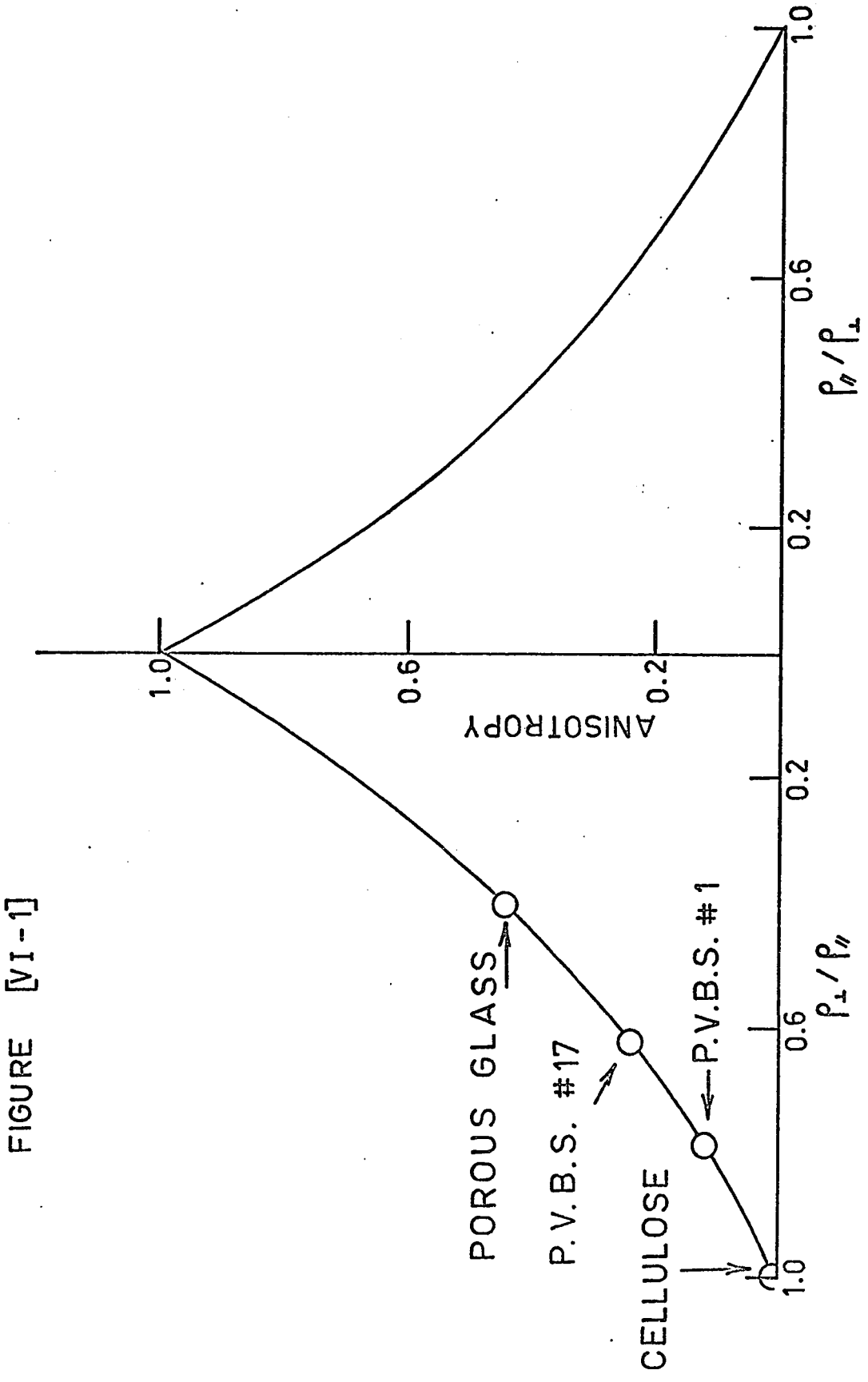
1.0
0.6
0.2
ANISOTROPY
1.0
0.6
0.2
$\rho_{\parallel}/\rho_{\perp}$
1.0
0.6
0.2
$\rho_{\perp}/\rho_{\parallel}$
POROUS GLASS
P.V.B.S. #17
P.V.B.S. #1
CELLULOSE

FIGURE [VI-1]

given in Table [VI-1] along with the results obtained parallel to the surface of the membrane from chapter V. From these measurements, the values for the anisotropy have been calculated, tabulated in Table [VI-1] and their locations plotted in Figure [VI-1].

3. Discussion

The value obtained for the anisotropy for cellulose membranes was zero within the errors of the measurement. This result would be expected from the manner in which the membranes were prepared (slow coagulation of viscose between porous porcelain sheets). The results show that they were uniform throughout. The results for these membranes are additional proof of the validity of the theories and apparatus used for both methods of measurement since the results not only agree independently with potassium chloride solution standards, but are consistent with each other.

The polyvinylbenzenesulfonate membranes do show anisotropy. The possible causes for this may be found in their method of manufacture. First, the membranes, polymerized thermally, would polymerize initially at the outer surface and then inward, toward the centre of the membrane. This suggests the possibility of a surface layer with properties different from those of the bulk of the membrane. Observations of the physical appearance of the membranes

TABLE [VI-1]

ELECTRICAL CONDUCTIVITIES AND ANISOTROPY OF MEMBRANES

MEMBRANE	CONCENTRATION KCl	ANISOTROPY	CONDUCTIVITY (ohm^{-1} cm^{-1}) PARALLEL	PERPENDICULAR
CELLULOSE	0.1 N	0	7.17×10^{-3}	7.12×10^{-3}
	0.05 N	0	3.76×10^{-3}	3.79×10^{-3}
	0.01 N	0	9.53×10^{-4}	9.45×10^{-4}
	0.005 N	---	5.45×10^{-4}	---
P.V.B.S. # 1	0.1 N	---	1.242×10^{-2}	---
	0.05 N	---	1.108×10^{-2}	---
	0.01 N	0.116	7.69×10^{-3}	9.74×10^{-3}
P.V.B.S. # 17	0.1 N	0.229	1.109×10^{-2}	1.77×10^{-2}
VYCOR	0.1 N	0.421	5.52×10^{-4}	1.35×10^{-3}

and their behaviour in liquids (they tend to assume a saddle-shaped configuration) support this idea. However, this model of the membrane will always result in a value of the anisotropy for the ratio $\rho_{\perp}/\rho_{\parallel}$ greater than unity, in contradiction to the results obtained here.

The second model of the membrane is concerned with the mobilities of the ions through the membrane. Since the membranes are polymerized from the outer edge inward, the polymer chains constituting the body of the membrane could become oriented across the narrowest dimension of the membrane possibly because of monomer flow during polymerization. This situation would allow a greater mobility of the ions in this direction compared with a direction perpendicular to it. As was shown in equation [II-56], the electrical conductivity is proportional to the sum of the mobilities of the ions in solution. This model can be thought of, then, as a large number of parallel elements across the narrowest dimension of the membrane so that their ends form the surfaces of the membrane. The anisotropy, in this case, would be in the direction obtained in the experiments. The actual situation is most likely a combination of these two models, with the second one predominating.

The porous glass membranes also showed anisotropy. This was probably also due to their method of preparation. Close inspection of all samples showed a fine line running through this type of membrane parallel to its faces. This type of porous glass is prepared by leaching a soft glass with a solution of phosphoric and hydrofluoric acids [79]. Since the product comes in sheets, the leaching would proceed predominantly from the large faces toward the centre of the sheet. The line in the membrane is likely caused by the overlapping of the leaching process from both sides of the sheet. Because this leaching was in one direction, it would be expected that the passage of a current should be more easy in this direction than in a direction perpendicular to it since the pores in the membrane would be largely oriented across the thickness of the sample and ions would be able to pass more easily in this direction. Therefore, in this case as well, the electrical conductivity could be expected to be, and is, larger in the direction perpendicular to the surface of the membrane than in the parallel direction.

No values for the anisotropy of membranes have been reported previously. In order to calculate it, independent measurements both perpendicular and parallel to the

membrane surface must be made. This is the first time that results have been obtained in both directions on the same membranes, and therefore made this calculation possible.

CHAPTER VII

THERMAL CONDUCTIVITY

1. Theory

(a) Introduction

The methods of measurement of the thermal conductivity in non-conductors usually rely on the difference of the thermal conductivity between the sample and the metal blocks which are used as the heat source and the heat sink [81-83]. A temperature gradient is set up across the sample and the heat flow across that sample is dependent upon the thermal conductivity of the sample.

The major problem encountered in the use of this method is a contact resistance between the sample and the metal blocks [84]. That is, the heat flow between the block and the sample is not continuous because of the presence of a small contact film between them. This causes an increase in the apparent temperature gradient across the sample since, in practice, this measurement can only be made with reasonable accuracy in the metal block. The resulting calculated value of the thermal conductivity will be lower than the actual value.

The most common method of minimizing this error is the application of pressure across the sample between the heat source and the heat sink. This should tend to reduce the size of the contact films and therefore make the metal-to-sample contact more closely perfect. For a solid sample, this method will work if the pressure required is not large enough to distort it. For ion-selective membranes, however, this is not acceptable. The membranes are saturated with solution and any excess pressure applied will not only squeeze the membrane and possibly change its characteristics, but will also squeeze some of the solution out of the membrane into the metal-sample interface. Therefore, applied pressure will probably not improve the thermal contact and may even make it worse. Theories are needed, then, to not only describe the operation of any apparatus used, but also to account for the presence of contact films between the sample and the heat source and heat sink.

A large number of possible steady state and non-steady state methods were investigated theoretically. Initially experiments were conducted using a steady state method. A series of thermocouples was placed along the side of the heat sink. The end farther from the sample, and the heat source, were kept at constant temperatures. A plot of

the temperature as a function of the distance from the sample along the heat sink then gave the required information for the calculation of the thermal conductivity. Several difficulties were found in this method. The time required to reach a steady state was long (about 2 hours) and therefore, there was a danger that the membrane would lose some of its solution due to evaporation during this time. This would change the characteristics of the sample and the results would be meaningless. Also, a large portion of the temperature drop was across the sample, leaving only about 10 percent of it along the length of the heat sink. This would have the effect of making the contributions of any uncertainties in the readings along the heat sink ten times as large. Difficulties were also encountered in keeping all of the thermocouples insulated from one another. Therefore, this method was discarded.

A non-steady state method was adopted finally and will be described in section (b) below.

(b) Theory of Thermal Conductivity Apparatus

This method applies a constant temperature to the top of the sample and the change in the temperature of a heat sink is measured as a function of time. The theory of this cell is similar to a problem studied by Carslaw and

FIGURE [VII-1]

THERMAL CONDUCTIVITY CELL

BOUNDARY CONDITIONS

FIGURE [VII-1]

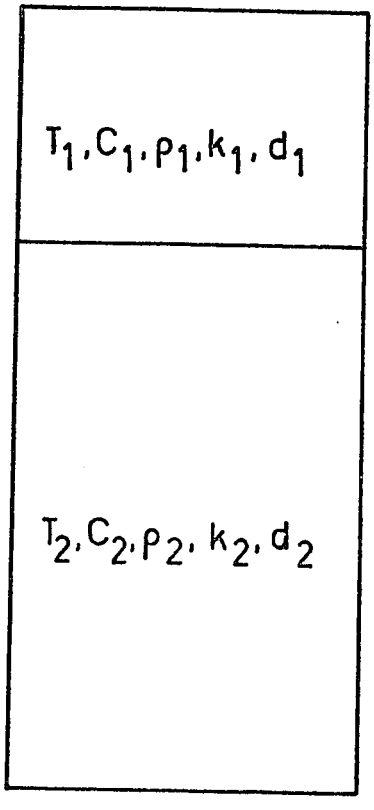

$x = -l, \quad -k_1 \partial T_1/\partial x = (T_s - T_1) H'$

$x = 0, \quad T_1 = T_2,$ and

$k_1 \partial T_1/\partial x = k_2 \partial T_2/\partial x$

$= (T_2 - T_1) H$

$x = a, \quad \partial T_2/\partial x = 0$

Jaeger [85], and involves a composite cylinder as shown in Figure [VII-1]. It is assumed that there is no radial heat flow. The top segment represents the sample and is defined by the quantities T_1, C_1, ρ_1, k_1, and D_1, where T is the temperature, C is the heat capacity, ρ is the density, k is the thermal conductivity and D is the thermal diffusivity which is defined as

$$D = k/C\rho \qquad [VII-1]$$

and the subscript refers to the sample section of the cylinder. The second segment represents the heat sink and is defined by the quantities T_2, C_2, ρ_2, k_2 and D_2.

In order to solve this problem, boundary conditions must first be set up and then the flow equation solved. The first condition is the condition at the beginning of the experiment:

$$t = 0, \quad -\ell \leq x \leq a, \quad T = T_o \qquad [VII-2]$$

Thus, the experiment starts out with the entire apparatus at a uniform temperature, T_o. The rest of the boundary conditions are shown in Figure [VII-1]. At any time after the start of the experiment, the heat source is at a temperature T_s. Because of the presence of a contact film between the heat source and the first segment of the composite cylinder (the sample segment), a radiation boundary condition is

used [86]:

$$t > 0, \quad x = -\ell, \quad -k_1 \, \partial T_1/\partial x = H'(T_s - T_1) \qquad \text{[VII-3]}$$

where

$$H' = k'/d' , \qquad \text{[VII-4]}$$

and k' is the thermal conductivity of the contact film which has a thickness d'.

A similar boundary condition applies on the other side of the sample segment:

$$t > 0, \quad x = 0, \quad -k_1 \, \partial T_1/\partial x = -k_2 \, \partial T_2/\partial x$$

$$= k(T_1 - T_2)/d = H(T_1 - T_2) \qquad \text{[VII-5]}$$

This boundary condition requires that the heat flow out of the sample segment is identical to the heat flow into the heat sink segment. That is, there should be no heat loss in the contact film between the two segments of the composite cylinder.

The final boundary condition concerns the other end of the heat sink (the second segment of the cylinder). It requires that no heat is lost out of the end of the heat sink:

$$t > 0, \quad x = a, \quad k_2 \, \partial T_2/\partial x = 0 \qquad \text{[VII-6]}$$

The problem can now be solved by applying these conditions to the one dimensional heat flow equation.

$$\partial T/\partial t = (k/C_\rho)\,\partial^2 T/\partial x^2 \qquad \text{[VII-7]}$$

The time dependence can be removed from this equation to make its manipulation less tedious with the use of the Laplace Transform [87]. The Laplace Transform of a time dependent function f(t) is defined by the equation

$$\bar{f}(p) = \int_0^\infty \exp(-pt)\ f(t)\ dt \qquad \text{[VII-8]}$$

where $\bar{f}$ is a function of p, and p is a number whose real part is positive and large enough to make the integral in equation [VII-8] convergent.

If both sides of the heat flow equation are multiplied by [exp(-pt)] and then integrated from zero to infinity with respect to time, the following result is obtained:

$$\int_{t=0}^{t=\infty} \exp(-pt)\,dt = \frac{k}{C_\rho}\frac{\partial^2}{\partial x^2}\int_{t=0}^{t=\infty} T\ \exp(-pt)\ dt \qquad \text{[VII-9]}$$

If the left hand side of this equation is integrated by parts, and equation [VII-8] employed, the result is the transformed heat flow equation.

$$\bar{T}-\bar{T}_o = (k/Cp\rho)\ d^2(\bar{T}-\bar{T}_o)/dx^2 \qquad \text{[VII-10]}$$

$\bar{T}$ is the transformed temperature, and $\bar{T}_o$ is the transformed temperature at the beginning of the experiment.

The general solution of this equation for a composite cylinder is the following [88]:

$$\bar{T}_i - \bar{T}_o = A_i \cosh(q_i x) + B_i \sinh(q_i x) \qquad i = 1,2 \qquad \text{[VII-11]}$$

$$q_i = (pC_i\rho_i/k_i)^{1/2}. \qquad \text{[VII-12]}$$

The subscript i refers to the segment of the cylinder in which the temperature is being measured. This means that there are four constants, A_1, A_2, B_1, and B_2, that must be determined by using the boundary conditions. The equations for these must be transformed in the same way as the flow equation. If this is done, the transformed boundary conditions are found to be:

(1) $t = 0, \quad -\ell \leq x \leq a, \quad \bar{T} = \bar{T}_o = T_o/p$ [VII-13]

(2) $t > 0, \quad x = -\ell, \quad -k_1 d\bar{T}_1/dx = H'(\bar{T}_s - \bar{T}_1)$ [VII-14]

(3) $t > 0, \quad x = 0, \quad -k_1 d\bar{T}_1/dx = -k_2 d\bar{T}_2/dx$

$$= H(T_2 - T_1) \qquad \text{[VII-15]}$$

(4) $t > 0, \quad x = a, \quad k_2 \, d\bar{T}/dx^2 = 0$ [VII-16]

The first condition has already been used in order to obtain equation [VII-10] and make it satisfy the initial conditions. The other three equations are sufficient to evaluate the four constants since the third condition is actually two equations.

Applying boundary condition (4) to equation [VII-11] gives the result

$$B_2 = -A_2 \sinh(q_2 a)/\cosh(q_2 a) \qquad \text{[VII-17]}$$

Boundary condition (3) is applied to give the following:

$$-k_1 q_1 B_1 = -k_2 q_2 B_2 = H(A_1 - A_2), \qquad \text{[VII-18]}$$

and finally, the second boundary condition can be applied to give the result

$$-k_1 q_1 [-A_1 \sinh(q_1 \ell) + B_1 \cosh(q_1 \ell)]$$
$$= H' [\bar{T}_s - \bar{T}_o - A_1 \cosh(q_1 \ell) + B_1 \sinh(q_1 \ell)] \qquad \text{[VII-19]}$$

$$[k_1 q_1 \sinh(q_1 \ell) + H' \cosh(q_1 \ell)] A_1$$
$$= H' [\bar{T}_s - \bar{T}_o] + [k_1 q_1 \cosh(q_1 \ell) + H' \sinh(q_1 \ell)] \qquad \text{[VII-20]}$$

Equation [VII-18] gives an expression for B_2:

$$B_2 = -H(A_1 - A_2)/k_2 q_2 , \qquad \text{[VII-21]}$$

which can be substituted into equation [VII-17] to give

$$H(A_1 - A_2)/k_2 q_2 = A_2 \sinh(q_2 a)/\cosh(q_2 a) \qquad \text{[VII-22]}$$

$$A_1 = A_2 (k_2 q_2 \sinh(q_2 a)/H \cosh(q_2 a)) \qquad \text{[VII-23]}$$

Again, from equations [VII-17] and [VII-18], an expression for B_1 can be obtained in terms of A_2.

$$B_1 = -\sigma A_2 \sinh(q_2 a)/\cosh(q_2 a) \qquad \text{[VII-24]}$$

where

$$\sigma = k_2 q_2 / k_1 q_1 \qquad \text{[VII-25]}$$

Now, the substitution of equations [VII-23] and [VII-24] into equation [VII-20] gives an expression which determines

A_2 in terms of the characteristic properties of the system:

$$A_2[k_1q_1\sinh(q_1\ell) + H'\cosh(q_1\ell)][k_2q_2\sinh(q_2a)/H\cosh(q_2a) + 1]$$
$$= H'[\bar{T}_s-\bar{T}_o] - A_2[k_1q_1\cosh(q_1\ell) + H'\sinh(q_1\ell)]\times$$
$$\sigma\sinh(q_2a)/\cosh(q_2a) \qquad \text{[VII-26]}$$

$$A_2 = (\bar{T}_s-\bar{T}_o)\cosh(q_2a)/\{[k_1q_1\sinh(q_1\ell)/H' + \cosh(q_1\ell)]$$
$$[k_2q_2\sinh(q_2a)/H + \cosh(q_2a)] + [k_1q_1\cosh(q_1\ell)/H'$$
$$+ \sinh(q_1\ell)]\ \sigma\sinh(q_2a)\} \qquad \text{[VII-27]}$$

Thus, the equations for the temperature in each segment can be written down:

$$\frac{\bar{T}_1-\bar{T}_o}{\bar{T}_s-\bar{T}_o} = \{[\cosh(q_2a) + k_2q_2\sinh(q_2a)/H]\cosh(q_2\beta x)$$
$$- \sinh(q_2a)\sinh(q_2\beta x)\}/Q \qquad \text{[VII-28]}$$

$$\frac{\bar{T}_2-\bar{T}_o}{\bar{T}_s-\bar{T}_o} = [\cosh(q_2a)\cosh(q_2x) - \sinh(q_2a)\sinh(q_2x)]/Q \qquad \text{[VII-29]}$$

where

$$Q = [k_1q_1\sinh(q_1\ell)/H' + \cosh(q_1\ell)][k_2q_2\sinh(q_2a)/H$$
$$+ \cosh(q_2a)] + \sigma\sinh(q_2a)[k_1q_1\cosh(q_1\ell)/H'$$
$$+ \sinh(q_1\ell)] \qquad \text{[VII-30]}$$

and

$$\beta = q_1/q_2 = [D_2/D_1]^{1/2} \qquad \text{[VII-31]}$$

The next step in the solution is the transformation of these equations back into their original time dependent form. This is accomplished by means of the inversion theorem of the Laplace Transform [87]. Its application to the result for the temperature in the second segment of the composite cylinder gives the following:

$$T_2-T_o = \frac{T_s-T_o}{2\pi i}\int_{\gamma-i\infty}^{\gamma+i\infty}\exp(pt)\cosh(q_2[a-x])\,dp/pQ \qquad [VII-32]$$

The limits of the integration are such that the quantity p is integrated over all imaginary space at some arbitrary constant real value. This equation can be solved by the implementation of Cauchy's theorem of Residues [89]. This theorem can be expressed by the equation

$$\oint_c f(p)\,dp = 2\pi i a_{-1} \qquad [VII-33]$$

where the integral is taken around a closed curve and a_{-1} are the residues of the integral, calculated from the equation

$$a_{-1} = \lim_{p\to a}(p-a)f(p) \qquad [VII-34]$$

and a is any point at which the argument of the integral, f(p), becomes infinite.

Since the temperature in the heat sink is what is important as far as experimental measurement is concerned,

T_2-T_o will be calculated by this procedure. For equation [VII-32], there are two poles at which the residue must be calculated. One is at p = 0, and the other is at the roots of the equation Q = 0. At p = 0, if equation [VII-12] is employed in Equation [VII-32] to convert each p to q_2 and the limit then taken as q_2 approaches zero (an equivalent condition), then the result obtained is

$$a_{-1} = \lim_{q_2 \to o} [q_2^2 D_2 (T_s-T_o)/2\pi i \; q_2^2 D_2]$$

$$= (T_s-T_o)/2\pi i \qquad \text{[VII-35]}$$

The evaluation of the residues at the other poles is more tedious. Let the roots of the equation Q = 0 be $i\gamma_m$. Then, from equation [VII-12],

$$p = -\gamma_m^2 D_2 . \qquad \text{[VII-36]}$$

The subscript, m, identifies each of the infinite number of roots of the equation being considered. By using equation [VII-12], the equation to be solved at each of these roots is

$$(a_{-1}) = \lim_{q_2 \to i\gamma_m} \frac{(T_s-T_o)\exp(q_2^2 D_2 t)(2q_2 D_2)\cosh(q_2[a-x])}{2\pi i q_2^2 D_2 Q} (q_2-i\gamma_m) \qquad \text{[VII-37]}$$

L'Hopital's rule [90] is now used. For an equation similar to that above, the following relationship is obtained:

$$\lim_{q_2 \to i\gamma_m} (q_2-i\gamma_m) f(q_2) = \lim_{q_2 \to i\gamma_m} \frac{1}{d(1/f(q_2))/dq_2} \qquad \text{[VII-38]}$$

From equation [VII-37], the function required for equation [VII-38] is

$$f(q_2) = \frac{(T_s-T_o)\exp(q_2^2 D_2 t)\cosh(q_2[a-x])}{2\pi i q_2 Q} \qquad [VII-39]$$

Thus

$$\begin{aligned} d(1/f(q_2))/dq_2 &= [2\pi i/(T_s-T_o)]\{\exp(-q_2^2 D_2 t)Q/\cosh(q_2(a-x)) \\ &\quad - 2q_2^2 D_2 t Q \exp(-q_2^2 D_2 t)/\cosh(q_2(a-x)) \\ &\quad - q_2(a-x)Q\sinh(q_2(a-x))\exp(-q_2^2 D_2 t)/\cosh^2(q_2(a-x)) \\ &\quad + [q_2 \exp(-q_2^2 D_2 t)/\cosh(q_2(a-x))]dQ/dq_2\} \end{aligned} \qquad [VII-40]$$

When this equation is substituted into equation [VII-38] and the limit taken as the root involved is approached, the first three terms in the above equation vanish and the final result for the residue at the m^{th} root is

$$(a'_{-1})_m = (T_s-T_o)\cosh(i\gamma_m[a-x])\exp(-\gamma_m^2 D_2 t)/(-2\pi\gamma_m(dQ/dq_2)) \qquad [VII-41]$$

where the derivative is evaluated at $i\gamma_m$ and

$$\begin{aligned} F(\gamma_m) = \frac{dQ}{dq_2} &= [\beta(\frac{k_1}{H'} + \ell)\sin(\beta\gamma_m\ell) + \beta^2 \frac{\gamma_m k_1 \ell}{H'}\cos(\beta\gamma_m\ell)] \\ &\quad \times [\cos(\gamma_m a) - \frac{k_2\gamma_m}{H}\sin(\gamma_m a) \\ &\quad + \sigma a\cos(\gamma_m a)[k_1\cos(\gamma_m\beta\ell) + \sin(\gamma_m\beta\ell)] \end{aligned}$$

$$+ \left[\cos(\gamma_m\beta\ell) - \frac{\gamma_m\beta k_1}{H'} \sin(\gamma_m\beta\ell)\right] \times$$

$$\left[a\left(\frac{k_2}{H} + 1\right)\sin(\gamma_m a) + \frac{k_2\gamma_m a}{H}\cos(\gamma_m a)\right.$$

$$\left. + \sigma\sin(\gamma_m a)\left[\beta\left(\frac{k_1}{H'} + \ell\right)\cos(\gamma_m\beta\ell) - \frac{\gamma_m\beta^2 k_1\ell}{H'}\sin(\gamma_m\beta\ell)\right]\right.$$

[VII-42]

The summation of the residues, according to equation [VII-32], gives the equation for the temperature in the heat sink, T_2-T_o.

$$\frac{T_2-T_o}{T_s-T_o} = 1 - 2\sum_{m=1}^{\infty} \exp(-\gamma_m^2 D_2 t)\cos(\gamma_m[a-x])/\gamma_m F(\gamma_m) \qquad [VII-43]$$

(γ_m) are the roots of the equation

$$[1 - \beta\gamma_m k_1 \tan(\gamma_m\beta\ell)/H'][1 - \gamma_m k_2 \tan(\gamma_m a)/H]$$

$$- \sigma\tan(\gamma_m a)[\beta\gamma_m k_1/H' + \tan(\gamma_m\beta\ell)] = 0 \qquad [VII-44]$$

The inversion theorem is applied in a similar manner to the temperature in the sample segment to obtain the following expression:

$$\frac{T_1-T_o}{T_s-T_o} = 1 - 2\sum_{m=1}^{\infty} \exp(-\gamma_m^2 D_2 t)\left[(\cos(\gamma_m a) - \frac{k_2\gamma_m}{H}\sin(\gamma_m a))\cos(\gamma_m\beta x) + \sin(\gamma_m a)\sin(\gamma_m\beta x)\right].$$

[VII-45]

Equations [VII-43] and [VII-45] are the complete solution to the problem of heat flow in a composite cylinder with one end insulated and the other at a constant temperature.

(c) Approximations to the Theory

The solution obtained for the thermal conductivity apparatus is theoretically correct, but several approximations can be made in order that it be of most use for the interpretation of experimental data.

The measurements of the temperature difference are to be made between the heat source at a constant temperature ($T_s - T_o$) and the heat sink at a temperature of $T_2 - T_o$. Therefore, $T_2 - T_s$ is the quantity that will be used for the calculation of the thermal conductivity and the approximations are therefore applied to it.

The first approximation to be made is the assumption that only the first root of equation [VII-44] is important when T_2 is calculated. Equation [VII-43] can then be written as

$$\frac{\Delta T}{T_s - T_o} = A \exp(-\gamma^2 D_2 t) \qquad [VII-46]$$

where

$$\Delta T = T_s - T_2 \qquad [VII-47]$$

and A is a constant depending on the characteristics of the system and the position in the heat sink at which the temperature is measured:

$$A = 2\cos(\gamma[a-x])/\gamma F(\gamma) \qquad [VII-48]$$

The temperature difference between the heat source and the heat sink decays exponentially as a function of time towards zero. If logarithms are taken of both sides of equation [VII-47], it is found that the logarithm of the temperature difference is directly proportional to the time from the beginning of the experiment. Thus, a plot of the logarithm of ΔT against the time will give a straight line relationship in which the slope, m, is related to the value of γ.

$$\ln(\Delta T) = \ln(A[T_S - T_O]) - \gamma^2 D_2 t \qquad [VII-49]$$

$$m = -\gamma^2 D_2 \qquad [VII-50]$$

This equation can therefore be used to obtain a value which can be substituted into equation [VII-44] to solve that equation for the thermal conductivity of the sample, k_1. However, because no direct value for H and H' is known, and because of the difficulties in evaluating this equation, further approximations must be made.

Equation [VII-44] is the equation which is manipulated since it relates the experimental slope (through

equation [VII-50]) to the thermal conductivity of the sample, k_1. If it is assumed that the thicknesses of the contact films is small, then both H and H′ will become large (from equation [VII-4]) and equation [VII-44] can be approximated by

$$1 - \sigma \tan(\gamma a) \tan(\gamma \beta \ell) = 0 \qquad \text{[VII-51]}$$

In order to take into account the presence of boundary layers, the approximation is treated in a different manner. It is first assumed that $\gamma\beta\ell$ is small compared to unity, and that therefore the tangent of this quantity can be replaced by the quantity itself. If this approximation is used in equation [VII-44] then the following is obtained:

$$\tan(\gamma a) \left[\frac{k_2 \gamma}{H} \left(\frac{\beta^2 k_1 \ell \gamma^2}{H'} - 1 \right) - \sigma\beta\gamma \left(\frac{k_1}{H'} + \ell \right) \right] = \frac{\beta^2 k_1 \ell \gamma^2}{H'} - 1 \qquad \text{[VII-52]}$$

This equation can now be manipulated by the use of equations [VII-25], [VII-31] and [VII-50], to obtain the following:

$$(m k_2 C_2 \rho_2)^{1/2} \left[\frac{\ell}{k_1} + \frac{1}{H'} + \frac{1}{H} - \frac{C_1 \rho_1 \ell m}{HH'} \right] \tan(\gamma a) = 1 - \frac{C_1 \rho_1 \ell m}{H'} \qquad \text{[VII-53]}$$

From this equation, several further approximations can be made. Firstly, the term $[\ell C_1 \rho_1 m/HH']$ is small compared to

the other terms in the factor since both H and H′ are large. Also m is small compared to both unity and ℓ. Therefore this term can be neglected. And, since m is small and H is large compared to unity, the term $[C_1\rho_1\ell m/H']$ can also be neglected. By adding these approximations, equation [VII-53] becomes

$$(mk_2C_2\rho_2)^{1/2}\left[\frac{\ell}{k_1}+\frac{1}{H'}+\frac{1}{H}\right]\tan(\gamma a) = 1. \qquad [VII-54]$$

Now, in order to determine the actual thermal conductivity it must be realized that the measurements have assumed that the sample fills the entire space between the heat source and the heat sink, including any boundary layers. Therefore, the apparent thermal conductivity is measured across three segments in series, but uses the thickness of only the sample segment. We can therefore define an "apparent thermal conductivity" to account for the effect of the contact films. From equation [VII-54],

$$1/k_{app} = 1/k_1 + (1/H' + 1/H)/\ell. \qquad [VII-55]$$

This equation can now be resubstituted into equation [VII-54] to obtain the result:

$$k_{app} = \ell(C_2\rho_2mk_2)^{1/2}\tan(a[mC_2\rho_2/k_2]^{1/2}) \qquad [VII-56]$$

Thus, an equation has been obtained which relates the measured thermal conductivity to the constants of the

system. From this, with the use of Equation [VII-55], the true thermal conductivity of the system can be found from a plot of $1/k_{app}$ as a function of the sample thickness.

2. Cell Design

Two different cells were used for the measurement of the thermal conductivity. One was made of brass which was silver plated in order to prevent corrosion on the surfaces which would be in contact with the sample. This apparatus was used for the measurement of the thermal conductivity of polytetrafluoroethylene. However, for ion-selective membranes, it appeared that the potassium chloride solution corroded even the silver surfaces of the heat source and heat sink. Therefore, a new cell was constructed of stainless steel. The design and operation of these cells were similar and the cell shown in Figure [VII-2] was the stainless steel model.

The heat sources in both designs were kept at constant temperature with water from a thermostatic bath. The water was brought through copper tubing down the middle of the heat source to within a few millimeters of the bottom. The bottom plate was made as thin as possible (about 1 mm) so that the face of the heat source in contact

FIGURE [VII-2]

THERMAL CONDUCTIVITY APPARATUS

The diagram is drawn to one-half actual size.

The large cross-hatched area is made from foamed polyurethane.

The recorder is located in the copper side of a copper-constantan thermocouple.

The heat sink and heat source are constructed of either silver-plated brass or stainless steel.

FIGURE [VII-2]

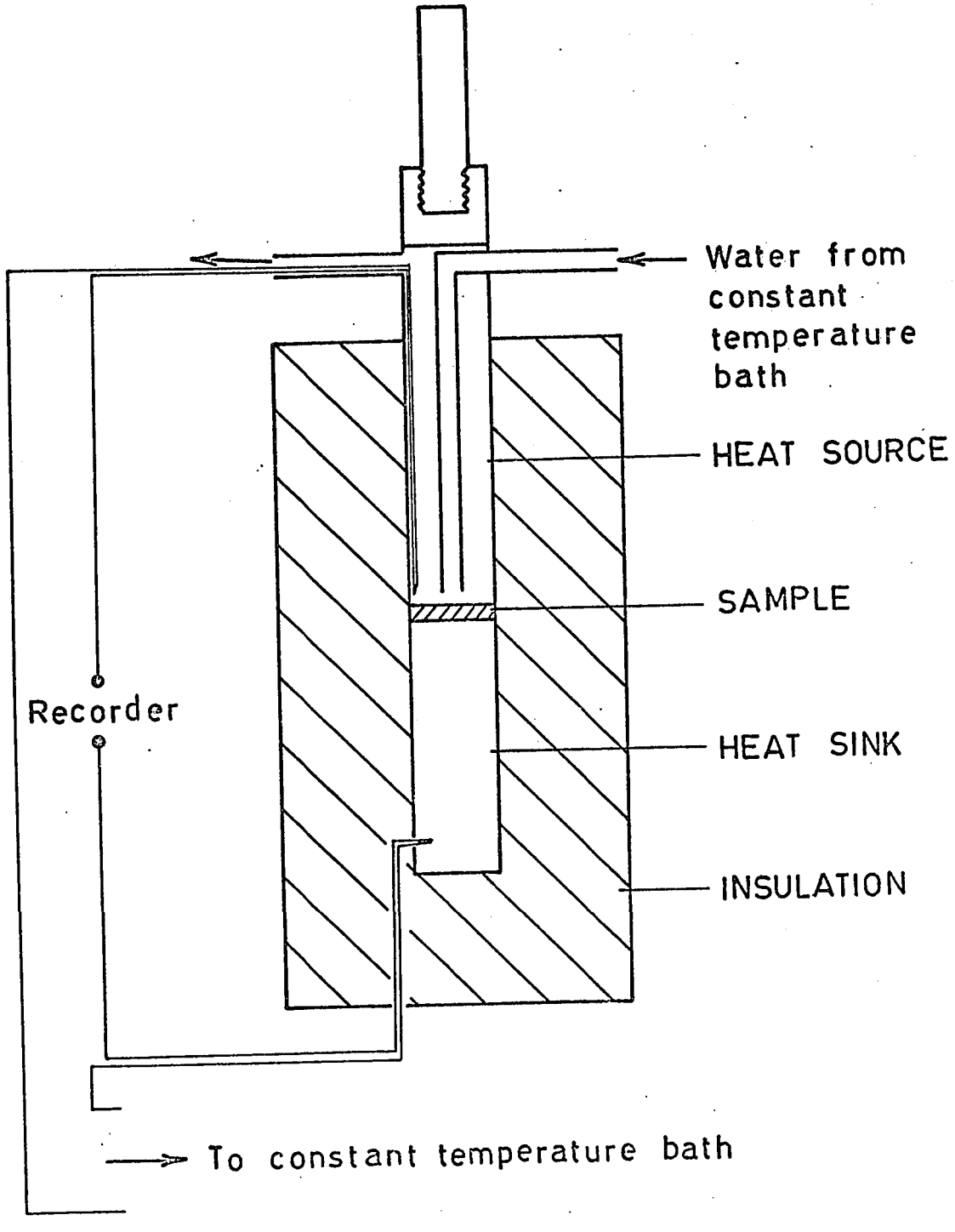
Water from constant temperature bath
HEAT SOURCE
SAMPLE
HEAT SINK
INSULATION
Recorder
To constant temperature bath

with the sample would be at the same temperature as the water. In the stainless steel model, only that part of the heat source below the inlet and outlet tubes was constructed of stainless steel. Above this, brass was used. Each heat source was equipped with a rod at the top where ring-shaped weights could be placed in order to supply enough pressure to achieve a reproducible contact film. Five weights of about 200 gm each were made for this purpose.

A stainless steel heat sink was made. It was 8.030 cm long and solid except for a small hole (about 1 mm in diameter) for the thermocouple drilled close to the end farther from the sample and 10 mm deep. The sample end was machined as smooth as possible. This block, both heat sources and the brass heat sinks were 25.0 mm in diameter. Three brass heat sinks were constructed. These were 8.26 cm, 4.54 cm, and 3.33 cm long. As before, a small hole for the thermocouple was drilled in each block. These were 6.665 cm, 3.190 cm and 2.235 cm from the sample end of the blocks. All three blocks were silver plated before they were used.

Polyurethane foam (Uniroyal 'Vibrafoam') was used as the insulation for the apparatus. A piece of glass tubing, 25.0 mm in outside diameter, formed the middle of the mold. It was sprayed with a polytetrafluoroethylene

spray so that the foam would not stick to it as the foam set. After the foam had set, the glass tubing was removed. A small hole was made in the insulation so that a thermocouple could be threaded through it and fitted into the small hole in the heat sink. The heat sink was then pushed into place in the bottom of the hole in the insulation with the thermocouple in place. A sample could now be placed on the top of the heat sink, and the heat source fitted on top of the sample to completely assemble the apparatus.

When the thermal conductivity was to be measured at elevated temperatures, the apparatus was inserted into a large glass tube to protect it from the water and the entire assembly was immersed in a thermostatic bath at the same temperature as the heat sink at the start of the experiment. A beaker was used to protect the bottom of the cell, and into it were placed several lead weights so that the apparatus would not float.

A cutter was constructed of brass that would cut samples that were 25.0 mm in diameter.

3. Measurement of the Constants of the System

(a) Heat Capacity and Density

The density of the two heat sinks and of the membranes was measured by first weighing them in air and then in water. Correction was made for the small piece of platinum wire used to hold the sample in the water. The density could then be calculated by the use of Archimedes' principle.

The heat capacities of the heat sinks were measured in the following way. A sample of the heat sink material was heated to a certain known temperature. A known amount of conductivity water was placed in a Dewar flask and the drift in its temperature was measured for several minutes. The sample was then placed into the water in the Dewar flask and the temperature change recorded until the drift was again constant. The temperature before and after the insertion of the sample was then extrapolated back to the midpoint of the temperature rise and the temperature difference between the two states at this point was noted. The experiment was repeated using water of the same volume as the original sample as a sample, the same amount of water in the Dewar flask, and the sample at a temperature high enough to make the final temperature approximately the same as that

when the actual sample was used. The heat gained by the water was then calculated, and that lost by the water sample so that the heat gained by the Dewar flask could be accounted for. This quantity corrected for the exact temperature rise plus the heat gained by the water when the metal sample was used was equal to the heat lost by the metal sample. Since its weight and the temperature change is known, the heat capacity of the metal could be easily calculated.

The temperatures of both the sample block and the water in the Dewar were recorded, by means of thermocouples, on a dual channel recorder. The sample used for the brass apparatus was the smallest heat sink. For the stainless steel apparatus, it was a small piece of the metal, weighing about 10 grams, from the block from which the apparatus was constructed.

(b) Calibration of Recorder and Thermocouple

A Sargeant recorder, model SR, was used for all measurements of thermal conductivity. In order to calibrate this recorder, the circuit shown in Figure [VII-3] was used. A small potential difference was measured across a precision decade resistance box. The resistance was changed by steps

and at each step the deflection of the recorder caused by that potential difference was noted. The potential difference for full scale deflection was measured on a potentiometer. Since the resistance across the variable resistance was directly proportional to the potential difference, a relationship between the potential difference and the deflection of the recorder in scale divisions over the complete range of measurement was obtained.

One copper-constantan thermocouple was used in each of the two thermal conductivity apparatus. In order to calibrate the thermocouple, one junction was placed in a constant temperature bath at about 25.0°C. The other junction was placed in a second thermostatic bath and close to it, the bulb of a N.B.S. precision thermometer number 37183 readable to ± 0.02 degrees. The temperature of this second bath was then varied in steps of about 0.4 degrees. The bath was allowed to equilibrate and a reading taken from both the thermometer and the recorder which measured the potential drop across the thermocouple. The process was continued until a full scale deflection was obtained on the recorder.

FIGURE [VII-3]

RECORDER CALIBRATION CIRCUIT

FIGURE [VII-3]

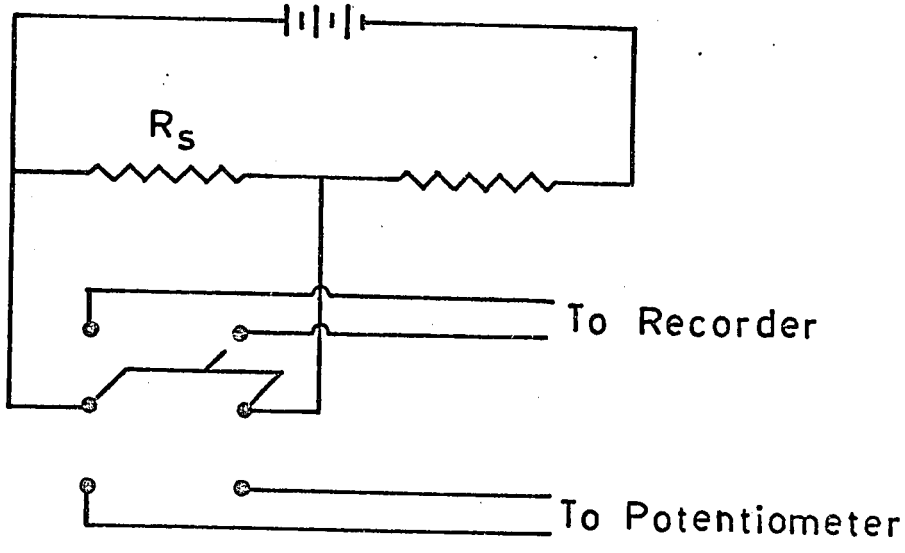

4. Polytetrafluoroethylene

(a) Experimental

The appropriate silver plated brass block, with the thermocouple in place, was put into the apparatus. A copper-constantan thermocouple was used for all measurements. The heat source was then placed in position so that it made contact with the heat sink. Water, at the temperature for the beginning of the experiment, was circulated through the heat source and the system was allowed to equilibrate. The heat source was then removed and a disc of polytetrafluoroethylene (Cadillac Plastics) (25.0 mm in diameter and of a known thickness), with a drop of silicone oil placed on each side, was placed on the top of the heat sink. The heat source was then replaced so that it made contact with the top of the sample, and several of the brass weights were placed on top of the heat source. The temperature of the water circulating in the heat sink was then raised 8 to 10 degrees. This was accomplished by bringing constant temperature water from another thermostatic bath at a higher temperature. This experimental set-up is shown in Figure [VII-4]. The temperature difference between the heat source and the heat sink was then recorded as a function of time on a Sargaent recorder. The recorder was run on the 1.25 mv

FIGURE [VII-4]

EXPERIMENTAL SET-UP

THERMAL CONDUCTIVITY CELL

S_1, S_2, S_3 and S_4 are clamps to control the water flow. If S_1 and S_2 are closed, and S_3 and S_4 are open, water at temperature T_1 will be pumped through the heat source. If S_1 and S_2 are opened while S_3 and S_4 are closed, then water at temperature T_2 will begin to circulate through the heat source.

FIGURE [VII - 4]

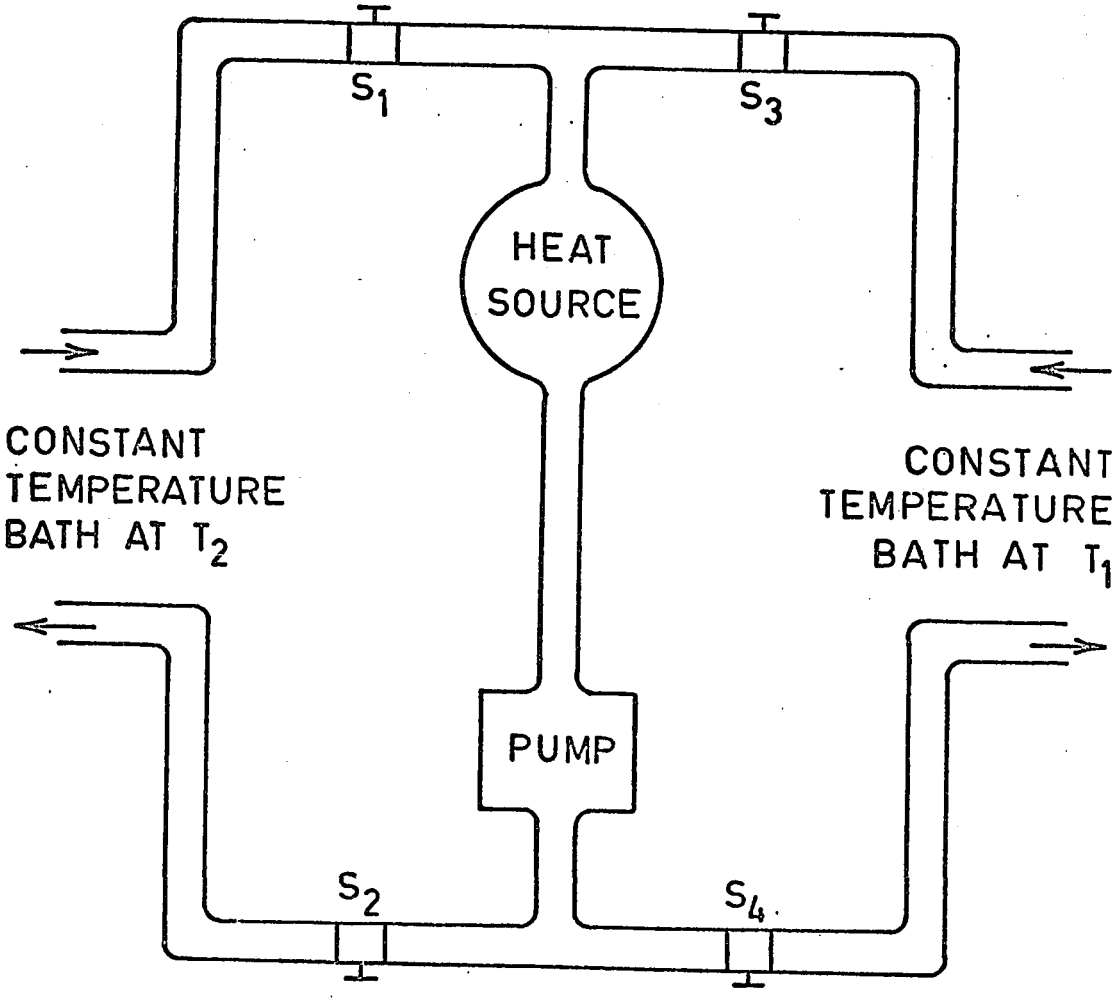
S_1
S_3
HEAT SOURCE
CONSTANT TEMPERATURE BATH AT T_2
CONSTANT TEMPERATURE BATH AT T_1
PUMP
S_2
S_4

scale fully attenuated so that the full scale deflection was caused by a signal of 0.404 mv. The recorder was calibrated as was described previously.

Six different thicknesses of polytetrafluoroethylene were measured in this manner.

(b) Results

The time dependence of the temperature difference across the sample and the heat sink was found to be, as expected, logarithmic. A typical curve obtained from the measurements conducted on a sample is shown in Figure [VII-5] and tabulated in Table [VII-1].

The calibration of the recorder revealed that, because of the small signal being measured, the potential was not a linear function of the scale divisions of the chart paper. Therefore, a curve was fitted to the voltage-scale division curve by use of a Fortran IV, non-linear least squares routine. In this method, the functional relationships could be arbitrarily chosen. Sine and exponential terms were used in order to take into account certain trends and irregularities that appeared in the curve. The following result was obtained:

TABLE [VII-1]

COMPARISON BETWEEN THEORETICAL AND THEORETICAL CURVES

P.V.B.S. #1 in 0.01 N. KCl

$T = 412.5\ [1.05392 \exp(-4.238\ t \times 10^{-4}) - 0.08698 \exp(-0.01078\ t)]$

TIME /MIN	RECORDER READING /mv EXPERIMENTAL	THEORETICAL TERM 1	THEORETICAL TERM 2	THEORETICAL TOTAL
0	404.0	437.0	35.9	401.1
2.5	404.0	413.7	7.1	406.6
5	389.8	388.5	1.4	387.1
10	344.7	342.2	.04	342.2
15	303.2	301.4	---	301.4
20	264.9	265.1	---	265.1
25	233.5	233.5	---	233.5
30	206.0	205.7	---	205.7
35	183.3	177.0	---	177.0
40	163.5	159.4	---	159.4
45	146.0	140.5	---	140.5
50	131.4	123.7	---	123.7

FIGURE [VII-5]

TYPICAL CURVE

THERMAL CONDUCTIVITY CELL

The results shown are for polyvinylbenzenesulfonate membrane #1 equilibrated in 0.01 N potassium chloride solution.

The experimental results are shown as points on the graph. The theoretical results were obtained from the equation

$$T = 412.5\ [1.05392\ \exp(-4.238\times10^{-4}) - 0.08698\ \exp(-0.01078t)]$$

which was obtained from equation [VII-43] and the data obtained. It is shown as a solid curve on the graph.

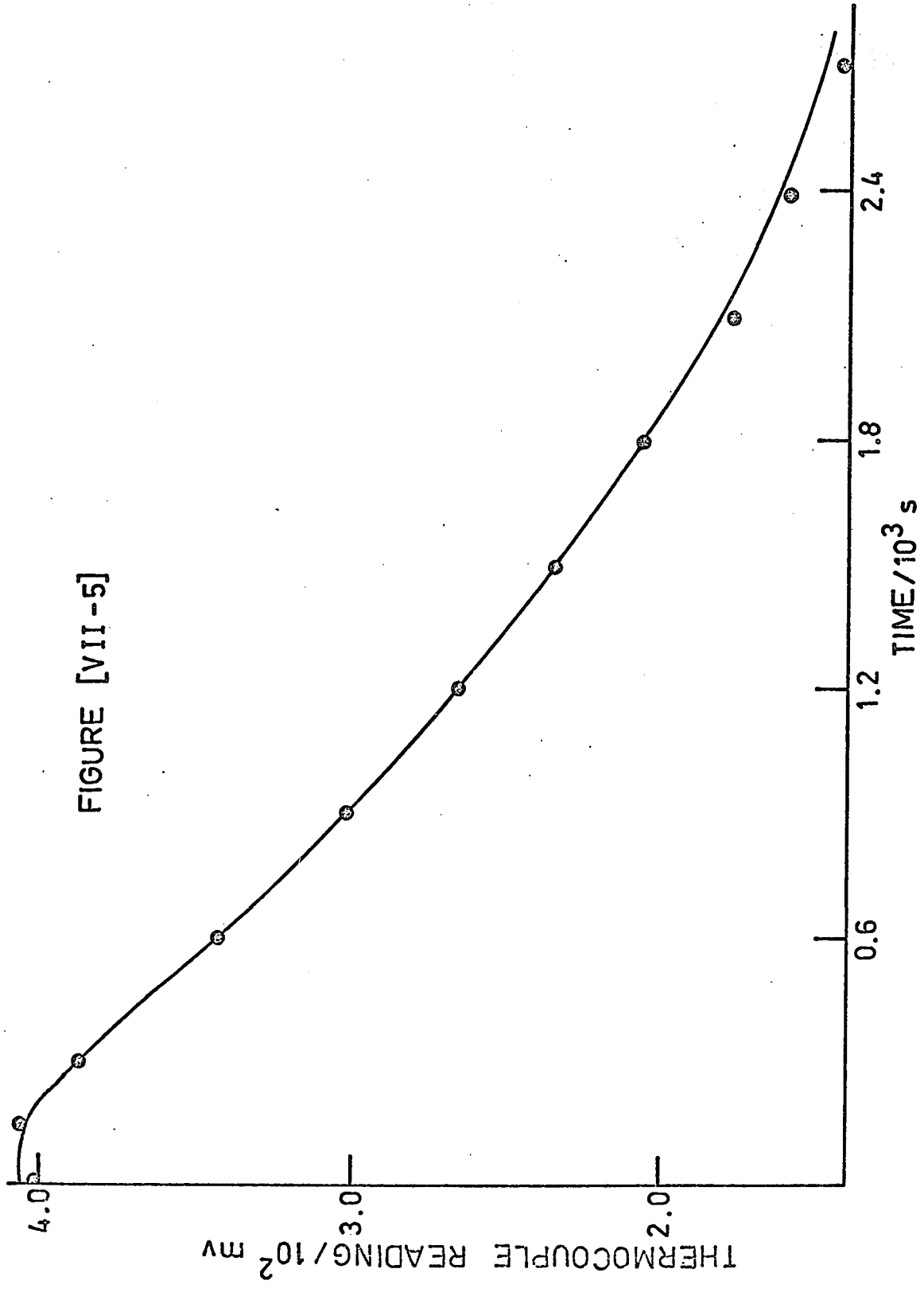

FIGURE [VII-5]

$$T = 99.271/x^2 - 25.245/x + 1.2902x + (0.02769x)^2 + (0.016687x)^3 + (0.0101791x)^4 + 3.1127 \sin(0.064981x) + 0.76764 \sin(0.139626x - 2.23402) + 2.3664 \exp(0.46x - 90.08) \quad \text{[VII-57]}$$

where T is the temperature measured by the thermocouple in millivolts and x is the deflection of the recorder pen in scale divisions. The maximum deviation from the experimental curve by this equation was about 1 scale division and considerably better than this along most of the curve. This was more than adequate for the analysis of results. It was also found that the point at which the recorder was zeroed did not affect this calibration.

The calibration of the thermocouple against temperature showed that the relationship between the potential difference across the thermocouple and the temperature was linear to within the accuracy of the measurements. This calibration is shown in Figure [VII-6], and in Table [VII-2].

The results from the six different thicknesses of polytetrafluoroethylene, measured using all three silver-plated brass blocks are shown in Table [VII-3]. A plot was made of the reciprocal of the apparent thermal conductivity against the inverse thickness of the samples, in order to obtain the intercept of equation [VII-55], the inverse of

TABLE [VII-2]

THERMOCOUPLE CALIBRATION

TEMPERATURE (scale divisions)	TEMPERATURE /mv	TEMPERATURE /°C
4.2	7.0	0.23
21.3	32.7	0.78
30.3	45.5	1.13
36.3	53.8	1.36
45.3	65.2	1.67
53.0	73.5	1.90
61.3	85.0	2.19
68.3	98.0	2.48
75.0	108.1	2.73
83.3	121.0	3.06
97.5	141.8	3.59
102.8	150.0	3.78
111.3	165.5	4.17
128.3	190.4	4.77
133.3	197.6	4.97
150.3	225.0	5.69
163.5	246.2	6.30

the actual thermal conductivity of polytetrafluoroethylene. This graph is shown in Figure [VII-7]. The value obtained was 0.301 J m^{-1} s^{-1} K^{-1}.

TABLE [VII-3]

RESULTS FOR POLYTETRAFLUOROETHYLENE

		a = 8.26 cm		a = 4.54 cm		a = 3.33 cm	
ℓ/cm	ℓ^{-1}/cm^{-1}	k	k^{-1}	k	k^{-1}	k	k^{-1}
0.154	6.4	0.282	3.55	0.281	3.56	0.280	3.58
0.102	9.8	0.267	3.74	0.268	3.75	0.276	3.63
0.0803	12.5	0.265	3.78	0.266	3.76	0.269	3.72
0.0566	17.7	0.253	3.95	0.250	4.00	0.251	3.98
0.0398	25.2	0.239	4.19	0.237	4.23	0.235	4.26
0.0267	37.5	---	----	0.212	4.72	0.216	4.63

(c) Discussion

The agreement of the results obtained from the thermal conductivity cell and the theory derived for it, as shown in Figure [VII-5] was very good. Only in two places did the graph deviate from an exponential relationship. As the run was started, a flat portion was observed. This could be taken into account by the higher terms of the theory (with H = H′ and very large) in equation [VII-45]. When the theoretical curve was corrected for these terms,

FIGURE [VII-6]

THERMOCOUPLE CALIBRATION

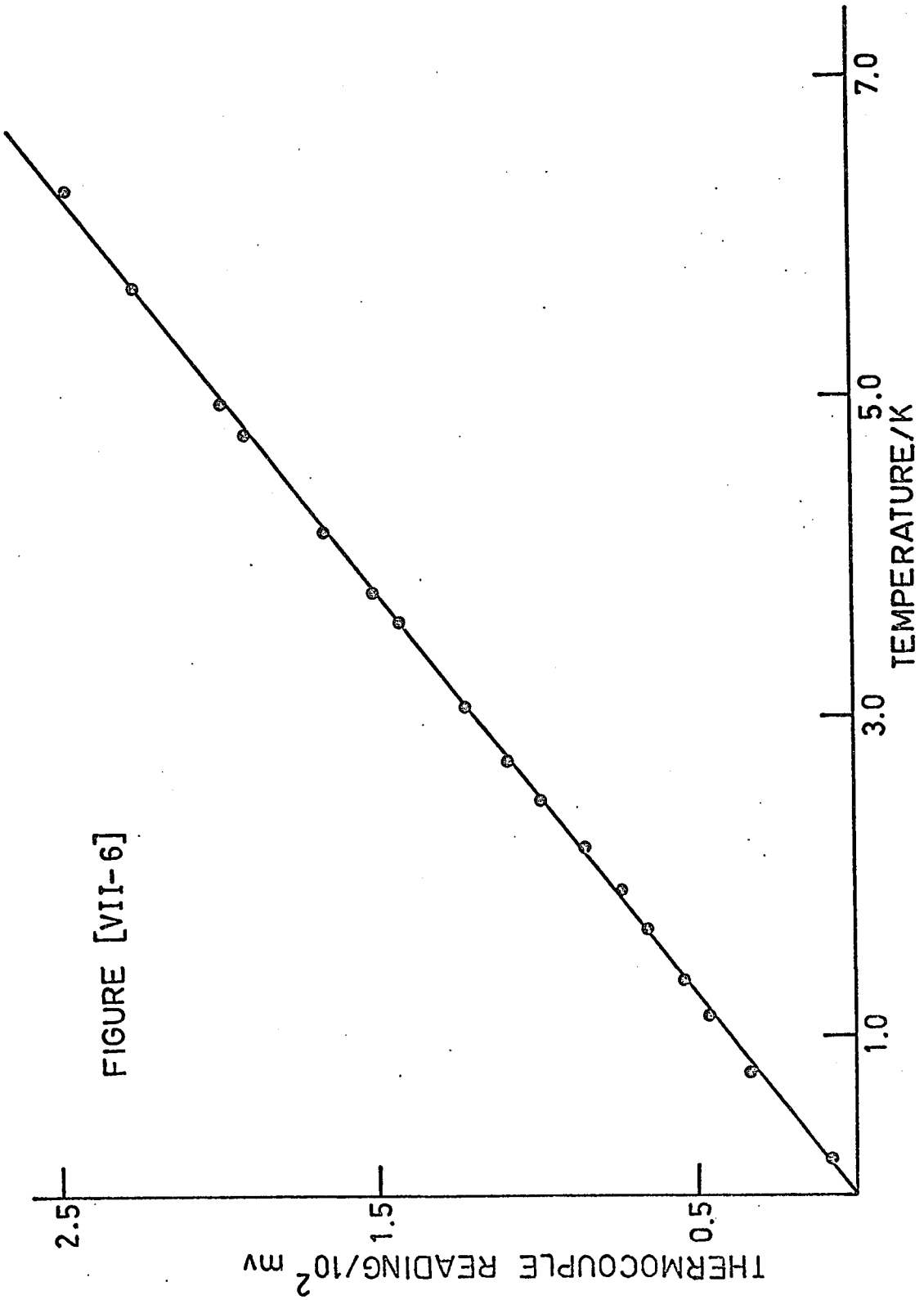
THERMOCOUPLE READING/10^2 mv
2.5
1.5
0.5
1.0
3.0
5.0
7.0
TEMPERATURE/K

FIGURE [VII-6]

FIGURE [VII-7]

RESULTS

THERMAL CONDUCTIVITY

POLYTETRAFLUOROETHYLENE

○ 8.26 cm heat sink

● 4.54 cm heat sink

□ 3.33 cm heat sink

◑ indicates coincidental results for the first two heat sinks

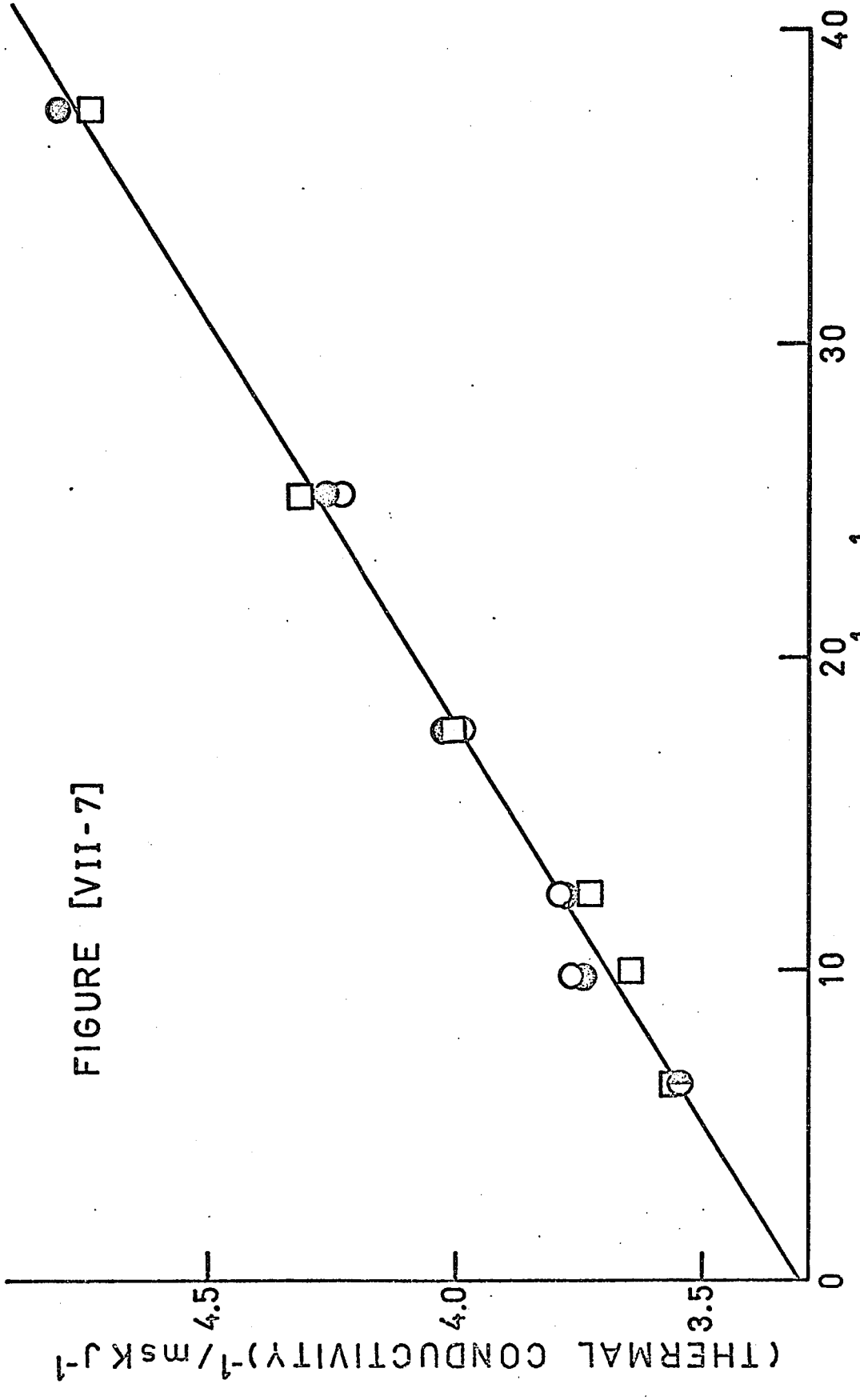
(THERMAL CONDUCTIVITY)$^{-1}$/mskJ^{-1}
4.5
4.0
3.5
0
10
20
30
40
(THICKNESS)$^{-1}$/cm^{-1}

FIGURE [VII-7]

this region of the theoretical curve coincides with experimental results. About two minutes after the start of a run, the effect of these higher terms in the equation was negligible. The curve again deviated from the predictions when the temperature difference between the heat source and the heat sink approached zero. The temperature was greater than expected, likely because of radial heat losses, losses through the thermocouple and losses through the bottom of the heat sink. This deviation was not observed for at least 25 minutes after the experiment was started. Therefore, a time of at least 23 minutes was always available for obtaining a useful curve.

The results were analysed in the following way. Points were read from the chart paper at equal time intervals of 12, 30 or 60 seconds, depending on the time required for the experiment. The logarithms of these points were fitted by computer with a linear least squares program and the slope of the logarithm against time plot was obtained, and the thermal conductivity calculated from equation [VII-56].

The temperature difference at the beginning and the end of each time interval used for the measurement was recorded, and from this the temperature difference across the sample was calculated using equation [VII-43]. The

temperature of the sample was then taken as the average of the initial and final temperature difference, subtracted from the temperature of the heat source.

A statistical analysis of the results showed a maximum standard error in the slope of the logarithm of temperature versus time plot of about 2 percent and an average of about 1 percent. The correlation coefficient for the results was consistently near 0.998.

Values of the thermal conductivity of polytetrafluoroethylene reported in the literature vary from .20 to .30 J m^{-1} s^{-1} K^{-1} [84,91,99]. Hsu et al [91] found that the value depended on the source of the material as well as the amount of annealing to which it was subjected. When this is taken into consideration, our value of 0.301 J m^{-1} s^{-1} K^{-1} is in good agreement with other work.

5. MEMBRANES

(a) Cellulose Membranes

(i) Experimental

The stainless steel apparatus was used for the measurement of membranes. As in the previous procedure the samples were cut into discs, 25.0 mm in diameter, and placed between the heat sink, with temperature T_o, and the

heat source at a temperature T_s, about 8 to 10 degrees higher.

The thermal conductivity of cellulose membranes of various thicknesses was measured in this way. One membrane was measured after equilibration in various concentrations of potassium chloride solution.

(ii) Results

The results of the apparent thermal conductivity of cellulose as a function of thickness are shown in Table [VII-4]. The membranes were equilibrated in 0.1 N potassium chloride solution. As with the polytetrafluoroethylene, the inverse of the apparent thermal conductivity was plotted as a function of the inverse of the thickness of the sample, as shown in Figure [VII-8] together with the results for polytetrafluoroethylene. This again gave a straight line as predicted from equation [VII-55]. The result obtained for the true thermal conductivity from the inverse of the intercept was 2.00 J m^{-1} s^{-1} K^{-1}. The results of the thermal conductivity as a function of external concentration are shown in Table [VII-5].

TABLE [VII-4]

THERMAL CONDUCTIVITY OF CELLULOSE

0.1 N POTASSIUM CHLORIDE SOLUTION

ℓ/cm	k/J $m^{-1}s^{-1}K^{-1}$	ℓ^{-1}/cm^{-1}	k^{-1}/m s K J^{-1}
0.113	0.598	8.93	1.67
0.183	0.778	5.46	1.28
0.232	0.866	4.31	1.15
0.315	0.980	3.17	1.02

$1/k_{app} = 0.667 + 0.113/\ell$

$k = 2.00$ J $m^{-1}s^{-1}K^{-1}$

TABLE [VII-5]

THERMAL CONDUCTIVITY AS A FUNCTION OF CONCENTRATION

CONCENTRATION	POLYVINYLBENZENESULFONATE J $m^{-1}s^{-1}K^{-1}$	CELLULOSE J $m^{-1}s^{-1}$ K^{-1}
0.0 N	0.235	--
0.005 N	0.241	0.786
0.01 N	0.246	0.774
0.05 N	0.253	--
0.1 N	0.254	0.778

the cellulose membrane of thickness 0.183 cm was used.

FIGURE [VII-8]

THERMAL CONDUCTIVITY

CELLULOSE MEMBRANES

AND

POLYTETRAFLUOROETHYLENE DISCS

The membranes were equilibrated in 0.1 N potassium chloride solution.

FIGURE [VII-8]

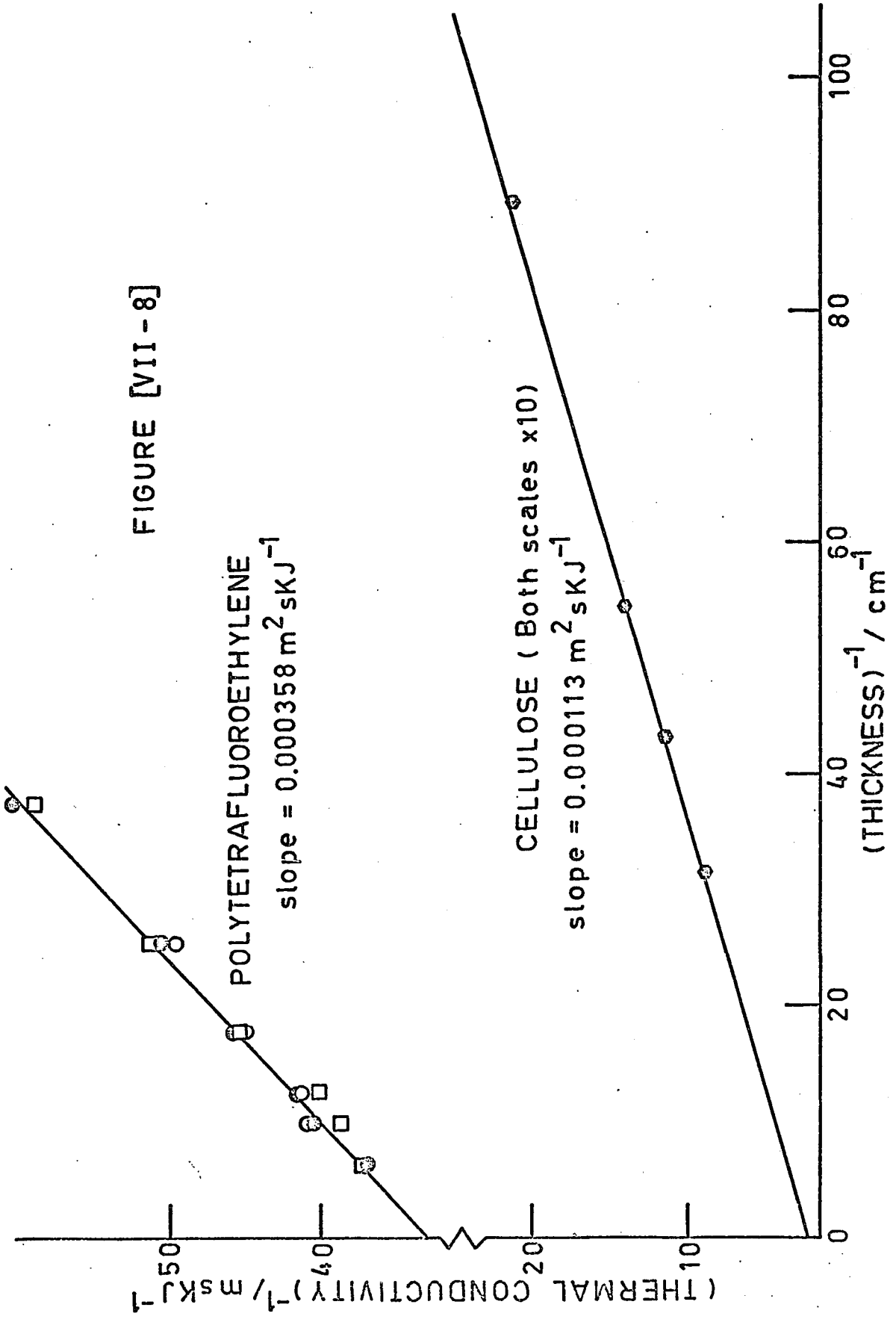
(THERMAL CONDUCTIVITY)$^{-1}$ / m s kJ^{-1}
10
20
40
50
0
20
40
60
80
100
(THICKNESS)$^{-1}$ / cm^{-1}
POLYTETRAFLUOROETHYLENE
slope = 0.000358 m^2 s KJ^{-1}
CELLULOSE (Both scales x10)
slope = 0.000113 m^2 s KJ^{-1}

(iii) Discussion

Estimation of the contact film thickness in the cases studied indicated that the values obtained were much larger than should be expected. For the case of silicone oil on polytetrafluoroethylene, the thickness was determined by micrometer measurements to be about 0.002 cm. This was about 50 times smaller than the result obtained from the slope of the inverse of the thermal conductivity against inverse thickness graph. This apparent discrepancy can be explained from the method by which the heat source was made. Since a fluid flow was used, a thermal diffusion layer between this fluid and the sample must be set up [92]. It is this layer which is allowed for by the theory. This film should be independent of the nature of the membrane but dependent on the flow velocity of the water in the heater block.

For cellulose membranes, the slope of this graph was about 1.13×10^{-4} $J^{-1}\ m^2\ s\ K$ as was shown in Figure [VII-8]. Therefore, if it is assumed that H' is much larger than H (that is, the layer next to the heater block much larger than the layer on the other side of the sample) then H' is the right order of magnitude for forced convection of a fluid of velocity u onto a surface of diameter δ [91].

$$H' = 0.008\ (u/\delta)^{\frac{1}{2}} \qquad \text{[VII-58]}$$

$$u = H'^{2}\delta/64 \times 10^{-6} = 7.1\ \delta \text{ cm/sec} \qquad \text{[VII-59]}$$

The water in the heat source was brought through a $\frac{1}{4}$ inch pipe, which corresponds to a flow rate of about 4.5 $cm^3\ s^{-1}$ for the experimental values of H' and δ. This value is in good agreement with the actual flow rate used in the experiments, 5.0 $cm^3\ s^{-1}$.

The same type of heat source was used for the experiments with polytetrafluoroethylene, and comparable flow rates were used. However, the slope of the line in Figure [VII-8] is significantly different from the result for cellulose membranes. The difference in the materials in the contact films should account for only a small portion of this difference. The probable answer for the discrepancy lies in the actual manufacture of the two heat sources.

The silver-plated brass heat source used for the polytetrafluoroethylene measurements was constructed from one piece of brass hollowed out from the bottom, and a brass disc soldered onto the bottom to complete the reservoir. A piece of brass tubing was then inserted through a hole in the side of the heat source, and pushed in until its end was situated close to the bottom of the heat source. Because

this necessitated bending the tubing, it is likely that the end of the tube was close to one side of the disc at the bottom, and at an angle off the perpendicular. This would result in a non-uniform flow onto the bottom of the heat source and therefore less efficient heat transfer. The uneven temperature profile across the bottom of the heat source is probably not important, since the thermal conductivity of the brass disc is much larger than that of the sample, and any temperature variations will be minimized before they enter the sample segment of the apparatus.

The stainless steel heat source was made in two pieces. The upper half, made of brass, was constructed with the brass tubing in place, and the lower half was soldered on so that the tube was centred in the heat source, and was perpendicular to the bottom. The resulting improvement of the flow properties of the water could account for the large reduction in the slope of the line for cellulose membranes in Figure [VII-8].

It is now possible to estimate the true thermal conductivities of other types of membranes. Since the slope of the graph is due almost entirely to the nature of the heat source and not the contact films, it can be assumed that this slope will stay the same for all other types of

membranes. Secondly, any discrepancy caused by the contact films for cellulose membranes should be approximately the same for other membranes, since these contact films will consist of the same material, i.e. potassium chloride solution.

(b) Porous Glass and Polyvinylbenzenesulfonate Membranes

(i) Experimental

The stainless steel heat source was used for all membrane measurements. Two porous glass membranes of slightly different thicknesses and polyvinylbenzenesulfonate membranes of varying capacity and water content were measured. One of these membranes was measured at temperatures from 25 to 45°C.

(ii) Results

The results obtained for porous glass membranes are shown in Table [VII-6]. The actual thermal conductivity was calculated from equation [VII-56] using the slope obtained from the cellulose results, and the change in the thermal conductivity predicted by these results was compared to the actual change.

The results for polyvinylbenzenesulfonate membranes were corrected for contact films by using the slope obtained from the cellulose data. The thermal conductivity results

TABLE [VII-6]

THERMAL CONDUCTIVITY OF POROUS GLASS

C_1 = 0.60 cal./gm

ρ_1 = 2.07 gm./cm^3

ℓ/cm	k_{app}/J m^{-1}s^{-1}K^{-1}	ℓ^{-1}/cm^{-1}	k_{app}^{-1}/msKJ^{-1}
0.490	1.728 ± .05	2.151	0.579
0.465	1.674 ± .1	2.041	0.598

Experimental change in k_{app}^{-1} = 0.019 J^{-1} m s K

Expected change (using slope from cellulose data)

= 0.012 J^{-1} m s K

k = 2.94 J m^{-1}s^{-1}K^{-1}

TABLE [VII-7]

THERMAL CONDUCTIVITY AS A FUNCTION OF WATER CONTENT

AND CAPACITY FOR POLYVINYLBENZENESULFONATE

Membrane	Volume fraction* Resin	Capacity /meq gm^{-1}	Degree of Swelling	k/J m^{-1}s^{-1}K^{-1}
1	0.483	1.72	2.08	0.933
9	0.504	1.77	1.99	0.808
11	0.370	2.47	2.71	1.380
12	0.530	2.24	1.89	0.767
13	0.492	2.30	2.04	0.933
17	0.775	1.03	1.29	0.245

* calculated for membranes in their H^+ form

obtained as a function of external concentration of potassium chloride solution using membrane 17 are shown in Table [VII-5] and are plotted in Figure [VII-9].

Polyvinylbenzenesulfonate membranes of varying volume fractions of resin were measured. The results, after being corrected using equation [VII-56], are shown in Table [VII-7], and plotted in Figure [VII-10].

The temperature dependence of the thermal conductivity of polyvinylbenzenesulfonate membrane number 17 was measured between 25° and 45°C. These results, are tabulated in Table [VII-8] and plotted in Figure [VII-11].

(iii) Discussion

The thermal conductivity of polyvinylbenzenesulfonate membranes increases with the volume fraction of water to values that are above the value for water alone. Considering the membrane as two separate phases, one of water and the other the membrane resin, leads to a maximum value for the conductivity [93].

$$k_{max} = v_r k_r + (1-v_r)k_w \qquad \text{[VII-60]}$$

where k_r is the thermal conductivity of the polymer resin, k_w is that for water, and v_r is the volume fraction of resin. This equation predicts values for the conductivity

FIGURE [VII-9]

THERMAL CONDUCTIVITY

FUNCTION OF CONCENTRATION

POLYVINYLBENZENESULFONATE

MEMBRANE 17

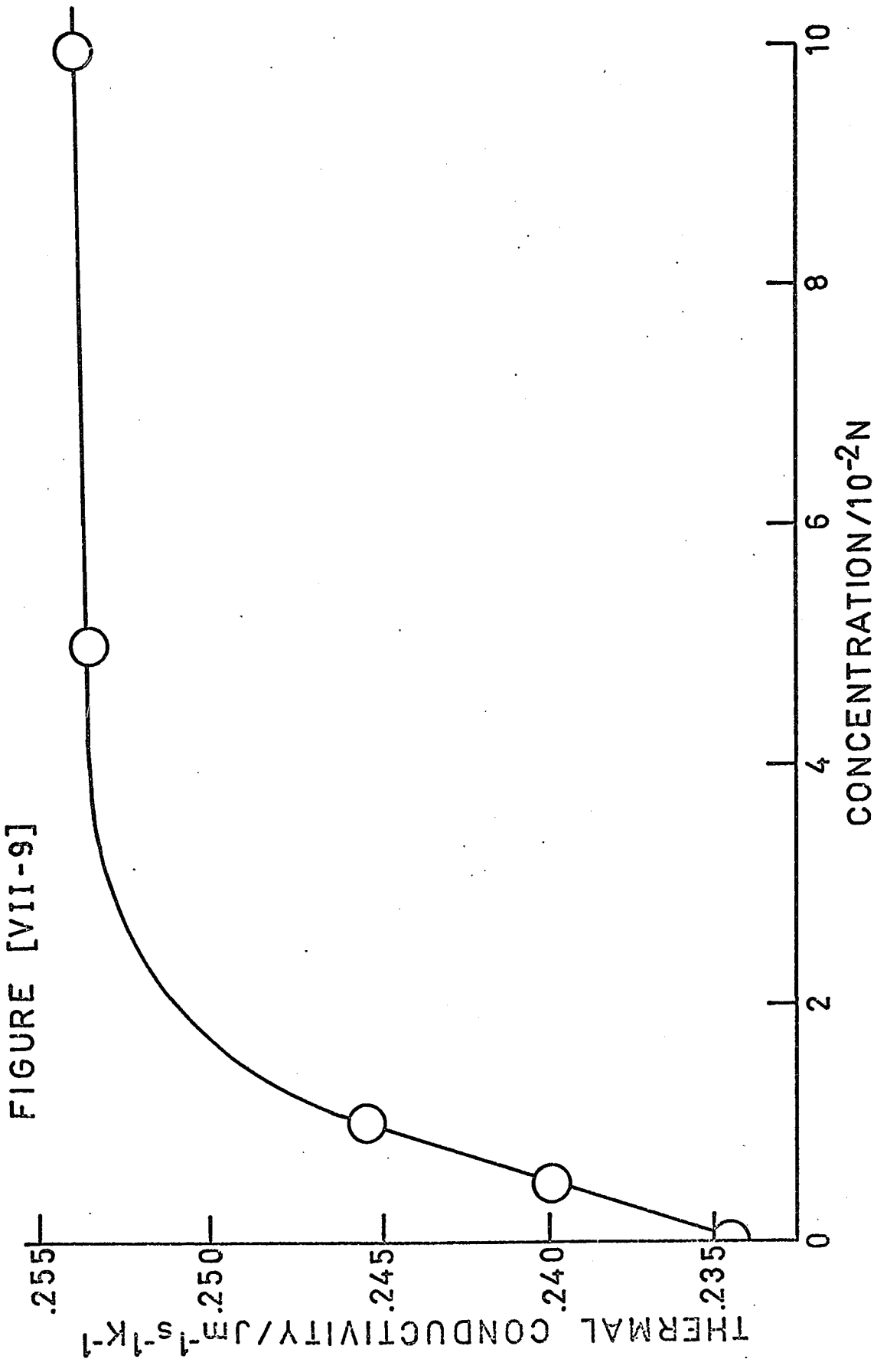
THERMAL CONDUCTIVITY/Jm⁻¹s⁻¹K⁻¹
.255
.250
.245
.240
.235
0
2
4
6
8
10
CONCENTRATION/10⁻²N

FIGURE [VII-9]

FIGURE [VII-10]

THERMAL CONDUCTIVITIES OF MEMBRANES

○ polyvinylbenzenesulfonate membranes

△ pure polystyrene

▤ water

Curve I -- maximum conductivity possible for membranes with water in its ordinary state.

Curve II - Theoretical conductivities for a random mixture of resin and "oriented water" (see text)

FIGURE [VII-10]

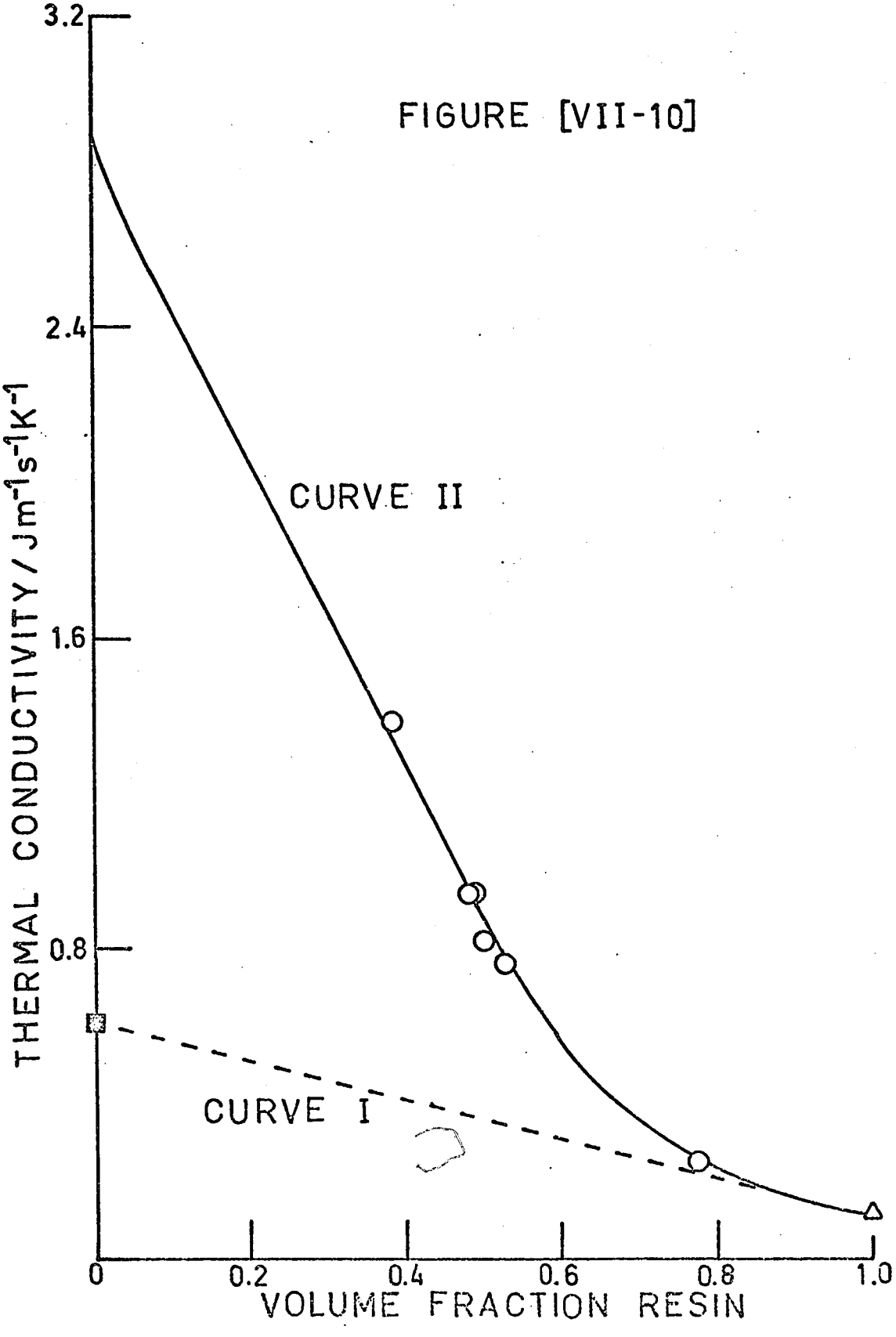

TABLE [VII-8]

THERMAL CONDUCTIVITY AS A FUNCTION OF TEMPERATURE

$T/^{o}C$	$k/J\ m^{-1}s^{-1}K^{-1}$
27.7	0.219
28.35	0.229
30.7	0.245
32.6	0.261
33.8	0.268
35.7	0.268
38.35	0.268
41.9	0.247
42.8	0.271
44.7	0.278
44.8	0.280
45.1	0.260
47.3	0.268
48.1	0.273

FIGURE [VII-11]

THERMAL CONDUCTIVITY

OF

POLYVINYLBENZENESULFONATE

AS A FUNCTION OF TEMPERATURE

0.1 N potassium chloride solution

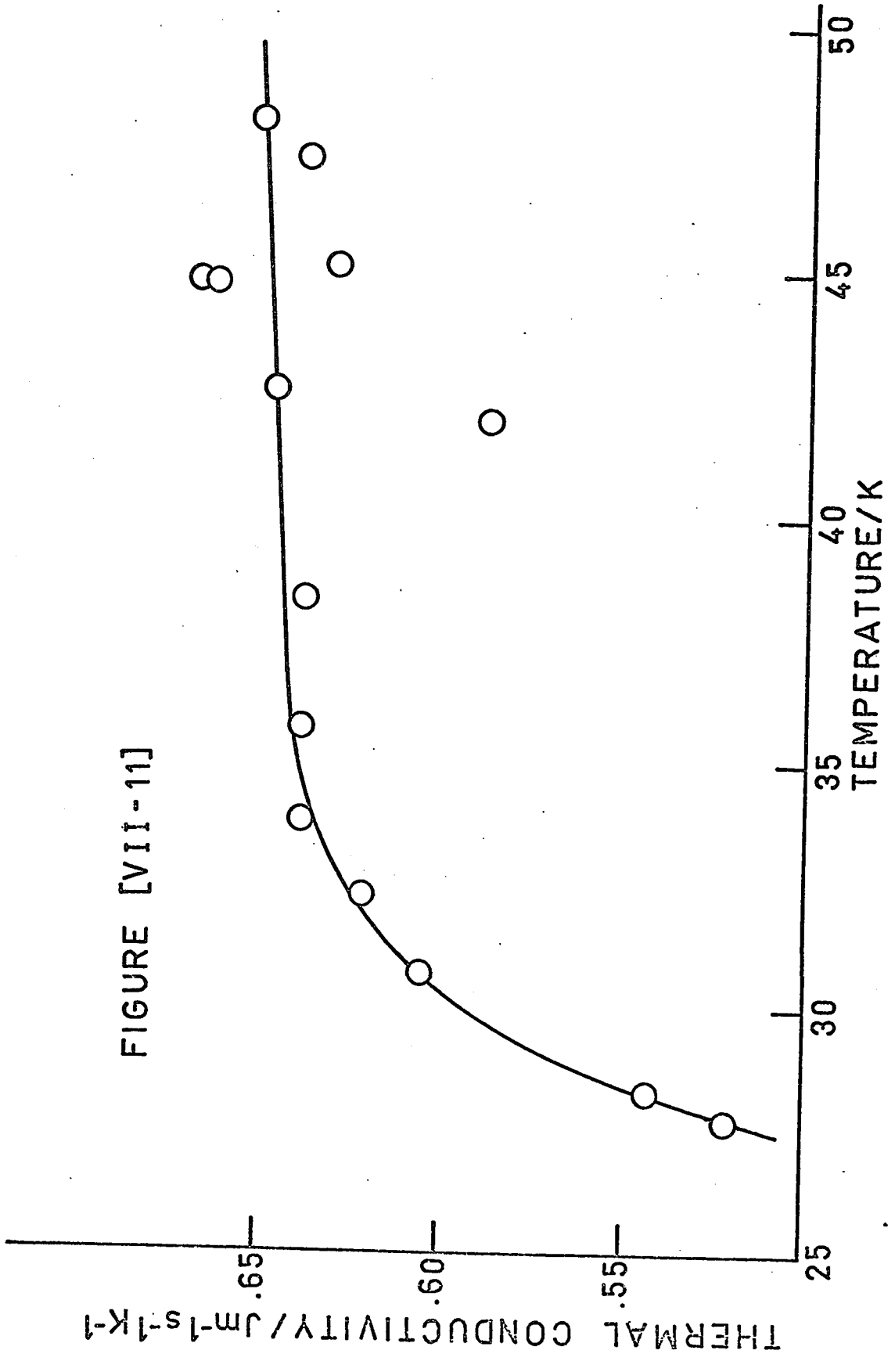

FIGURE [VII-11]

that are intermediate to the values for pure water and for pure resin. The values obtained, however, are above this maximum.

The application of Irreversible Thermodynamics leads to a term involving the pressure difference set up across the membrane as was derived in equation [II-52]. This term, however, is always negative and cannot account for the discrepancy unless a convective conductivity is set up from a flow caused by this pressure difference. The size of this pressure difference, calculated from measurements of thermo-osmosis and mechanical permeability on these membranes is found to be negligible [94], and therefore is not likely to cause such a large effect.

Another possible explanation involves errors in the measuring system itself. According to Tye [95], large errors are possible in thermal conductivity measurements. However, the consistent smoothness of the results and the apparent agreement with the value obtained for pure polystyrene obtained by others [99], 0.12 J $m^{-1}s^{-1}K^{-1}$, suggests that this is not the case.

Finally, the increased thermal conductivity could be explained by the nature of the water present in the membrane. The presence of the electrical double layer (or

surface forces on the resin matrix) would tend to order the water molecules causing the thermal conductivity to increase. If the membranes are treated as a random mixture of two phases, then an expression can be derived to relate the thermal conductivity to the thermal conductivity of the two phases and to their volume fractions [93,97]. This equation assumes that the single phases in the correct proportions are embedded in a random mixture of the same two phases which has a conductivity equal to the conductivity of the two-phase assembly which is being calculated.

$$k = \{(2-3v_r)k_w + (1+3v_r)k_r + [((2-3v_r)k_w + (1+3v_r)k_r)^2 + 8k_r k_w]^{\frac{1}{2}}\}/4 \qquad \text{[VII-61]}$$

If this equation is used to fit the results for polyvinylbenzenesulfonate , as is shown in Figure [VII-10], the value for the thermal conductivity of the resin agrees closely to that for polystyrene, but the value for the water phase is 2.85 J $m^{-1}s^{-1}K^{-1}$, compared to a reported value for water of 0.61 J $m^{-1}s^{-1}K^{-1}$ [98]. The value for ice is 2.25 J $m^{-1}s^{-1}K^{-1}$ at $0^{\circ}C$ increasing to 2.85 J $m^{-1}s^{-1}K^{-1}$ at $-50^{\circ}C$ [96]. These data suggest a highly ordered orientation of water within the membranes causing a substantial increase in the thermal conductivity of this phase. Other models

that embedded one phase in a continuous second phase were not successful in fitting the experimental results. This suggests that the two phases, water and resin, can be treated as continuous throughout the membrane.

The variation of the thermal conductivity of polyvinylbenzenesulfonate membranes with concentration is plotted in Figure [VII-9]. Since the membranes swell as the concentration of external electrolyte becomes smaller, it would be expected that this effect would cause the conductivity to decrease with increasing concentration since this represents an increase in the volume fraction of resin. However, the results in Figure [VII-10] show an exactly opposite trend. It appears that this concentration effect is caused by more than just the swelling of the membranes.

The temperature variation of the thermal conductivity of a polyvinylbenzenesulfonate membrane is shown in Figure [VII-11]. This variation is smooth between 20° and 45°C and shows no abrupt transitions. According to Ueberreiter *et al* [12], this suggests that the membrane matrix is constructed in such a way that the main body of the system is composed of short vibrating chain segments. If these segments were long, there would be abrupt transitions in the thermal conductivity when a high enough

temperature was reached to excite these chains. For short chain segments, there would be a gradual excitation of the chains at different temperatures and the thermal conductivity against temperature curve would be smooth. Independent experiments using a differential scanning calorimeter to measure the relative heat capacity with temperature showed no abrupt changes, supporting this conclusion.

CHAPTER VIII

SUMMARY

The purpose of this work was to find suitable methods for the measurement of the electrical and thermal conductivities of ion selective membranes with a wide range of physical properties and to use these methods to determine these two quantities for several types of membrane.

Several different kinds of apparatus were used for the measurement of the electrical conductivity perpendicular to the surface of the membrane. It was found that the best condition for measurement was the use of platinized platinum electrodes which were very close to, but did not touch the surface of the membrane. If shiny platinum electrodes were used which touched the surface of the membrane, large and unpredictable polarization effects made the acquisition of accurate results difficult. A technique using mercury electrodes in contact with the membrane was also studied and found to be useful. For the measurement of ion-selective membranes with a high electrical conductivity, polarization effects were once again encountered. These effects introduced a capacitance large enough to make balancing the

bridge impossible. If, however, a standard 100 ohm resistor was put in series with the cell, the readings were reasonable and the polarization effects were not as large as for the previous method.

Both of these methods worked well with an electrical conductivity of the same order of magnitude and lower than the electrical conductivity of the supporting electrolyte. For higher values of the electrical conductivity, the error in the results became fairly large. For the mercury electrode cell, this increase in error was caused by the polarization effects noted above. These could be accounted for to a reasonable extent and the values obtained should be accurate to within one percent. The platinized platinum electrode cell suffered from another problem. There was a small amount of electrolyte between the electrodes and the membrane. For highly-conducting membranes, the resistance of the electrolyte became much larger than the resistance across the membrane itself. Therefore, the total error in the measurement of the total resistance across the cell was imposed on a small portion of the total measurement. Also, any small error in reproducing the exact amount of pressure and therefore any squeeze on the membrane will produce a large error in the measurement. The percentage

error was therefore greatly increased. The errors involved could be as high as 35 percent.

Therefore, only the use of the mercury electrode cell was feasible for high electrical conductivity. The precision of the two apparatus at low conductivities was found to be equivalent.

A theory to take into account any part of the membrane not between the electrodes was also tested. It was found to work well if the electrodes were sufficiently close to the faces of the membrane (with several millimeters). If the electrodes were too far away, the electrical conductivity calculated was a function of the fraction of the surface not between the electrodes and was lower than the expected value.

With the aid of irreversible thermodynamics, it was found that the proper treatment of the electrical conductivity in cellulose and polyvinylbenzenesulfonate membranes assumes that the entire area of the membrane is available for ion transport. This idea is in variance with current pore models which do not allow for motion of the chains in the membrane matrix. For porous glass, a much more rigid membrane, a pore model was found to be more adequate, suggesting that the actual situation can vary between these two extrema.

A method for the determination of the electrical conductivity parallel to the membrane surface was also studied. It relied on the thickness of the sample and not on all three dimensions as with previous types of cells. In this method, two measurements were required using four electrodes, and a theory based on the mapping properties of Laplace's equation. The cell was found to work well for all types of membranes.

The anisotropy of the electrical conductivity of the three types of membranes was studied. The electrical conductivities perpendicular and parallel to the membrane surface were obtained using the methods described above. The cellulose membranes were found to show no anisotropy. The anisotropy of porous glass and polyvinylbenzenesulfonate membranes could be explained by their methods of manufacture.

A method was developed for measuring the thermal conductivity of ion-selective membranes, taking into account any contact layers produced on the faces of the membrane as measurements were being taken. A complete theory of the apparatus was derived and appropriate approximations made in order to make the theory useable. The theory and cell were tested using polytetrafluoroethylene discs and it was found that the values obtained could adequately account for

contact resistances. Using several thicknesses of the polytetrafluoroethylene, the linear relationship that was expected between the inverse of the apparent thermal conductivity and the inverse of the thickness of the discs was found. The results showed a precision of within 2 percent. It was found that a large part of the slope of this line was caused by thermal convection across the heat source from the circulated water. This problem could be corrected by either an improved heat source design or a faster flow of circulated water. The smaller value of the slope would then give results with less inherent error.

The thermal conductivity of cellulose was measured for various thicknesses of this membrane and the corresponding graph of the inverse thermal conductivity versus inverse thickness was plotted. It was then assumed that the slope of this line could be used for all membranes in order to calculate the true thermal conductivity when contact films were absent.

The thermal conductivity of cellulose was found to be independent of the concentration of the supporting electrolyte.

The thermal conductivity of porous glass was determined at two slightly different thicknesses and these

results confirmed, within experimental error, the assumption concerning the slope of the inverse thermal conductivity curve.

The thermal conductivity of the polyvinylbenzene-sulfonate membranes was measured as a function of the volume fraction of resin. The results suggested that the water within the membrane behaves anomalously because of the orientation of water molecules within the electrical double layer of the membrane matrix. When an appropriate value of the thermal conductivity of the water in the membrane is used, the results show good agreement with theory for a random mixture of two phases.

The thermal conductivity of polyvinylbenzene-sulfonate membranes was measured as a function of external concentration of electrolyte. This effect was not explainable by the swelling of membranes and was thought due to more complex factors. It was found that the thermal conductivity increased smoothly with temperature, indicating relatively short chain segments within the membrane.

Thus, methods for measuring the electrical and thermal conductivities of ion-selective membranes have been found and established as acceptable and accurate methods. These quantities were measured for several varieties of

ion-selective membranes in an attempt to characterize these systems and to prove the operation of the cells. The use of these results with others obtained for these membranes should be useful in the constructing of a theory for membranes and in the manufacture of membranes with specified properties for specific purposes.

REFERENCES

(1) Tuwiner, S.B., Diffusion and Membrane Technology, Reinhold Publishing Corp., New York, 1962.

(2) Shedlovsky, T., (ed.) Electrochemistry in Biology and Medicine, Wiley and Sons Inc., New York, 1955.

(3) Helfferich, F., Ion Exchange, McGraw-Hill Book Co., New York, 1962.

(4) Brydges, T.G., D.G. Dawson, and J.W. Lorimer, J. Polymer Sci., 6, 1009 (1968).

(5) Kirkwood, J.G., Ion Transport Across Membranes, H.T. Clarke (ed.), p. 119, Academic Press Inc., New York, 1954.

(6) Helfferich, F., Ion Exchange, p. 323, McGraw-Hill Book Co., New York, 1962.

(7) Kittel, C., Introduction to Solid State Physics, 3rd edition, Wiley and Sons Inc., New York, 1966.

(8) Lakshminarayanaiah, N., Chem. Rev., 65, 491 (1965).

(9) Helfferich, F., Ion Exchange, p. 6, McGraw-Hill Book Co., New York, 1962.

(10) Helfferich, F., Ion Exchange, p. 79, McGraw-Hill Book Co., New York, 1962.

(11) Donnan, F.G., Chem. Rev., 1, 73 (1924).

(12) Ueberreiter, V.K., and E. Otto-Laupenmuhlen, Kolloid-Zeitschrift, 133, 26 (1953).

(13) Haase, R., Zeit. Phys. Chem., N.F. 51, 315 (1966).

(14) Thompson, H.S., J. Roy. Agr. Soc. Engl., 11, 68 (1850).

(15) Lemberg, J., Z. deut. geol. Ges., 22, 355 (1870).

(16) Harm, F., and A. Rumpler, 5th Intern. Congr. Pure Appl. Chem., 1903, 59.

(17) Juda, W., and W.A. McRae, J. Amer. Chem. Soc., 72, 1044 (1950).

(18) Kressman, T.R.E., Nature, 165, 568 (1950).

(19) Lakshminarayanaiah, N., Transport Phenomena in Membranes, Academic Press Inc., New York, 1969.

(20) Graydon, W.F., and R.J. Stewart, J. Phys. Chem., 59, 86 (1955).

(21) Lorimer, J.W., E.I. Boterenbrood, and J.J. Hermans, Discussions Faraday Soc., No. 21, 150, 198 (1956).

(22) Altug, I. and M.L. Hair, J. Phys. Chem., 72, 599 (1968).

(23) Manecke, G., and K.F. Bonhoeffer, Z. Electrochem., 55, 475 (1951).

(24) Barrer, R.M., J.A. Barrie, and M.G. Rogers, Trans. Faraday Soc., 58, 2473 (1962).

(25) Subrahmanyan, V., and N. Lakshminarayanaiah, J. Phys. Chem., 72, 4314 (1968).

(26) Hills, G.J., J.A. Kitchener, and P.J. Ovenden, Trans. Faraday Soc., 51, 719 (1955).

(27) van der Pauw, L.J., Philips Res. Repts., 13, 1 (1958).

(28) Staverman, A.J., Trans. Faraday Soc., 48, 176 (1952).

(29) de Groot, S.R., Thermodynamics of Irreversible Processes, North Holland Publishing Co., Amsterdam, 1952.

(30) de Groot, S.R., and P. Mazur, Non-equilibrium Thermodynamics, North Holland Publishing Co., Amsterdam, 1962.

(31) Katchalsky, A., and P.F. Curran, Non-equilibrium Thermodynamics in Biophysics, Harvard University Press, Cambridge, 1965.

(32) Caplan, S.R., and D.C. Mikulecky, in J.A. Marinsky ed., Ion Exchange, Vol. 1, Marcel Dekker Inc., New York, 1966.

(33) Hanley, H.J.M., in H.J.M. Hanley, ed., Transport Phenomena in Fluids, Marcel Dekker, New York, 1969.

(34) Mikulecky, D.C., in H.J.M. Hanley, ed., Transport Phenomena in Fluids, Marcel Dekker, New York, 1969.

(35) Helfferich, F., Ion Exchange, Chapters 7 and 8, McGraw-Hill Book Co., New York, 1962.

(36) Dresner, L., J. Phys. Chem., 67, 1635 (1963).

(37) Kobatake, Y., and H. Fujita, Kolloid-Z., 169, 58 (1964).

(38) Kobatake, Y., and H. Fujita, J. Chem. Phys., 41, 2963 (1964).

(39) Churaev, N.V., and B.V. Deryagin, Doklady Phys. Chem., 166, 471 (1966).

(40) Churaev, N.V., B.V. Deryagin, and P.P. Zolotarev, Doklady Phys. Chem., 183, 935 (1968).

(41) Onsager, L., Phys. Rev., 37, 405 (1931); 38, 2265 (1931).

(42) Miller, D.G., in H.J.M. Hanley, ed., Transport Phenomena in Fluids, Marcel Dekker, New York, 1969.

(43) Tyrrell, H.J.V., Diffusion and Heat Flow in Liquids, Butterworths,

(44) Katchalsky, A., and P.F. Curran, Non-equilibrium Thermodynamics in Biophysics, pp. 153-9, Harvard University Press, Cambridge, 1965.

(45) Meares, P., and H.H. Ussing, Trans. Faraday Soc., 55, 244 (1959).

(46) Kedem, O. and A. Katchalsky, Trans. Faraday Soc., 59, 1918, 1931, 1941, (1963).

(47) Helfferich, F., Ion Exchange, Sect. 7-3, 7-4, McGraw-Hill Book Co., New York, 1962.

(48) de Groot, S.R. and P. Mazur, Physica 23, 73 (1957).

(49) Greene, R.F. and H.B. Callen, Phys. Rev. 88, 1387 (1952).

(50) Rice, S.A. and F.E. Harris, Zeit. physik. Chem. (N.F.) 8, 207 (1956).

(51) Marinsky, J.A., in J.A. Marinsky, Ion Exchange, Vol. I., Marcel Dekker, Inc., New York, 1966.

(52) Danielli, J.F., The Permeability of Natural Membranes, p. 343, MacMillan, New York, 1943.

(53) Eyring, H., R. Lumry, and J.W. Woodbury, Record Chem. Progr. (Kresge-Hooker Sci. Lib.), 10, 100 (1949).

(54) Corning Glass Works, Technical Products Div., 'The Use of Porous Glass No. 7930 as a Chromatographic Medium'. Feb. 28, 1961.

(55) Helfferich, F., Ion Exchange, Sect. 4-3, McGraw-Hill Book Co., New York, 1962.

(56) MacInnes, D.A., The Principles of Electrochemistry, p. 83, Dover Publications Inc., New York, 1961.

(57) Janz, G.J., and J.D.E. McIntyre, J. Electrochem. Soc., 108, 272 (1961).

(58) Feates, F.S., D.J.G. Ives, and J.H. Pryor, J. Electrochem. Soc., 103, 580 (1956).

(59) Shoemaker, D.P., and C.W. Garland, Experiments in Physical Chemistry, p. 384, McGraw-Hill Book Co., 1962.

(60) Reitz, J.R., and F.J. Milford, Foundations of Electromagnetic Theory, 2nd edition, p. 125, Addison-Wesley Pub. Co., Reading, Mass., 1967.

(61) Tranter, C.J., Integral Transforms in Mathematical Physics, 2nd edition, Wiley and Sons Inc., New York, 1959.

(62) Abramowitz, M., and I.A. Stegun, Handbook of Mathematical Functions, Dover Publications Inc., New York, 1965.

(63) Model Pk-1A Platinizing Kit, Operating Instructions, Industrial Instruments Inc., Cedar Grove, New Jersey.

(64) Benson, G.C. and A.R. Gordon, J. Chem. Phys. 13, 473 (1945).

(65) Robinson, R.A., and R.H. Stokes, Electrolyte Solutions, 2nd ed., pp. 93-95, Butterworths, London, 1959.

(66) Gregor, H.P., Research and Development Report. No. 193, Office of Saline Water, U.S. Department of the Interior, Washington, D.C., May 1966.

(67) Kawabe, H., H. Jacobson, I.F. Miller and H.P. Gregor, J. Coll. Interface Sci., 21, 79 (1966).

(68) Breslau, B.R., and I.F. Miller, Ind. Eng. Chem. Fundamentals, 10, 554 (1971).

(69) Katchalsky, A., in B.E. Conway and R.G. Barradas, eds., Chemical Physics of Ionic Solutions, John Wiley and Sons, Inc., New York, London, Sydney, 1966.

(70) Mazur, P., and J.Th.G. Overbeek, Rec. trav. chim., 70, 83 (1951).

(71) Stewart, R.J., and W.F. Graydon, J. Phys. Chem., 61, 164 (1957).

(72) Harned, H.S., and B.B. Owen, The Physical Chemistry of Electrolytic Solutions, 2nd ed., p. 172, Reinhold Publishing Corp., 1950.

(73) Brydges, T.G., Ph.D. Thesis, University of Western Ontario, 1966.

(74) Chambers, J.F., J.M. Stokes and R.H. Stokes, J. Phys. Chem., 60, 985 (1956).

(75) Kreysig, E., Advanced Engineering Mathematics p. 568, Wiley and Sons, Inc., New York, 1964.

(76) Spiegel, M.R., Complex Variables, p. 201, Schaum Publishing Co., New York, 1964.

(77) Spiegel, M.R., Complex Variables, p. 238, Schaum Publishing Co., New York, 1964.

(78) Ives, D.J.G., and G.J. Janz, Reference Electrodes, p. 205, Academic Press Inc., New York, 1961.

(79) Haller, W., J. Phys. Chem., 42, 686 (1965).

(80) Hills, G.J., A.O. Jakubovic and J.A. Kitchener, J. Polymer Sci., 19, 382 (1956).

(81) Joffe, A.F., Can. J. Phys., 34, 1342 (1956).

(82) Ballard, S.S., K.A. McCarthy and W.C. Davies, Rev. Sci. Instr., 21, 905 (1950).

(83) Harvalik, Z.V., Rev. Sci. Instr., 18, 815 (1947).

(84) Eierman, K., and K.-H. Hellwege, J. Polymer Sci., 57, 99 (1962).

(85) Carslaw, H.S., and J.C. Jaegar, Conduction of Heat in Solids, p. 319, Clarendon Press, Oxford, England, 1959.

(86) Carslaw, H.S., and J.C. Jaegar, Conduction of Heat in Solids, p. 18, Clarendon Press, Oxford, England, 1959.

(87) Kreysig, E., Advanced Engineering Mathematics, p. 540, Wiley and Sons, Inc., New York, 1964.

(88) Kreysig, E., Advanced Engineering Mathematics, p. 208 Wiley and Sons Inc., New York, 1964.

(89) Kreysig, E., Advanced Engineering Mathematics, p. 700, Wiley and Sons Inc., New York, 1964.

(90) Thomas, G.B., Calculus and Analytic Geometry, part 2, 3rd edition, p. 815, Addison-Wesley Publishing Co. Inc., Reading, Mass., 1961.

(91) Hsu, K.-L., D.E. Kline, and J.N. Tomlinson, J. Appl. Poly. Sci., 9, 3567 (1965).

(92) Carslaw, H.S., and J.C. Jaegar, Conduction of Heat in Solids, p. 20, Clarendon Press, Oxford, England, 1959.

(93) Pratt, A.W., in R.P. Tye, ed., Thermal Conductivity, Vol. 1, p. 301, Academic Press, London and New York, 1961.

(94) Chan, S.H., and J.W. Lorimer, private communication.

(95) Tye, R.P., in R.P. Tye, ed., Thermal Conductivity Vol. 1, p. IX, Academic Press, London and New York, 1961.

(96) Ratcliffe, E.H., Phil. Mag. 1, 1197 (1962).

(97) Brailsford, A.D., and K.G. Major, Brit. J. Appl. Phys., 15, 313 (1964).

(98) Ziebland, H., in R.P. Tye, ed., Thermal Conductivity Vol. 2, p. 146, Academic Press, London and New York, 1961.

(99) Brennan, W.P., B. Miller and J.C. Whitwell, J. Appl. Poly. Sci. 12, 1800 (1968).

APPENDIX I

```
C       CALCULATION OF THE CORRECTION FACTOR FOR MEMBRANE
C       OVERLAP IN ELECTRICAL CONDUCTIVITY CELLS USING
C       THE FORMULA
C           R = RO + L*(1.0 - (16.0/PI**2)*SN)
C       SN = SUM OVER ODD POSITIVE INTEGERS, Q, OF
C            (1/Q**2)*(I1(ALPHA)/I1(BETA))*
C              (I1(BETA)*K1(ALPHA)-I1(ALPHA)*K1(BETA))
C       ALPHA = PI*A/L
C       BETA = PI*B/L
C       'A' IS THE RADIUS OF THE ELECTRODES
C       'B' IS THE RADIUS OF THE MEMBRANE
C       'L' IS THE THICKNESS OF THE MEMBRANE
C       I1(X) AND K1(X) ARE MODIFIED BESSEL FUNCTIONS OF
C       THE SECOND KIND.
C
C
C       NUMBERS CONCERNING K1(X) MUST BE CALCULATED IN
C       DOUBLE PRECISION SINCE THE FINAL RESULT IS ABOUT
C       1.0E-08 TIMES THE LARGEST TERM.  DOUBLE PRECISION
C       GIVES 16 FIGURES.
C
```

```
C
      DOUBLE PRECISION DANB2, DBNB2, DAN, DBN, DANEXP,
     1 DBNEXP, FACIN, GAB2, GBB2, TERMKA, TERMKB, AIPRT1,
     2 DCOUNT, AKPRT1, AKPRT2, BKPRT1, BKPRT2, ANFAC,
     3 ANFAC1, BIPRT1
C
C        READ VALUES FOR PI*A/L AND PI*B/L
C
13    READ (5,1) ALPHA, BETA
1     FORMAT (2F8.5)
      IF (ALPHA.LT.0.1) STOP
      WRITE (6,14)
14    FORMAT (1H1, 33H   ALPHA      BETA       CORRECTION )
      TRMSN1 = 0.0
      TRMSN2 = 0.0
C
C        DO LOOP TO CALCULATE THE TERMS IN THE SUMMATION IN
C        THE EQUATION.
C
2     DO 3 N = 1, 15, 2
      E = N
      ALPHAN = ALPHA*E
      BETAN = BETA*E
```

```
      DIFF = 0.0
      IF (ALPHAN.LT.10.0) GO TO 4
      IF (BETAN.GT.10.0) GO TO 5
C
C        IF THE ARGUEMENT IS LESS THAN 10.0, THE BESSEL
C        FUNCTION IS CALCULATED USING A SERIES EXPANSION TO
C        AN ACCURACY OF 6 FIGURES.
C
4     ANFAC = 1.0D0
      ANEXP = EXP(ALPHAN)
      BNEXP = EXP(BETAN)
      DANB2 = DBLE(ALPHAN)/2.0D0
      DBNB2 = DBLE(BETAN)/2.0D0
      DAN = 2.0D0*DANB2
      DBN = 2.0D0*DBNB2
      DANEXP = DEXP(DAN)
      DBNEXP = DEXP(DBN)
      FACIN = 0.0D0
      GAB2 = DLOG(DANB2) + 0.5772156649015329
      GBB2 = DLOG(DBNB2) + 0.5772156649015329
      TERMIA = (ALPHAN/2.0)/ANEXP
      TERMKA = (1.0D0/DAN + DANB2*(GAB2 - 0.5D0))*DANEXP
      TERMIB = (BETAN/2.0)/BNEXP
```

```
      TERMKB = (1.0D0/DBN + DBNB2*(GBB2 - 0.5D0))*DBNEXP
      AIPRT1 = 1.0D0
      BIPRT1 = 1.0D0
      CORFAC = BETAN
C
C           DO LOOP FOR CALCULATING THE TERMS IN THE
C           SERIES EXPANSION OF BESSEL FUNCTIONS.
C
      DO 5 L=1,30
      COUNT = L
      DCOUNT = DBLE(COUNT)
      ANFAC = ANFAC*DCOUNT
      ANFAC1 = ANFAC*(DCOUNT + 1.0D0)
      FACIN = FACIN + 1.0D0/DCOUNT
      IF (ALPHAN.GT.10.0) GO TO 6
      AKPRT1 = GAB2 - FACIN - 1.0D0/(2.0D0*DCOUNT + 2.0D0)
      AIPRT1 = ((DANB2**(2.0D0*DCOUNT + 1.0D0))/ANFAC1)/ANFAC
      TERMIA = TERMIA + AIPRT1/ANEXP
      AKPRT2 = AKPRT1*DANEXP
      TERMKA = TERMKA + AKPRT2*AIPRT1
C
C           **TEST** ENSURES THE CONVERGENCE OF THE BESSEL
            FUNCTIONS
```

```
      TEST = AIPRT1*ANEXP
      IF (BETAN.GT.10.0) GO TO 3
6     BKPRT1 = GBB2 - FACIN - 1.0D0/(2.0D0*DCOUNT + 2.0D0)
      BIPRT1 = ((DBNB2**(2.0D0*DCOUNT + 1.0D0))/ANFAC1)/ANFAC
      TERMIB = TERMIB + BIPRT1/BNEXP
      BKPRT2 = BKPRT1*DBNEXP
      TERMKB = TERMKB + BKPRT2*BIPRT1
      IF (ALPHAN.LT.BETAN) GO TO 7
      GO TO 3
7     TEST = BIPRT1*BNEXP
3     IF (TEST.LT.1.0E-06) GO TO 5
      WRITE (6,8)
8     FORMAT (1H0, 45HBESSEL FUNCTION HAS NOT CONVERGED IN
     1 30 TERMS)
5     IF (ALPHAN.LT.10.0) GO TO 9
C
C          IF THE ARGUEMENT IS GREATER THAN 10, THE BESSEL
C          FUNCTION IS CALCULATED BY A POLYNOMIAL
C          APPROXIMATION(ABRAMOWITZ AND STEGUN [62])
C          ACCURATE TO AT LEAST 5 FIGURES.
C
      CORFAC = BETAN - 0.90*ALPHAN
C
```

```
C           **CORFAC** ENSURES THAT THE NUMBERS CALCULATED
C           DO NOT EXCEED THE UPPER LIMIT OF NUMBER MAGNITUDE
C           IN THE COMPUTER--- ABOUT 10**38.
C
      IF (CORFAC.GT.40.0) GO TO 10
      TENTHA = 0.10*ALPHAN
      TNAEXP = EXP(TENTHA)
      AB375 = ALPHAN/3.75
      AB200 = ALPHAN/2.0
      AFFACI = 0.39894228 - 0.03988024/AB375 - 0.00362018/
     1 AB375**2 + 0.00163801/AB375**3 - 0.01031555/AB375**4
     2 + 0.02282967/AB375**5 - 0.02895312/AB375**6
     3 + 0.01787654/AB375**7 - 0.00420059/AB375**8
      TERMIA = AFFACI/ALPHAN**0.5
      AFFACK = 1.25331414 + 0.23498619/AB200
     1 - 0.03655620/AB200**2 + 0.01504268/AB200**3
     2 - 0.00780353/AB200**4 + 0.00325614/AB200**5
     3 - 0.00068245/AB200**6
      TERMKA = AFFACK/ALPHAN**0.5
      DIFF = BETAN - ALPHAN
      IF (DIFF.GT.7.0) GO TO 10
9     IF (BETAN.LT.10.0) GO TO 11
      TNBEXP = EXP(CORFAC)
```

```
      BB375 = BETAN/3.75
      BB200 = BETAN/2.0
      BFFACI = 0.39894228 - 0.03988024/BB375
     1 - 0.00362018/BB375**2 + 0.00163801/BB375**3
     2 - 0.01031555/BB375**4 + 0.02282967/BB375**5
     3 - 0.02895312/BB375**6 + 0.01787654/BB375**7
     4 - 0.00420059/BB375**8
      TERMIB = BFFACI/BETAN**0.5
      BFFACK = 1.25331414 + 0.23498619/BB200
     1 - 0.03655620/BB200**2 + 0.01504268/BB200**3
     2 - 0.00780353/BB200**4 + 0.00325614/BB200**5
     3 - 0.00068245/BB200**6
      TERMKB = BFFACK/BETAN**0.5
11    CONTINUE
C           CALCULATION OF THE CORRECTION FACTOR
C
      TRMSN1 = TRMSN1 + TERMIA*TERMKA/E**2
      IF (DIFF.GT.7.0) GO TO 3
      TRMSN2 = TRMSN2 + (TERMIA**2)*TERMKB*(TNAEXP/TNBEXP)
     1 **2/(TERMIB*E**2)
3     CONTINUE
10    SN = TRMSN1 - TRMSN2
      FCNCOR = 1.0 - 16.0*SN/(3.14159**2)
```

```
      WRITE (6,12) ALPHA, BETA, FCNCOR
12    FORMAT (2F10.6, F15.10)
      GO TO 13
      END
```

END OF REEL

ARC-30